A modeling perspective on *Candida albicans*' interactions with its human host

D i s s e r t a t i o n

zur Erlangung des akademischen Grades

d o c t o r r e r u m n a t u r a l i u m

(Dr. rer. nat.)
im Fach Biophysik

eingereicht an der
Mathematisch-Naturwissenschaftlichen Fakultät I
Humboldt-Universität zu Berlin

von
Katarzyna Marta Tyc

Präsident der Humboldt-Universität zu Berlin:
Prof. Dr. Jan-Hendrik Olbertz

Dekan der Mathematisch-Naturwissenschaftlichen Fakultät I:
Prof. Stefan Hecht, PhD

Gutachter/innen:
1. Prof. Dr. Dr. h. c. Edda Klipp
2. Prof. Dr. Alistair Brown
3. Prof. Dr. Peter Hammerstein

Tag der mündlichen Prüfung: 4.12.2012

Abstract

Mathematical modeling approaches facilitate the analysis of dynamic properties of mechanisms triggering specific functions of biological systems. Through this work I aim to shed light on various aspects of host-pathogen interactions. Depending on the type of available data, different computational techniques are being explored.

In Chapter 3, I discuss a dynamic mathematical model of heat shock stress response activated in the fungus *Candida albicans*. The model in form of ordinary differential equations reveals several features of the system, such as acquired thermotolerance and a perfect molecular adaptation to the thermal insult. The study is relevant in the context of host-pathogen interactions since development of fever is a primary host response to fungal invasion.

The human pathogen *C. albicans* can adapt to a variety of environmental conditions. This flexibility is an important feature of the fungus' virulence. The dynamics of *C. albicans* virulence factors, e.g., yeast to hyphae transition, and defense mechanisms of the host determine the state of the fungi, i.e. whether to act as a commensal or as a foe. In Chapter 4, I explore rules that trigger the dynamics of a fungal population influenced by host phagocytic cells. Through application of an agent-based modeling technique, I investigate effects of potential drug treatments on fungal populations and their effectivity in the fungal clearance.

In Chapter 5, I analyze the dynamics of candida yeast and hyphae populations assuming pairwise interactions influenced by hagocytic cells and nutritional conditions. Two models are presented that look at the fungal interactions from different perspectives. The first model is based on game theory principles. From the study it can be hypothesized that during the course of infection the evolutionary game dynamics shift from Snowdrift game dynamics toward Prisoners' dilemma. In the second model, I examine switching rates between yeast and hyphae. The model reveals that phenotypic variations may occur in order to increase the fitness of the population.

Keywords: systems biology, Candida albicans, heat shock response, host-pathogen interactions, ODE model, agent-based model, pairwise interactions, game theory

Zusammenfassung

Ansätze der mathematischen Modellierung ermöglichen die Analyse der dynamischen Eigenschaften biologischer Systeme und den Einfluß spezifischer Funktionen. Das Ziel dieser Arbeit ist es verschiedene Aspekte der Interaktionen zwischen Wirt und Krankheitserregern zu analysieren. In Abhängigkeit von den verfügbaren Daten werden verschiedene Rechenmethoden angewandt.

In Kapitel 3 diskutiere ich ein dynamisches mathematisches Modell der zellulären Antwort auf Hitzeschockstress im Pilz *Candida albicans*. Das Modell in Form von gewöhnlichen Differentialgleichungen erörtert mehrere Aspekte des Systems, wie z.B. die erworbene Thermotoleranz und eine perfekte Anpassung an die Beanspruchung durch die Temperaturwechsel. Im Rahmen der Interaktionen zwischen Wirt und Krankheitserreger ist die Studie relevant, da die Entwicklung von Fieber eine primäre Antwort des Organismus auf eine Pilzinvasion ist.

Der Krankheitserreger *C. albicans* kann sich an unterschiedlichste Umweltbedingungen anpassen. Diese Flexibilität ist ein wichtiger Aspekt der Virulenz des Pilzes. Die Dynamik von *C. albicans* Virulenzfaktoren, wie z.B. der Übergang vom Hefe- zum Hyphenstadium, und die Abwehrmechanismen des Wirts bestimmen den Zustand des Pilzes, d.h. ob er als Kommensale oder Krankheitserreger vorkommt. In Kapitel 4 untersuche ich die Regeln, die der Dynamik der Pilzpopulation zu Grunde liegen und wie diese z.B. von der Aktivität von phagozytischen Zellen des Wirtsimmunsystems beeinflusst werden. Mit Hilfe einer agenten-basierten Modellierungstechnik untersuche ich die Auswirkungen potenzieller medikamentöser Behandlungen von Pilzpopulationen und ihre Effektivität.

In Kapitel 5 analysiere ich die Dynamik der *C. albicans* Hefe- und Hyphenpopulationen unter der Annahme, das zwischen den Individuen beider Populationen paarweise Wechselwirkungen bestehen, die zusätzlich von Fresszellen und Ernährungsbedingungen beeinflusst werden. Zwei Modelle werden vorgestellt, die die Pilzinteraktionen aus verschiedenen Perspektiven betrachten. Das erste Modell basiert auf den Prinzipien der Spieltheorie. Aus dieser Studie lässt sich die Hypothese aufstellen, dass sich im Verlauf der Infektion die evolutionäre Spieldynamik von der Snowdrift Spieldynamik in Richtung Gefangendilemma verschiebt. Im zweiten Modell untersuche ich die Umschaltraten zwischen Hefen und Hyphen. Das Modell zeigt, dass in Pilzpopulationen die Ausprägung verschiedener Phänotypen der Grund für die erhöhte Überlebensfähigkeit der Population sein könnte.

Schlagwörter: Systembiologie, Candida albicans, Hitzeschock, Wirt-Pathogen Interaktionen, Differenzialgleichungsmodell, agenten-basiertes Modell, paarweise Interaktionen, Spieltheorie

Acknowledgments

First, I would like to thank **Prof. Edda Klipp** for giving me the opportunity to be a member of the Theoretical Biophysics group at the Humboldt Universität zu Berlin, and for guidance throughout the work presented in this thesis.

I am indebted to **Prof. Al Brown** for many discussions on the heat shock project, and I am thankful to **Michelle Leach**, who worked on the experimental part of the heat shock project. I am grateful to **Prof. Bernhard Hube** for many stimulating discussions on the subject concerning host-pathogen interactions and to **Prof. Peter Hammerstein** for critics on the application of the game theory formalism.

To the entire group of **Theoretical Biophysics**, especially **Clemens Kühn** for discussions and criticism concerning the mathematical models of host-pathogen interactions presented in this thesis, for a crash course on the agent-based modeling technique and valuable support while implementing models presented in this thesis.

To people who contributed to the process of improving the structure and readability of this thesis, many thanks especially to **Katja Tummler**, **Matteo Barberis**, **Marcus Krantz** and **Thomas Handorf** for their constructive criticism. I am especially indebted to my friend **Adriana Supady** who has patiently supported my well being, in my ups and downs, throughout my PhD, and who has commented on the entire manuscript providing me with countless valuable suggestions.

To the European Commission for funding through the FINSysB Marie Curie Initial Training Network (PITN-GA-2008-214004). I am glad I could make part of the **FINSysB consortium**.

To my family and friends, **Ania**, **Gabrysie dwie** and **Ruda**; **Sabina**, **Lucyna** and **Grzegorz**. Foremost, I am grateful to **Nicola**, who has been there and whose encouragement helped me to arrive to this point.

Contents

1. Biological systems meet mathematics

1.1. Introduction

Dysfunction of the human immune system can give rise to the development of a plethora of infectious diseases. In this case, these infections are more spread and their associated mortality rate is higher than that of cancer [Alberts et al., 2002]. In this contest particularly, fungal infections are an enormous health-care problem. Human fungal pathogens attack severely ill or immunocompromised patients and the number of incidences remains unacceptably high. In most cases, severe fungal infections are caused by the endogenous strains, i.e., present in our microflora. Nevertheless, the number of invasive fungal infections (IFIs) acquired in the intensive care units (ICUs) has been continuously increasing since the 1980s. *Candida* species account for the majority of the fungal infections acquired in hospitals, which are often referred to as nosocomial candidiasis. The fungus *Candida albicans* has been noted as the most frequent isolate causing IFIs [Pfaller, 1996, Evans, 2010] and its associated mortality rate ranges from 40% to 60%. The treatment and prevention of IFIs require better understanding of the biology of endogenous fungal infections as well as those with exogenous background. At-risk patients are in danger of their floral strains but there are also other factors potentiating the development of IFIs. For instance, fungal infections may occur due to use of medical devices, e.g., catheter placement, or any other contact with the environment, e.g., contact with hospital staff as pathogens can survive on hands or clothes.

The yeast *C. albicans* is an especially interesting pathogen as it is normally found in the human microflora with main reservoir being gastrointestinal (GI) tract where it displays a commensal style of life. However, the same strain that resides in the GI tract can become pathogenic and cause serious damages to its host [Miranda et al., 2009]. Common risk factors for developing candidiasis include neutropenia, application of broad spectrum of anti fungal drugs or immunodeficiency induced by e.g., chemotherapy. Other factors like, for instance, placement of a catheter or even burns may also facilitate the entrance of a pathogen and favor its dissemination. In most cases however, colonization of the host's mucosa, i.e., development of *thrush* precedes dissemination. Number of virulence factors enable the fungus to colonize the host's mucosa. In this sense, virulence factors represent the strength of the fungus in destroying host defense strategies and in disseminating, which can lead to systemic candidiasis. During the colonization and the following dissemination phase, the fungus is exposed to environmental changes and has to adapt constantly in order to survive in new niches. In order to spread within the host, the fungus has to cross natural host barriers, such as epithelial cells and endothelial cell

layer. In parallel it has to evade the innate immune response.

Mathematical models proved to be an useful tool in revealing the underlying nature of observed biological phenomena. Through applications of diverse mathematical techniques, we can help to understand the biology of fungal disease and to develop novel therapeutic strategies. Strikingly, although fungal infections are an important clinical problem, not much focus has been made on the mathematical modeling of this fungus or of any other fungal pathogen. We are, however, at the beginning of the road and only the continuous elaboration of the mathematical models, supported with experimental data, will enable us to reach the main goal: a successful treatment of fungal infections.

In this thesis, I explore the mutual dependencies of *C. albicans* and its human host and I apply several computational techniques for their investigation. The intriguing aspect of the yeast is its association with warm-blooded animals and hence, most of the time, it is living in stable thermal conditions. Yet the fungus has retained the general heat stress response. The heat shock adaptation in the fungus is interesting for number of reasons. First, exposure of cells to elevated temperatures increases their survival in otherwise lethal temperatures, a phenomenon called acquired thermotolerance [Zeuthen & Howard, 1989]. The activation of the conserved heat shock transcription factor Hsf1 regulates genes of the heat shock family proteins and hence, it triggers the production of heat shock proteins, Hsps. It was shown that the morphogenetic yeast-hyphae transition, induced by a temperature upshift from 23°C to 37°C, evokes Hsps [Dabrowa & Howard, 1984]. Germ tube formation is a key virulence factor of the pathogen [Lo et al., 1997] and the process is regulated by Hsp90 via Ras1-PKA signaling pathway [Shapiro et al., 2009]. Moreover, Hsps are immunogenic [Binder, 2006] and since broad immune responses are applied to fight e.g., infectious diseases, Hsp-vaccines are being developed. Hsps are the most abundant proteins in the cell and they allow *C. albicans* to adapt to thermal insult, which is important for virulence. In this work I present a detailed mathematical model of the molecular mechanism activated during a heat shock response in the pathogen. The process activated upon development of fever by the host, which is only one of the first responses to invading pathogens.

Fungi invasion results in, e.g., an activation of the innate immune system and recruitment of phagocytic cells to the infected tissue. A scenario where immune cells are in search for intruder cells becomes a case study for host-pathogen interactions. I elaborate on that and present models of such interactions later in this thesis. Through agent-based models (ABMs) we can assess the population dynamics and understand the interaction of microbes with host immune cells. ABM is used here to study the effect of a hypothetical drug treatment on population dynamics. A game theoretical approach allows us to consider these interactions as games between two players, the fungus and the host immune system. A thorough investigation of the rules that define this game can help us to understand what are the winning strategies for the host in fighting the microbe.

1.1.1. Objectives

A better understanding of the biology of *Candida* infections along with the development of novel anti fungal therapy strategies and diagnostic techniques are essential for fighting the microbe. Only a in-depth analysis of host-pathogen interactions will enable us to successfully fight fungal infections. New diagnostics and therapeutic approaches are the center of research in the *Candida* scientific community.

Computational techniques allow for a thorough dissection of the available experimental data. Recently, a lot of emphasis has been laid on mathematical models. Only precisely constructed and validated mathematical models can give us hints on the nature of the host-pathogen interactions. In order to invade the host, the pathogen *C. albicans* has to adhere to the host cells and cross natural host barriers. This process is very complex and only partially understood. However, it is well known that there are several cues allowing the fungi invasion. A morphological transition triggered by multiple environmental stimuli [Biswas et al., 2007] appears to be a crucial factor. The fungus can reprogram its gene expression pattern and switch from unicellular spherical yeast form to multicellular elongated hyphal form which is more suitable to cross the host barriers [Filler & Sheppard, 2006]. The fungal infection evolves further as fungi cells continue to spread with the bloodstream to different organs. The exact mechanism of how the fungus is interacting with its host and how it is able to escape the host immune response is not yet precisely understood and lies at the heart of the research on the pathogenesis of fungal infection. The host innate immune system is the key element in fighting the microbe. Only when both the pathogen and the host are confronted and studied in the context of mutual temporal dependencies, understanding the biology of fungal infections is possible.

Mathematical models have great potential to elevate the understanding of host-pathogen interactions and help to construct novel approaches for treatments of the fungal infections. This can be achieved by considering predictions of the model on drug applications and their dosage. Systems biology is a field that helps to elucidate these problems and with a broad spectrum of techniques allows us to precisely formulate them in mathematical terms.

In this work I study the pathogenesis of *C. albicans* infection. Through mathematical modeling I dissect experimental data and propose the structure of the molecular mechanism activated in the pathogen when invading the human host. During fungal invasion the host develops fever and the microbe has to adapt to the thermal insult. A dynamical model describing these processes is discussed in the light of the infection progress and is supported with experimental data. Simulations of the model revealed a molecular memory in the system which was also validated by the experiments. Hence, through analysis of temporal behavior of the model's variables we can give new insights into our understanding of how molecular interactions lead to a specific function.

In a next step I discuss a project where the focus is given on the interaction of the pathogen with neutrophils, a specific type of innate human immune cells. The problem

is approached using an agent-based modeling technique. The developed model is further used to discuss possible applications to treatment strategies, like drug therapies.

Within this context a game theoretical formulation of the problem was established. I look at the interactions as a game played by host cells and invading fungi. Based on the literature I assign two strategies to the fungus: it exists either in a yeast form or in a hyphae form. The host is not explicitly modeled and only the current status of its immune system influences the outcome of the game. In the model I consider features like various recognition strengths of the host regarding both fungi cell types [Moyes et al., 2010]. Significant differences in eliminating of one form of the fungi by innate immune cells are also taken into account [Jacobsen et al., 2012]. I investigate these complex dependencies and present a game theoretical model considering the activities of the microbe when facing its host.

1.1.2. Structure of the thesis

The development of tools and computational techniques that aid a better understanding of the pathogenesis of fungal infections is vital for effective anti fungal treatment. In order to understand the observed phenomena in biological systems, different mathematical modeling approaches were developed [Machado et al., 2011, Karlebach & Shamir, 2008]. Through this work I aim to shed light on the nature of host-pathogen interactions by using different established modeling techniques. For the first time, those are applied to study the mutual interactions between *C. albicans* and its human host. I start from a thorough description of the human opportunistic pathogen *C. albicans*, elucidating the complexity of its nature in Chapter 2. In the same chapter the process of infection development is sketched. The changes in environmental cues associated with colonization of different host niches are highlighted. These are important to understand the complex nature of the host-pathogen interactions. In the next chapters I propose different approaches that can be used for studying these mutual dependencies and present models with various levels of detail. In Chapter 3, I begin with an ordinary differential equation (ODE) model. ODE models are frequently utilized to study nonlinear dynamics of both signaling pathways and gene regulatory networks. The presented ODE model is further used to make testable predictions. Particularly, the model in Chapter 3 discusses the problem of heat shock stress response in the fungus while invading the human host. The stress is presented as the induction of fever which is the primary host response to an invading pathogen. In Chapter 4, another modeling technique is presented. Agent-based models are tools often applied to study population dynamics and cell-cell interactions within the population. I apply this technique to investigate the interactions between different morphological fungus forms and a specific type of human innate immune cells. Finally, in Chapter 5, I present another technique with potential applications to study host-pathogen interactions. A game theoretical model of *C. albicans* population, consisting of yeast and hyphae cell types as players in the game, is presented. To study the equilibrium profile of the population I apply evolutionary game theory, in particular

replicator equations. These are elaborated to first provide explanations to some real biological population data. At the end of Chapter 5, a new possible application of the framework is sketched and discussed.

1.2. 'Living cells as molecular networks'

1.2.1. Systems biology

As pointed out in [Kitano, 2002], system-level understanding of living organisms is a leading aspect of biology. Biologists aim to tackle the full functionality of organisms, through the identification and characterization of molecules the organisms are composed of. Along structural and functional characterization of the molecules they investigate how these interact and trigger a cell function. The need to ease the understanding of the organization of the inner content of the cell gave rise to systems biology. Systems biologists helps to elucidate the molecular mechanisms triggering the functionality of the cell through mathematical models. More precisely, mathematical models help to assess the problem of how the complex molecular interactions give rise to a specific function of the cell. Mathematical models of molecular interactions forming networks are used to make predictions of the behavior of such systems. Although we often have to deal with sparse experimental data available, there are essential information that cannot be disregarded when constructing a mathematical model. As such, we should take into account the following aspects whenever possible [Bruggeman & Westerhoff, 2007]:

- molecular interactions and (co-)regulation; connection of various metabolites with proteins and mRNAs;
- spatial distribution of molecules in the cell in time, i.e., spatio-temporal dynamics;
- above aspects also when the cell is challenged with different environmental conditions (stress signals, nutrients, drugs) and perturbations within the cell.

Systems biology approach can be divided into bottom-up and top-down approaches [Bray, 2003, O'Malley & Dupre, 2005, Bruggeman & Westerhoff, 2007]. Through an application of computational techniques, in the *top-down* view of systems biology, we can extract the basics of molecular properties of the studied system from experimental data. The top-down systems biology approach can be simplified as follows.

Top-down systems biology:

$$DATA\,(-omics\,data) \longrightarrow MODEL \longrightarrow PARAMETERS.$$

Supported with '-omics' data (proteomic, transcriptomic, metabolomic) we can model molecular systems and extrapolate their molecular properties. For instance, changes in the concentrations of the molecules are being used to support mathematical models and these are then used to assess the kinetic constants, or to understand the formation of

molecular complexes, for example, in terms of association and dissociation constants. The *top-down* systems biology integrates '-omics' data into models where groups of molecules are interconnected or co-regulated. These models are then used to predict new regulatory events in the molecular systems. Subsequent experimental testing of the predictions can further strengthen the model's predictive power.

Bottom-up approach uses molecular properties to predict system's behavior.

Bottom-up systems biology:

$$PARAMETERS \longrightarrow MODEL \longrightarrow DATA\,(-omics\,data).$$

The *bottom-up* derived models differ in accuracy levels depending on the source of the used parameters. Many parameters, e.g., constants describing physico-chemical properties of enzymes participating in specific reactions, cannot be determined experimentally nowadays. Their values are appraised based on parameter estimation techniques (see §1.4.1), and thus, are unlikely to reflect the 'true' parameters. This aspect clarifies the accuracy issue of the models.

In general, *bottom-up* systems biology connects molecules to identify the behavior of the bigger system. For instance, the steady-state fluxes in the model are not fitted to the data. The data are only used for validation of the model. The ultimate goal of the *bottom-up* approach is to merge models of single pathways to predict the behavior of the entire cellular system.

The model of *C. albicans* adaptation to a heat stress presented in Chapter 3 is an example of the top-down systems biology approach. Supported with the proteomic and transcriptomic data we estimate the parameters of the model, we identify molecular regulatory circuits and new behavioral properties of the system.

1.2.2. Data integration, data dissection

Mathematical modeling

Every species, in order to survive, has adapted to the fluctuations in the outer world. We use mathematical models as tools for expressing the observed adaptation behavior. Examples are, amongst others, a population growth and coexistence of distinct species, which are fighting for common nutritional resources or, zooming in, interacting molecules within a cell. All these processes can be approximated with a set of suitable mathematical functions. These functions form what we call a mathematical model.

Microbiologists aim to understand the principles of the organism's response to a variety of external signals as only a complete picture of all cellular responses will provide us with strategies for fighting diseases. Through the analysis of the structure of the system and its dynamics, systems biology is a framework for bridging the gap between molecular interactions and the behavior of biological systems. Consequently, mathematical models depend on data. Mathematical models, when supported with experimental data, provide us with an idea on the structure of the system and the various interconnections of the

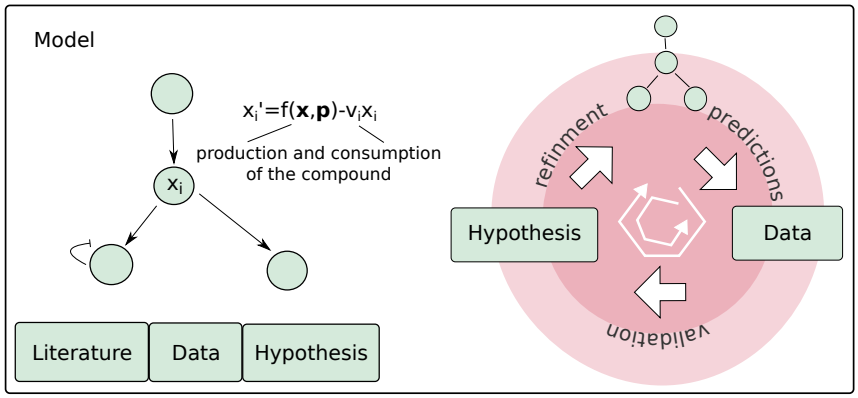

Figure 1.1.: Modeling workflow. (Left) Mathematical models are based on data from literature and new experiments. The structure of an investigated system is influenced by the data driven hypothesis, our knowledge and intuition. (Right, clockwise) The model's predictions are later tested in experiments. The new data set is used for validation of the hypothesis. If discrepancies between the model and the data occur, the model has to be refined. (Right, counter clockwise) A process where a 'new' data set is used to refine the model's structure. In order to validate the 'refined' model we need yet again subsequent data sets.

compounds. To increase the validity of the considered model, we go through an iterative cycle as depicted in Figure 1.1. The integration of literature-driven knowledge and new observations is inherent in a model development process. We have to keep in mind, that a model is only a schematic representation of reality. Usually, it includes only a subset of processes involved in the studied phenomena and hence, the model has to be further validated. Thorough investigation of the functionality of the system provides us with hypotheses on the system's behavior when some conditions are imposed. These should then be tested experimentally to support the model structure or, in the case the hypotheses are not reproducible in the experiments, to refine the model.

The first step in model creation is to collect experimental data for our model. Then, with the help of the literature, we establish a backbone of the model and in combination with hypothesis driven by the data, we adjust the model appropriately. If we are interested in the dynamical behavior of the system time course experimental data are needed. In this case, for mathematical modeling, the most suitable approach will be to work with ordinary differential equations (ODEs) since with help of ODEs we can simulate the temporal evolution of the system. However, we will still have to define the kinetic rate laws that drive the system's dynamics. For each compound in the model we define production and degradation rates and how the interactions of the compounds influence the mass flow. We will have to parameterize the model (see §1.4.1). Only when the model is able to reproduce the experimental data, we will begin with model validation. Sometimes we have to go back to the structure of the model and adjust it according to the attained experimental results. During this process, we learn new prop-

erties of the system and gain new information about the mechanism of the considered system.

Importance of mathematical models

Let $\mathcal{M}$ be a 'working' model that describes properties of compound x. By comparing simulations of the model $\mathcal{M}$ to experimental data we can validate hypothesis made for x when constructing the model. The unknown parameters of the model can be estimated and then the parameterized model can be used for making testable predictions. Predictions of the model are the simulations of the system when changing, for example, the strength of stimuli, perturbing parameters, or deleting a compound from the model structure. Computational modeling of biological systems is an approach that helps to direct a way for making necessary experiments.

Modeling cellular signaling processes

The analysis of biological processes that occur in a cell can be facilitated using mathematical models. Eukaryotic cells perceive signals from the environment via receptors present on the membrane. Those signals are then processed through different molecules in the cytoplasm to the nucleus. Transmission of the signal from the cytoplasm into the nucleus is facilitated by the activation of **transcription factors** (TFs). TFs shuttle between the cytoplasm and nucleus and control the expression of genes. This allows the cells to respond to environmental changes, but also react to any abnormalities that may occur within the cell. The cells' response processes are driven by the activation of **signaling pathways**. A specific sequence of different proteins is activated in response to stimuli, either mechanical or chemical. The signal is transmitted from one protein to another triggering the functional activity of the subsequent proteins. Despite a plethora of molecules in the cell, whenever the cell is challenged with the same external signal, the same sequence of proteins will be activated. The last element in a cascade is usually a TF. Once activated, it enters the nucleus and triggers the expression of specific genes, allowing the cell to adapt to the changes in the environmental conditions. The whole process is termed with a **stress response**. Interestingly, for eukaryotic cells, many biological processes have been conserved without considerable divergence in the pathway's structure even between different organisms and species. Based on that, the yeast *Saccharomyces cerevisiae* often serves as a model organism for studying biological processes. For instance, in Chapter 3, I discuss a computational model of molecular processes activated upon heat shock stress in the yeast *C. albicans*, and whose structure was influenced basing on the knowledge of the molecular interactions in the baker's yeast.

Transcriptional networks are another type of regulatory networks in the cell, where regulation can be both positive or negative. The major divergence between signaling pathways and transcriptional networks is in the fact that the elements constituting transcriptional networks are not proteins but genes, which encode proteins. Consequently,

we design the network topology by connecting two genes g_1 and g_2 with a arrow, directed from the first one to the latter, if the gene g_1 encodes a transcription factor t_1 which in turn regulates the expression of g_2.

Identification of compounds that constitute pathways is a challenge, especially when considering a variety of proteins present in the cell, for example, *C. albicans* has more than 6000 genes. Reconstruction of the pathway can also be a hard task due to cross talks with other pathways, e.g., some proteins can pass signal to a distinct set of proteins. Features like feedback or feedforward regulation are also commonly found in biological systems and they further complicate the identification of crucial compounds. Mathematical models are even more important in this context. If the model's simulations fail to reproduce the experimental data, it can be a consequence of omitting the necessary feedback or feedforward steps. This, in turn, can direct the experiments to the identification of missing compounds.

This section was partially based on [Alon, 2006] and I strongly encourage its reading.

1.3. Computational methods vs. biological systems

Interacting molecules are the foundation of the function of living organisms. Models of biological systems are approximations of these processes and their power is predictive nature. One of the goals of systems biology is to identify, through deep understanding of temporal molecular interactions, a source of any disfunction in cellular processes.

Biological processes can be represented by different mathematical formalisms. Depending on the type of available data and the question we want to address, we can choose between (i) models that describe the system's behavior only qualitatively, (ii) continuos models and (iii) stochastic models. The latter two account for aspects that regard relative changes rather than qualitative one (see for instance [Karlebach & Shamir, 2008]).

The next section covers three computational methods applied to study various biological processes. The first method that I introduce uses a set of ordinary differential equations. As next, in order to get the reader familiar with the approach used in Chapter 4, the agent-based modeling technique will be discussed. At the end, principles of game theory are briefly presented.

1.3.1. Modeling with set of ordinary differential equations

Dynamics of biological processes are commonly modeled with set of ordinary differential equations (ODEs) [Klipp et al., 2007]. ODEs are collections of reaction rates, i.e., mathematical formulae that describe temporal behavior of a given system. For the following irreversible reaction with two state variables x_1 and x_2

$$x_1 \rightarrow x_2 \tag{1.1}$$

the **reaction rate r** is defined as the slope of the time course plot divided by the stoichiometric coefficient of that variable. Since from one molecule of x_1 one molecule of x_2 is produced, the stoichiometric coefficient of x_1 is -1 and of x_2 is 1. Hence,

$$r = -\frac{dx_1}{dt} = \frac{dx_2}{dt}.$$

Most bio-chemical reactions obey one of the three differential rate laws (i) zero- (ii) first- and (iii) second-order reaction; $r = k$, $r = k \cdot x_1$, $r = k \cdot x_1^2$ respectively. If we assume that the reaction (1.1) is a first order reaction, i.e., $r = kx_1$, then we arrive at following equation

$$\frac{dx_1}{dt} = -kx_1. \tag{1.2}$$

We see that the differential rate law (1.2) gives a relationship between the rate of change of a variable and the concentration of this variable. The solution of (1.2) provides us with an integrated rate law

$$x_1(t) = x_1^0 e^{-kt}$$

i.e., what is the time evolution of the concentration of the variable x_1 over time with x_1^0 as initial condition.

The temporal behavior of a complex system can be captured with a set of ODEs. Below I present a scheme for a construction of an ODE model which is largely based on [Klipp et al., 2009]. If we assume we have n variables in the model, we can then determine following equation for each model variable x_i

$$\frac{dx_i}{dt} = f_i(x_1, \ldots, x_n, p_1, \ldots, p_k, t), \tag{1.3}$$

where each x is a variable in the model, p are the parameters and t is the model time. The functions f_i cover all the processes that take place in the system. The processes like production or activation enter the right side of the equation (1.3) with a positive sign, while deactivation, consumption or degradation enter the equation with a negative sign.

All processes together form a system of n state variables and m reactions, what can also be represented by ODEs in a matrix form

$$\frac{d\mathbf{x}}{dt} = \mathbf{N}\mathbf{v}. \tag{1.4}$$

In the above, $\mathbf{N}$ is a $n \times m$ stoichiometric matrix whose N_{ij}^{th} entry provides us with an information whether the i^{th} variable is connected with the j^{th} reaction. A positive value of N_{ij} indicates accumulation of the i^{th} compound and a negative value its consumption.

$$\mathbf{v} = (v_1, \ldots, v_m)^T$$

is a vector of all reaction rates with

$$v_i := v_i(x_1, \ldots, x_n, p_1^i, \ldots, p_k^i, t).$$

Velocities of most of the reactions are described by either Mass Action (MA) kinetics or Michaelis-Menten (MM) kinetics. The MA kinetic rate is proportional to the probability with which the compounds will collide. The probability of the collision is proportional to the amount of molecules in the system. The volume of the considered system also influences the process. Taken together, we can say, that the MA kinetic rate is proportional to the concentrations of the molecules and is captured in the following formulae

$$v_i = p_i \prod_j x_j.$$

The MM kinetic in turn is a model of enzymatic activity and is described by

$$v_i = \frac{\mathrm{v}_{\max}\, x_i}{x_i + K_M}.$$

Characteristic to the MM rate law is that an enzyme catalyzing a reaction has its upper activity limit. Half of the maximal velocity of the reaction $\mathrm{v}_{\max}$ is met when enzyme concentration is equal to the K_M value, called Michaelis-Menten constant. An increase of the enzyme concentration, even when in great excess to the K_M value, will not speed up the reaction due to saturation effects.

1.3.2. Agent-based modeling

Agent-based models (ABMs) emulate systems composed of elements that can behave individually. It is a computational technique suitable to study systems where spatio-temporal distributions of elements, possibly affected by stochastic processes, are considered. ABMs gained much attention in social and economical sciences [Bonabeau, 2002], but lately they have been also applied to biological systems (see references in §4.1). An inherent feature of ABMs are decision-making agents. The interactions between individual agents are defined by a set of rules. The rules include how the agents should behave, move or replicate. Naturally, these include parameters what in turn can make an ABM deterministic but also stochastic processes can easily be incorporated. The agents are existing in a predefined spatial environment and their decisions may be affected by the environment and *vice versa* the agents may influence environmental attributes. At each discrete model-time step agents are assessing their state and make decisions based on the rules that define them. ABM capture emergent phenomena where interactions among independent entities lead to global patterns. Thus, ABM can also be used to identify rules of the agents necessary to observe a pattern of interest.

The advantage of choosing ABM lies in the possibility to describe rules governing the behavior of the agents. Contrary to other computational techniques, e.g., ODE

models, where description of dynamics of the system often leads to non-linear expression. Moreover, it is easy to enlarge ABM as we can insert additional independent agents at any time. A downside of the approach might be the fact that a code of the program might evolve to even thousands of lines which makes it difficult to handle at this end.

1.3.3. Principles of game theory

The concept of game theory was first introduced by John von Neumann in 1928 and then published as [Neumann & Morgenstern, 1944]. Game theory can be applied to study various situations where interacting individuals have to make a certain decision in order to win. Winning the game is not necessarily reflecting the fact of beating the opponent. In some cases, the win is the best possible outcome under given circumstances. Game theory methods allow us to study such problems. Given two or more individuals, where one does not know what the others will do, we can derive what decision would be the best to make in order to assure winning always the highest score possible. Below I give examples of two games with two players, i.e., *two-person games* where each player can choose between two strategies. Naturally depending on the strategies that both players acquire, the outcome of the game changes. These information can be stored in a table, which is called a *payoff matrix*. Every time a game is played, it is assumed that players are aware of the content of the payoff matrix, but they do not know what the other player will do.

Formal representation of a game

When describing concepts from the field of game theory, as a reference, I mainly consider [Webb, 2007]. In order to establish a game we need players and we have to specify strategies that each of them can play. Furthermore, we need to define the payoffs for playing each of the strategies. In a game with n players, where each player i can choose between k^i strategies, let $\mathcal{S}^i = \{S^i_1, \ldots, S^i_{k^i}\}$ represent the set of possible strategies for the player i. Let $\Omega = \mathcal{S}^1 \times \ldots \times \mathcal{S}^n$ be a $k^1 \times \ldots \times k^n$ dimensional table representing all possible strategies profiles, i.e., combinations of players' strategic choices. Each cell in the Ω table provides us with the payoffs which are always given in an ordered sequence from player 1 to player n. In other words, each cell is an ordered set of real valued payoffs that gives us an information on how much a player i wins when playing a strategy from the set $\mathcal{S}^i$ against strategic choices of the remaining players. The player's payoff for playing certain strategy is always affected by choices made by the opponents. In the game, *Nash equilibrium* represents a strategy profile, i.e., a cell in the table Ω, such that, while strategies of the opponents are fixed, the player i has no incentive to deviate from its current strategy, and the same holds for all the other players.

Below, I recall two games which are considered to be canonical examples. I decided to present these examples here also because I refer to them later in the thesis in Chapter 5.

Prisoner's dilemma

The Prisoner's dilemma game is a model that explains why sometimes individuals do not cooperate although it would be beneficial for both players to do so. The game is often explained by referring to a situation where two persons are convicted of a crime. In this example, because the police do not have enough evidences for their conviction, both persons are separated, and then they are offered the same deal. They can either cooperate with each other and tell nothing to the police, or provide the police with information sufficient to put the other one in jail, i.e., defect. In case both cooperate, they will serve three years of prison. If only one prisoner defects, he will be set free and the other will serve ten years of prison. In case both defect, both will be conducted for five years of prison.

		Player 2	
		cooperate	defect
Player 1	cooperate	$-3, -3$	$-10, 0$
	defect	$0, -10$	$-5, -5$

Table 1.1.: Payoff matrix in the Prisoner's dilemma game. Each cell contains an ordered couple. The first numbers in each of the table cell are payoffs for the player 1, the second for the player 2.

Analyzing the game one can see that each of the players will tend to defect in order to minimize its own imprisonment. Since both persons have tendency to do so, at the end both will serve five years of prison. We can also see that remaining silent and cooperating would be more advantageous for them. The situation where both defect is a Nash equilibrium of this game.

Game of chicken

The game of chicken (or the Hawk-Dove game or Snowdrift game) models a conflict between two players, such that no player wants to yield to the other one. However, a situation where both players do not yield leads to the worst possible outcome of the game. Common example for an illustration of the game considers a situation on a narrow road where two cars are approaching each other from opposite directions. Obviously at least one has to swerve otherwise both will collide. In the game the one that swerved is called a chicken.

		Player 2	
		swerve	stay
Player 1	swerve	$0, 0$	$-2, 2$
	stay	$2, -2$	$-5, -5$

Table 1.2.: Payoff matrix in the game of chicken. The first numbers in each of the table cell are payoffs for the player 1, the second for the player 2.

The analysis of the game reveals that there are two possible Nash equilibria. One Nash equilibrium reflects the scenario where the first player swerves and the other drives straight. The second Nash equilibrium represents the situation where the players exchange the strategies, i.e., the first player drives straight and the other swerves.

1.4. Models and parameters

1.4.1. Parameters in the model

A mathematical model employes a set of parameters which governs the dynamics of the system. The problem begins to rise when we want to simulate a particular behavior of the system so that it follows experimental observations. To achieve this we need to set the parameters of the model appropriately. If we deal with models of cellular pathways, it will quickly appear to us that the parameters for individual reactions are in most cases unknown and only few can be found in the literature. Here, also caution has to be exercised by addressing following questions.

- Do the data from the literature refer to the same organism strain as the one we consider?
- Are the experimental conditions the same?
- Do the parameters reflect the same granularity level in the model?

With the help of time course experimental data, we can estimate parameters such that the model follows the desired dynamics. Estimation of model parameters is an extensively studied problem and currently there are many algorithms developed for this purpose. Thereby, we can distinguish between local and global optimization methods [Moles et al., 2003, Baker et al., 2010]. Both methods aim at minimizing the difference between experimental data and model simulation. While global methods search the entire parameter space, looking for the global minimum of such a distance and the corresponding set of parameters, they are computationally more challenging and time consuming than local optimization methods. On contrary, the local optimization methods are faster but they could find only a local minimum without providing the best solution.

I will start from a detailed description of the parameter estimation problem and then give a brief overview of the estimation techniques. Parameter estimation in the model is an inverse problem with an objective function being the set of model parameters that fits the best the data.

Let $\mathcal{M}(\mathbf{x}(t), \mathbf{p})$ be a dynamic model with t being the model time. The model is described by n variables $\mathbf{x}(t) = (x_1(t), \ldots, x_n(t))$ and employes m parameters $\mathbf{p} = (p_1, \ldots, p_m)$. Suppose we have experimental data $y(t)$ for a finite number of time points, $t_1, \ldots, t_j$ of a variable $x_k(t)$ in our model. The inverse problem aims at finding a set of parameters $\mathbf{p}^*$ such that $\mathcal{M}(\mathbf{x}(t), \mathbf{p}^*)$ is the best approximation of the observed

behavior. To this end, we use an optimality criterion that aims at minimizing the sum of squared residuals (RSS). With a given set of parameters $\mathbf{p}$ the model gives us the values $\mathcal{M}_k(\mathbf{x}(t_i), \mathbf{p})$ for $i \in (1, \ldots, j)$ for the variable $x_k(t)$. At each time point t_i we obtain an error from the model's approximation (see also Figure 1.2):

$$\epsilon_i = |y(t_i) - \mathcal{M}_k(\mathbf{x}(t_i), \mathbf{p})|.$$

The solution of the optimization problem is the set of parameters $\mathbf{p}^*$ such that

$$\sum_{i=1}^{j} |y(t_i) - \mathcal{M}_k(\mathbf{x}(t_i), \mathbf{p}^*)|^2 = \min_{\mathbf{p}} \sum_{i=1}^{j} \epsilon_i^2 = \min_{\mathbf{p}} \sum_{i=1}^{j} |y(t_i) - \mathcal{M}_k(\mathbf{x}(t_i), \mathbf{p})|^2.$$

In the case that we have experimental data for only l model variables we can specify their importance and priority during the estimation by specifying the weights ω_k, with $k \in (1, \ldots, l)$. Then the optimization problem can be reduced to minimizing the following

$$\mathrm{RSS}^{\omega} := \sum_{k=1}^{l} \mathrm{RSS}_k$$

where

$$\mathrm{RSS}_k := \sum_{i=1}^{j} \omega_k \epsilon_i^2 = \sum_{i=1}^{j} \omega_k |y(t_i) - \mathcal{M}_k(\mathbf{x}(t_i), \tilde{p})|^2.$$

In the above formula, we assume the weight ω_k to be the same for all time points for the variable x_k. We can highlight the importance of a specific time point i by including $\omega_{k,i}$ instead. For instance, the maximum likelihood method takes ω_k such that $\omega_k^{-1} = \sigma_k^2$, with σ_k^2 being the variance of noise in the measurements, assuming the noise is the same for all time points. In more detail, the method assumes the measurement errors are following a Gaussian distribution with mean $\mu = 0$ independently for each time point [Klipp et al., 2009]. The maximum likelihood method finds the parameter set such that the likelihood function L takes the maximum value

$$L(\mathbf{p}|y(t)) = p(y(t)|\mathbf{p}), \tag{1.5}$$

where $p(y(t)|\mathbf{p})$ is a probability density to reproduce the data set $y(t)$ by a given model $\mathcal{M}$ when given a parameter set $\mathbf{p}$. Hence, the method of maximum likelihood is equivalent to minimizing the RSS (see [Klipp et al., 2009] for derivation), where

$$\ln L(\mathbf{p}|y(t)) = -\frac{1}{2\sigma_k^2} \sum_{i=1}^{j} |y(t_i) - \mathcal{M}_k(\mathbf{x}(t_i), \mathbf{p})|^2.$$

Most mathematical models that require parametrization are nonlinear and with constrained dynamics. Hence, these problems are often nonconvex and the application of

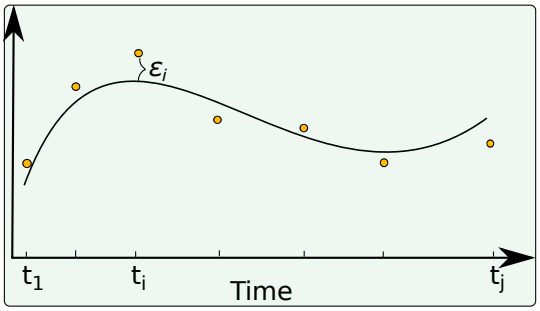

Figure 1.2.: Illustration of the error associated with a parameter estimation technique. The model captures the general trend observed in the experimental data with some inaccuracy on the single data point level. ϵ_i is a measure for the difference between experimental data point at time t_i and simulation of the model at this time.

local optimization methods, for instance, the standard Levenberg-Marquardt method, does not provide us with the optimal solution. One way to overcome this problem is to repeat the optimization tasks with varying initial conditions for every run. Although one solution can appear several times, there is no guaranty it is the globally optimal one. Global optimization tasks are used to surmount the problem. They can be distinguished into two groups: deterministic and stochastic methods. Deterministic strategies are in theory the most accurate but the computation time increases exponentially with the size of the problem. Hence, stochastic methods are often chosen to avoid the expensive computation time. The downside of this approach is that the solution might be solely the approximation of the optimal one, but this is still satisfactory in most cases. Just to name some of the global optimization algorithm, there are methods of estimating the model parameters based on the evolution in biology, known as evolutionary computation method (see [Moles et al., 2003] and references therein). These contain the Evolutionary Programming, Genetic Algorithms and Evolutionary Strategies. I use Evolutionary Programming method in Chapter 3.

The solution of the optimization task is not always unique. Due to this fact *parameter identifiability* becomes an issue. Research on this topic has been progressing during the last years and tools are being developed to aid the problem of systems identifiability [Bellu et al., 2007]. The more data points we have the higher is the likelihood that the system is identifiable. For instance, suppose that a variable x accumulates linearly under certain conditions. The information that it takes the value x^* at the single time point t^* is not enough to fully determine its temporal dependencies and the parameters of the model

$$x(t) = a \cdot t + b$$

are non-identifiable. We can also say, a model is not identifiable if a solution to the equation (1.5) is not a unique one.

To illustrate another problem, let us consider the following example. Suppose that two substrates x_1 and x_2 take part in a reaction. Both substrates are converted to the

final product x at rates k_1 and k_2, respectively. The mass flow in the reaction could thus be expressed by the following equation

$$x = k_1 x_1 \cdot k_2 x_2.$$

If values of the parameters are assigned based on sparse data we speak of *overfitting*. As such, in the above example, if we are provided solely with the value of x, we can not tell what are the contributions of x_1 and x_2 and hence, we can not assess the values of k_1 and k_2. One way to surmount the problem is to avoid the *overdetermination* and to merge together some of the information, e.g., $k = k_1 k_2$ in the above example. We could adjust the structure of the model by ignoring some of the intermediate steps.

All biological systems involve several interconnected components. For instance, the adaptation to an osmotic stress in bakers yeast *S. cerevisiae* involves several modules [Klipp et al., 2005]. Signal transduction pathways interfere with gene regulatory networks and these with metabolic pathways. We need large amount of data in order to derive a predictive mathematical model. Once this is possible we can establish a *fine-grained* model, that is, a model that describes components of the system in detail. When only sparse data are available we might opt for a *coarse-grained* model that consists of larger components with lower granularity. For instance, we can reduce each module leaving out some of the details. Such system is surely deprived of some information but it might be the only way to avoid overfitting. On the other side the predictions of the model would become more reliable and hence we increase the predictive power of the model.

In some cases it is convenient however to first divide a large model into small subsystems and estimate the parameters separately [Kühn et al., 2007]. Afterwards the subsystems can be joined together. I use this strategy when estimating the parameters for heat shock model (see Chapter 3).

1.4.2. Sensitivity analysis

Dynamic biological processes are often described by set of ordinary differential equations (ODEs). Parameters determine the temporal behavior of such systems and there are existing techniques that allow us to identify the parameters that control the model dynamics. As such, sensitivity analysis (SA) is a method that investigates an extent to which a model's parameter influences system's dynamics. SA technique referred to as metabolic control analysis (MCA, [Higgins, 1963, Heinrich & Rapoport, 1974]) was initially founded to study metabolic pathways. The method was devoted to the analysis of changes in enzymes concentrations (and hence affecting the fluxes) on steady state of metabolic system (for a concise historical overview see [Westerhoff, 2008]). Important to note is the fact, that MCA addresses the problem where we investigate how small perturbations in the parameters impact steady state value of the system. Since only small deviations from the nominal trajectory are considered the method can be classified as a

local SA technique. Examples of application of global SA techniques to dynamic models can be found in [Marino et al., 2008].

Currently, MCA has extended its application to ODE models [Klipp et al., 2009]. It can be applied to analyze dynamic models of both gene regulatory networks or signal transduction pathways. When modeling regulatory pathways it might be of more interest to look at changes along entire trajectories rather than at steady state only (upon perturbations in model parameters). Calculation of time dependent control coefficients might be a solution [Ingalls & Sauro, 2003]. With help of time dependent control coefficients we can observe whether a parameter exerts behavioral changes all along the considered trajectory or only at the early stage or maybe on a long time scale, with no visible changes at the beginning of the simulations. These can not be addressed by standard MCA. An example for the application of the method, mathematical fomulation and derivation of the coefficients is also given in §3.2.2.

To finalize, SA is often applied to reveal level of robustness of studied system. We note that robust systems exhibit little effect on the overall system's dynamics upon perturbation in parameter values. Whereas highly robust systems exhibit little or none dynamical change even to structural changes. This might be due to redundancy in the system or a feedback.

2. Biological background of yeast *Candida albicans*

Most of the fungi are ubiquitous in the environment and humans are exposed to them by inhaling the spores or small yeast cells. By 1995 it was estimated that there are about 72,000 species recognized and in total about 1.5 million fungal species existing in the whole world [Hawksworth, 1991]. This implies less than 5% of the fungi species are known so far. A small fraction of these, about 400 species, consists of plant pathogenic species and even lower number consists of human pathogenic species. From these only few human fungal pathogens are able to cause a real health problem rather than only esthetic ones. *Candida albicans* is an example of human pathogenic fungus, which is most frequently isolated from patients suffering from fungal invasion. This fungus has gained much of attention as *C. albicans* infections are difficult to treat and the associated mortality is more than 30% nowadays [Netea et al., 2008].

In the last decade a significant increase in cases of people suffering from *Candida* infection was reported. *C. albicans*, together with *C. glabrata*, is a major fungus from the genus, since it causes the majority of infections. In many cases patients are suffering from superficial mucosal or vaginal infection, i.e. *thrush*, but the immunocompromised individuals are exposed to live threatening deep sited invasive *Candidiasis*. The most dangerous are blood stream infections, which often end in death. There are some explanations for the reason of *Candida* infection's explosion. For instance, the use of chemotherapy against cancer. Patients suffering from immuno-not-competent system, like AIDS/HIV patients, neutropenic individuals, neonates or transplant recipients, are also susceptible to the fungal infection. In each of the patients group the type of infection caused by the fungi can vary from superficial to severe systemic diseases. This overall increase in cases suffering from *Candidiasis* raises the already high treatment expenses and only few cases end with success because of the lack of highly efficient anti fungal drugs. Because of that there is a need for novel anti fungal therapies against the pathogen. The combination of bioinformatics and mathematical modeling to dissect experimental data is a powerful approach to study biology of this human fungal pathogen.

2.1. *Candida albicans*: a human fungal pathogen

The fungus *C. albicans* is frequently called opportunistic human fungal pathogen. It is a yeast from the phylum *Ascomycota* and family *Saccharomycetacease*, therefore closely related to the yeast model organism *Saccharomyces cerevisiae*. There are many similar-

ities at the molecular level between the two species as many genes are shared. Because of good understanding of biological processes in *S. cerevisiae*, and based on the genetic similarity, many mechanisms have been discovered also in this pathogen.

C. albicans is an habitant of oral and vaginal mucosa and gastrointestinal tracts, with the latter one being the main reservoir. It can be present in two forms, yeast and hyphal, and hyphae development is required for pathogenesis. It is normally harmless and commensal of oral mucosa. It can adapt to wide range of environmental conditions, even though it is not found in a soil alive. These suggest that the fungus has specifically evolved to live in the human host. It is an extremely flexible microbe able to sense and rapidly adapt to subtle changes in the outer world. It responds to many stress signals, like oxidative or osmotic stress, nutritional conditions or anti fungal drug treatment and it can also sense physical changes like osmotic pressure or temperature. The adaptation processes play an extremely important role in the fungus live pattern. Thus, stress responses are extensively studied in order to address the key molecules responsible for adaptation. Adaptability also plays a role in the virulence of the fungi, because it allows the microbe to recognize the changes in the environment and to establish an infection in immunocompromised patients via activation of appropriate responses. Information from the outside influences gene expression patterns and specific molecular pathways process the signal to the nucleus. Many of these pathways have been already elucidated [Hall et al., 2009, Biswas et al., 2007]. The mitogen activated protein kinase pathways (MAPK) play a special role in fungal virulence [Roman et al., 2007]. In fact, most of the environmental stimuli activate MAP kinases, which are involved in cell fate specification, intensity of the stress response, etc.

2.1.1. Stress responses

In the systemic infections *C. albicans* is spread over different body parts. Distinct organs display various pH or oxygen concentration, nutritional conditions, etc., nevertheless this pathogen has evolved to survive by developing different signaling responses activated after the dissemination. It is thus crucial for the fungus to respond quickly and adapt to new conditions. Among many stresses encountered during the invasion process we can distinguish the following:

- Osmotic shock. Central to this response is the activation of the HOG pathway. This is the most extensively studied signaling pathway and the general molecular mechanism of osmotic adaptation is conserved from bacteria to humans. Many predictive mathematical models for osmotic adaptation in the yeast *S. cerevisiae* are already constructed [Klipp et al., 2005, Zi et al., 2010, Kühn et al., 2010]. During the evolution *C. albicans* has lost Sho1 branch for osmotic adaption retaining only Sln1 membrane sensor [Cheetham et al., 2007]. Upon sensing hyper-osmotic conditions Sln1 activates a phosphorelay cascade, which in turn activates MAP kinase cascade and consequently the Hog1 protein. Activated Hog1, a transcription factor, induces specific genes necessary for stress adaptation. Accumulation

of an osmolyte, glycerol, is considered to be the crucial at this point. Osmotic stress is an example where signaling pathways and gene regulation interplay with metabolism. In fact, during the osmotic challenge the production of some enzymes is regulated and this in turn tunes the metabolic processes in order to allow the cells to adapt.

- Thermal shock. Heat shock stress initiates the expression of heat shock genes necessary for adaption [Morimoto, 1993]. All eukaryotic cells are responding to the thermal changes in a similar fashion. Even *C. albicans*, although obligately associated with warm blooded host, has retained the general heat shock response [Nicholls et al., 2009]. Upon thermal upshift many proteins unfold causing malfunction of many signaling and regulatory pathways. Misfolded proteins bind Hsp90, leading to its dissociation from a complex with the conserved heat shock transcription factor Hsf1. This event results in the rapid and transient activation of Hsf1, which upregulates the expression of heat shock family genes HSPs. The genes products, especially the chaperone Hsp90, inhibit the activity of Hsf1 via its dephosphorylation. In Chapter 3 an elaborate predictive model of heat shock response dynamics is presented.

- Nutritional conditions. Nutrients availability controls cell growth and proliferation via the highly conserved Tor proteins [De Virgilio & Loewith, 2006]. The Tor signaling pathway is present in all eukaryotes, from bacteria to human, and it displays similar functionalities: regulates autophagy, transcriptional stress response and protein synthesis. In *C. albicans*, Tor1 exhibits a negative control upon cell-cell adhesion, e.g., important for biofilm formation. It repressess the transcritpional activity of two regulators, Bcr1 and Efg1, that induce adhesin Als1 and Als3 production, important for cell-cell adhesion [Bastidas et al., 2009]. Nutritional conditions also exhibit the control over morphogenetic switch with Tor1 as a central component to that response [Bastidas et al., 2009].

- Oxidative and nitrosative stress. This type of stress is encountered during host pathogen interactions, i.e., when the immune system gets activated in order to fight against the invading microbe. Fungi cells are exposed to oxidative and nitrosative stresses when engulfed by immune cells like monocytes, macrophages or neutrophils. Activated phagocytic cells are producing both reactive oxygen and nitrogen species, which kill the invading pathogen.

- Exposure to anti fungal drugs. In order to fight the invading fungi different therapies strategies based on the antimicrobial drug treatments are used. The development of a drug is based on a prior knowledge of the key molecules that help the microbe to act as a foe. If a key molecule in the organism is characterized, it is possible to develop a drug that targets it and disrupts its function. As an example, we can consider an antibiotic which targets a protein important for a proper DNA

replication. DNA replication in turn affects directly cell division and therefore, the growth of the single cell, and consequently of the whole population. The drug treatment can result in elimination of the invading microbe. However, *C. albicans* is an eukaryote and because of its cell wall, the outer layer of the fungus is composed of molecules that are also present in a human host. Thus, developing drugs that target the fungus without causing an harm to the host is a difficult task.

2.2. Virulence factors

C. albicans displays two forms of living, commensal state and pathogenic state, which are determined based on the mutual interactions between the human host and the fungi. Depending on the host state of health, for instance, the degree of the patient's immunodeficiency, the pathogen can cause either mucosal infections, i.e., *thrush* or deep sited systemic infections. However, the ability to cause an infection by the fungus is determined by different virulence factors (VFs) that allow the pathogen to interact with the host and enable penetration of host natural barriers. In this context, we refer to pathogenicity as ability of an organism to cause disease and to virulence as degree of pathology caused by an organism. Depending on the environmental conditions, a pathogenic organism can exhibit different levels of virulence, i.e., damage done to the host. The progress of the disease is very complex and the exact mechanism is not fully understood. Malfunctioning immune system or unbalanced microflora are strong signals for the fungi to act as a pathogen, however the virulence factors that endow the fungi to establish an infection differ depending on the kind of infection, e.g., mucosal or systemic, as well as on site and stage of infection. It seems that a single factor enabling *C. albicans* to cause a disease does not exist. However, a list of VFs widely investigated that play a significant role in the whole process is available and some are discussed in this section.

2.2.1. Morphogenesis

Many environmental stimuli trigger the phenotypic switch in the fungus *C. albicans*, for instance, cultures cultivated at 37°C on medium with serum, neutral pH, nutritional starvation or $C0_2$ availability. The stimulus affects the fungus genotype resulting in the changed expression profile of specific genes. Such modifications result in the phenotypic change. Hyphae formation is a property that has attracted the most attention in *Candida* community. It was shown that non filamentous fungi are avirulent [Lo et al., 1997]. Hyphae development increases the ability of the fungus to attach to epithelial and endothelial cells. Because of germ tube formation, *C. albicans* is able to penetrate the tissue, either by induced endocytosis [Filler & Sheppard, 2006, Dalle et al., 2010] and active penetration when meeting oral endothelial cells, or via active penetration, when invading the intestinal cells [Dalle et al., 2010]. Hyphae are present throughout the infection process. Hence, studying signaling pathways that induce the phenotypic change

(Figure 2.1) has been considered relevant to provide new strategies for anti fungal drug treatments and discoveries of potential drug targets.

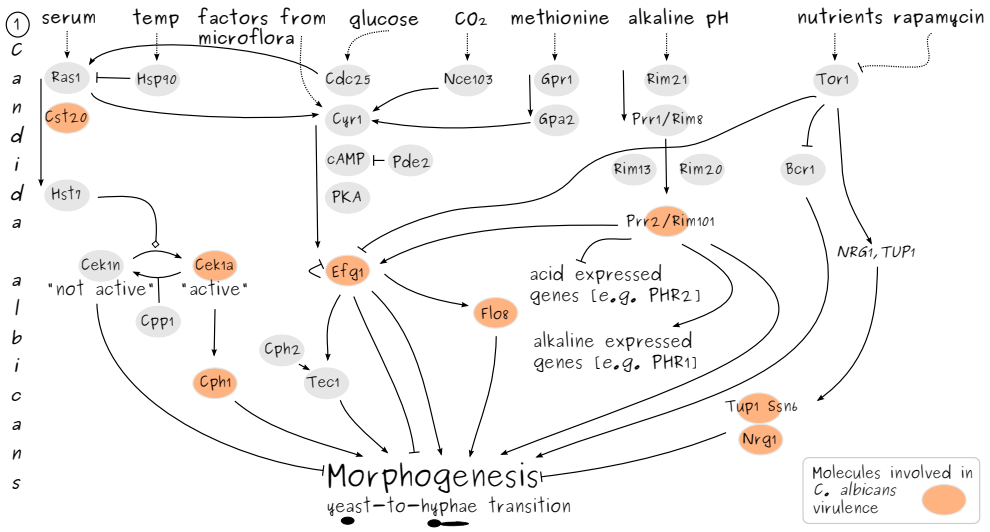

Figure 2.1.: Several environmental conditions influence the process of hyphae development by the fungi. Each of the stimuli regulates other signaling pathway.

Two transcription factors (TFs), Cph1 and Efg1, are considered to play the central role in fungi morphogenetic switch. Both are required to induce the most efficient phenotypic switch, as mutants lacking one of the two TFs are not completely off the hyphae [Whiteway, 2000, Brown & Gow, 1999], whereas $\Delta cph1\Delta efg1$ double mutant is not able to form hyphae. This suggests that the phenotypical switch is transmitted via Cph1 or Efg1. In addition, many molecules involved in the signaling of morphological switch are involved in the virulence of *C. albicans*, as mutants lacking those molecules are either partially or completely unable to cause systemic disease in a mouse model. This molecules are highlighted in orange in Figure 2.1. For example, the TF Flo8 is essential for hyphae development in *C. albicans* as well as for the expression of hyphae specific genes, and the mutant $\Delta flo8$ is avirulent in mouse model of systemic infection [Cao et al., 2006]. As indicated in Figure 2.1, pathways controlling the switch between the yeast and hyphae are activated upon variety of stress signals.

2.2.2. Cell wall proteins and related features

Fungal **cell wall proteins** (CWPs) are the first molecules that are in direct contact with the host. The components of the fungal cell wall can have various functionality. Some control the permeability of the fungal cell wall, other called adhesins (Hwp1, Hwp2, Ece1, Hyr1, Als family) initiate the fungal adhesion to host cells. For example, Hwp1 is believed to play a major role in the recognition of mammalian transglutaminases. This protein binds covalently to the host molecules connecting thus *C. albicans* to its host,

therefore Hwp1 play an important role in the colonization of host tissue. Another class of proteins can direct the biofilm formation. Some components of the cell wall function as receptors that sense the environmental signals and transmit them into a cell, thus activating appropriate signalling pathways. Other proteins are responsible for nutrient sensing or transport, e.g., amino acid sensing: Csy1, Csh3, Gap1, Gpr1; ammonium sensing: Mep1, Mep2; nitrogen: Gcn4. For *C. albicans* characteristic to phenotypic transition are cell wall rearrangements. During hyphae development many specific genes are induced coding for several adhesins, proteins that enhance the attachment to the host cells, and also genes secreting Sap proteins to the outer layer that facilitates the penetration of the host barriers.

Several studies indicate that hyphae formation is an important feature when invading the host cells and **adhesion** is crucial during the infection process. However, the efficiency of the adhesion to epithelial cells is different depending on the morphology of the fungi and the type of epithelium [Dalle et al., 2010]. Once the fungus adhere to an epithelial cell, it can then invade the host via induced endocytosis or active penetration. Whereas the internalization of the oral epithelial cells occurs by both mechanisms, the intestinal cells invasion is possible only by active penetration [Dalle et al., 2010]. *C. albicans* can enter the blood stream either via gastrointestinal mucosa or via intravascular catheter. Afterwards, in order to escape from the blood stream, *C. albicans* must cross the endothelial cells layer lining out all the blood vessels. At least three scenario that explain how this might function have been described [Filler & Sheppard, 2006]. First, leukocytes phagocytize the microbe and then during extravasation transport the fungus outside the blood stream. Second, fungus can simply cross through the endothelial cell, for example, in kidney where it is more fenestrated. Third, via induced endocytosis. The invasion protein Als3 binds to other proteins on the endothelial cell surface, and this process indirectly cause the rearrangement of the endothelial cell microfilaments that in turn initiate the internalization. Even dead cell of both types, yeast and hypha, can adhere to oral and intestinal epithelium [Dalle et al., 2010]. But killed yeast cells are not internalized by any of the cell types, in contrary to hyphal cells that are internalized only by the oral cell type.

Quorum sensing mechanism is present in variety of bacterial species and it serves as a type of communication between cells, which do not necessary have to be of the same species [Bassler & Losick, 2006]. The quorum sensing molecule for *C. albicans* is farnesol and it exerts a negative regulatory function on the yeast to hyphae transition. It activates the transcription factor Tup1, which is a negative regulator of the morphogenetic switch (see Figure 2.1) and central to the farnesol response in *C. albicans* [Kebaara et al., 2008]. Farnesol not only inhibits the filamentation but also downregulates the expression of certain genes which are necessary for biofilm formation. By quorum sensing mechanism fungi cells are able to sense the number of neighboring cells as well as to communicate to each other the presence of other microorganisms or chemical molecules in their vicinity that could have a negative impact on them. Cells are able to sense farnesol molecule

concentration in the environment and change expression of genes accordingly. Cells not only sense the molecules but also secrete new ones, with the concentration of the molecules in the external space increasing proportionally with the population growth. There are no transcriptional changes in the cell until a threshold is reached. After crossing a threshold concentration, cell starts to differently express the genes in order to appropriately respond to the changes in the surrounding environment. Such mechanism can be used, for instance, to direct biofilm formation or to regulate other virulence factors.

Biofilm formation is a problem occurring mainly in hospitals. *C. albicans* biofilms are often formed on medical devices, like intravascular catheter, connected to the patient. Upon contact with a surface, fungi population grows and cells attach to the surface, then they develop hyphae and pseudohyphae [Deveau & Hogan, 2011]. A mature biofilm is a structure composed of *Candida* yeast cells, hyphae and also pseudohyphae covered by an extracellular matrix. Biofilms are difficult to clear due to their particular resistance to the known anti fungal drugs and they often lead to a life-threatening systemic disease. Quorum sensing molecule, farnesol has negative impact on biofilm formation, meaning it reduces the biofilm size.

2.2.3. Hydrolases

Hydrolase is an enzyme that breaks the chemical bond during the hydrolysis (Eq. 2.1).

$$\text{A-B} \xrightarrow{\text{H}_2\text{O}} \text{A-OH} + \text{B-H} \tag{2.1}$$

Secretion of hydrolases helps the fungal invasion of epithelium. The immuno-competent host is susceptible to the fungal invasion. *C. albicans* can enter the bloodstream, however the fungal dissemination to different body organs become possible only after endothelial cell line penetration [Biswas et al., 2007]. This is accomplished partially because of the production of hydrolases, and for this reason the production of hydrolytic enzymes is considered to be another virulence factor. In general *C. albicans* can secrete three types of hydrolases:

- Aspartic proteases that breaks the proteins.
- Phospholipases class B that cleave the acyl chains present in acyl chlorides, acid anhydrides (upon contact with water they form organic and non organic acids), esters and salts. The main phospholipase of class B is Plb1, however Δ*plb1* mutants do not show a difference during epithelial cell invasion, neither oral nor intestinal, as compared to the parental strain [Dalle et al., 2010]. This led to the conclusion that fungus invades both cell lines independently of Plb1 enzyme activity [Dalle et al., 2010]. In contrast, after histological examination of a liver in an infant mouse model, the parental strain and the revertant strain, i.e., after reintroducing PLB1 gene, show similar virulence strength whereas the *plb1* mutant was

significantly less virulent. It had reduced capability of penetration of the host cells [Mukherjee et al., 2001]. Also other studies indicate reduced virulence of the *plb1* mutant [Leidich et al., 1998, Ghannoum, 1998]. Therefore, Plb1 might play a role during the dissemination process, for example, by facilitating the penetration of the host barriers.

- Lipases that breaks fats. They are considered not to play a role during epithelial invasion.

The first group of hydrolases consists of lytic enzymes able to digest the surface of the epithelium making the fungus a way to get through this barrier [Filler & Sheppard, 2006]. Some of them, called aspartic proteases, are secreted by members of the family of SAP genes. The genes *SAP*1-3 play a role during the superficial infection, whereas *SAP*4-6 are expressed in hyphal cells and during the systemic infection or even during an escape from macrophages. The proteases Sap1-6 have a positive impact on the *C. albicans*'s ability to invade the epithelial cells. SAPs facilitate the penetration of host cells by the fungus. In particular, they stimulate induced endocytosis, as the killed hyphal cells mutants lacking *SAP*1-3 and *SAP*4-6 exhibit a reduced uptake [Dalle et al., 2010].

2.2.4. Phenotypic switching and mating

The fungus *C. albicans*, unlike *S. cerevisiae*, lacks a complete sexual cycle. There are however conserved molecules structurally and functionally similar to those participating in mating process in *S. cerevisiae*, i.e., pheromone response pathway. *C. albicans* is able to switch phenotypically between white oval yeast cell and elongated opaque cells. The opaque cells are shown to be more effective in mating and only the strains homozygous for MTL-a or MTL-α locus strains, for instance, WO-1 strain, are able to switch the phenotype [Miller & Johnson, 2002, Bennett & Johnson, 2005, Noble & Johnson, 2007]. Opaque cells exhibit changes in the structure of the surface. Phenotypical switching impacts the adaptability to distinct host sites and influences virulence during different stages or types of infection. White cells are more virulent in systemic infection and opaque cells are more successful in infecting the skin or in cutaneous infection models [Bennett & Johnson, 2005]. Although the switching occurs at very low probability, and there is always a mix of both, i.e., negligible fraction of one type within the colony of second form, specific growth media as well as environmental signals can induce the switch [Ramirez-Zavala et al., 2008, Bennett & Johnson, 2005]. Both cell types differ only in the phenotype, while the genotype remain unchanged, and they differ only in the gene expression pattern.

The following sections are based on:

Tyc KM, Klipp E (2011) Modeling Dissemination of Pathogenic Fungi within a Host: A Cartoon for the Interactions of Two Complex Systems.

J Comput Sci Syst Biol S1:001. doi:10.4172/jcsb.S1-001

2.3. Host-pathogen interactions

C. albicans is a human commensal mainly found in the gut and gastrointestinal flora. In the commensal state, the fungi live in equilibrium with other microflora organisms and host cells from the immune system. These interactions, along with variety of physical and chemical environmental signals, control the size of the candida population. Disruption of a healthy floral balance leads to an increased growth of the fungal population, and subsequently to the fungal colonization of the epithelial cells. In some cases, as the process continues, the fungi penetrate to deeper body parts that eventually lead to a fungal dissemination with the blood stream, leading to a systemic candidiasis [Pittet et al., 1994]. Patients with weakened immune system are especially susceptible to deep-seated fungal infections [Zupanić-Krmek & Nemet, 2004].

C. albicans when residing in a yeast form is tolerated by the host who does not take any steps to clear the fungi, e.g., through an activation of the immune response, which is a primary host's defense mechanism, even though in immunocompromised patients the benign *C. albicans* yeast cells can switch their morphology, and appear more pathogenic and invasive. In general, *C. albicans* is a flexible fungus able to adapt to very harsh conditions. The fungus adjusts its gene expression pattern according to pH, temperature, nutritional conditions, oxygen availability, etc. These are usually influenced by the life style of the fungus that changes from a commensal to a pathogenic in a weakened host. In this view, the fungi experience the changes in environmental conditions due to a invasion and a dissemination. In Figure 2.2 I point out different host barriers the fungi have to cross during the course of infection. In the same figure, I also illustrate various host defense strategies the fungi are challenged with, what is also summarized in the text below (see also [Munro et al., 2006]).

The *C. albicans* cells, the habitants of the human microflora, are in constant contact with human epithelium. The epithelial cells form the very first host barrier the fungi have to cross, and it is achieved by a penetration of the host cells. The fungal invasion is anticipated with colonization of the epithelium (Figure 2.2, (1)). An increased population growth is accompanied by the yeast to hyphae transition that occurs in the fungal population. The phenotypic transition is an important virulence factor mainly because hyphae are considered to be the invasive form [Lo et al., 1997, Moyes et al., 2010, Netea & Kullberg, 2010].

Epithelial cells are equipped with different recognition mechanisms that are differ-

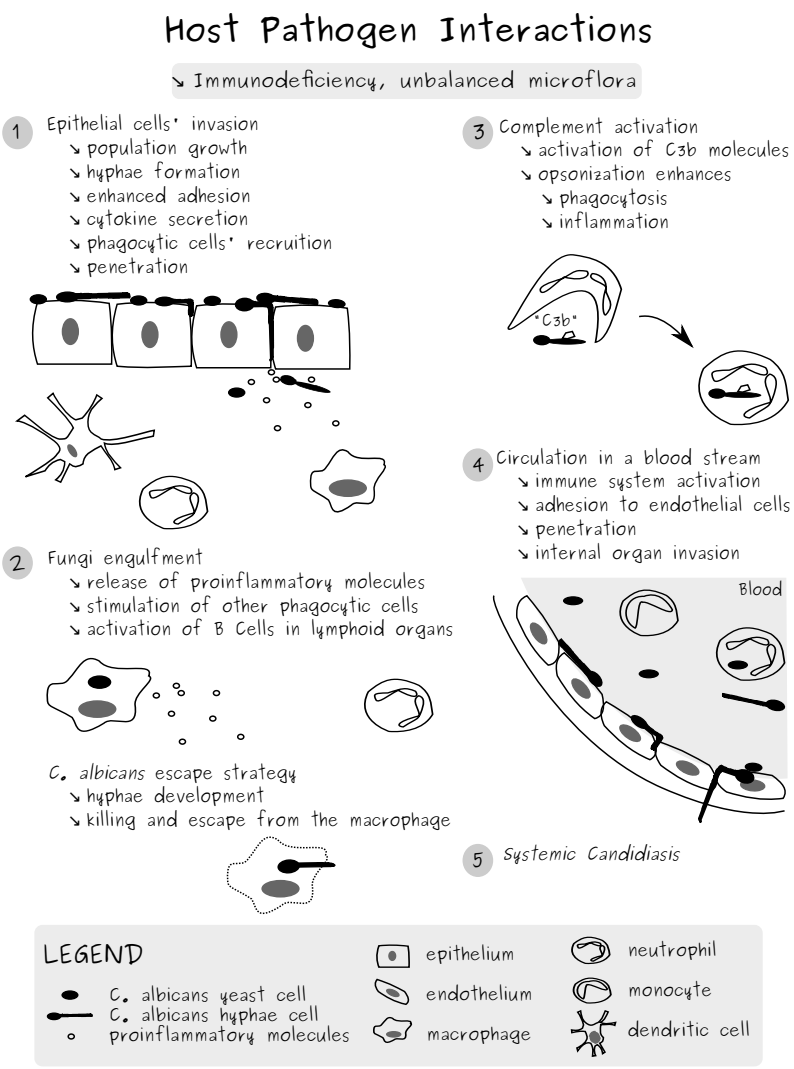

Figure 2.2.: Host - *C. albicans* interactions. Unbalanced microflora facilitates fungal invasion. The process begins with an increased rate of population growth and enhanced yeast to hyphae transition - a switch necessary for adhesion to epithelial cells. (1) Upon contact with hypae, epithelial cells secrete pro-inflammatory molecules, which act as chemoatractants for phagocytic cells. (2) Innate immune cells engulf the pathogen and release other pro-inflammatory molecules. *C. albicans* can escape from macrophages, but not neutrophils, by developing hypha. (3) Complement pathway is important in fighting the microbe. Its stimulation results in activation of C3b molecules. These bind the surface of the pathogen and become a target for other phagocytic cells. (4) The fight with immune cells continues in the blood stream. Hyphae attach to the endothelium and penetrate it either by forming hyphae or inducing their own uptake. (5) Due to a circulation in a blood stream, *C. albicans* is able to reach internal organs and cause systemic disease is some patient group.

entially activated upon contact with yeast and hyphae. The recognition mechanisms consist of so called, the first phase and the second phase [Moyes et al., 2010]. Increased burden of the hyphae form results in the activation of the secondary phase that triggers inflammatory response. This in turn causes the activation of the host innate immune response, and recruitment of the phagocytic cells to the site of infected tissue (Figure 2.2, (2)). In an early phase, upon sensing the fungi the host can also activate the complement that is another type of the host's defense mechanism (Figure 2.2, (3)). Stimulation of the complement pathway results in the activation of C3b molecules that subsequently bind to the surface of the pathogen, the process called opsonization [Zipfel et al., 2008]. Activated C3b molecules help the macrophages to target the pathogen.

Since the penetration of the host cells continues, the fungal cells can eventually enter the blood stream, and thus develop a candidemia. All the types of blood vessels are lined by endothelial cells which form another host's barrier that *C. albicans* has to cross (Figure 2.2, (4)). The fungus can attach to endothelium despite of flowing with the bloodstream [Wilson & Hube, 2010]. The attachment itself induces endocytosis of the *C. albicans* fungi by endothelial cells, a strategy that appears to be a common one for fungi that invade non-phagocytic host cells [Filler & Sheppard, 2006]. Severely ill patients are at high risk of developing disseminated candidiasis (Figure 2.2, (5)).

2.3.1. The infection cycle of *C. albicans*

C. albicans causes the majority of fungal infections, and oral candidiasis is the most frequent type of infection observed. The potential risk factors for developing fungal infections are considered to be: either (i) therapies that weaken the immune system of the host, e.g., chemotherapy, or (ii) therapies that result in a disruption of the floral balance, e.g., due to antibacterial drug treatments. However, it is not clear what exactly determines the patient's susceptibility to developing oral infection, for instance, rather than other mucosal infection or disseminated candidiasis. It was however observed that patients with HIV and compromised functionality of the T-Cell mediated immunity are more likely to develop oral fungal infections.

Disruption of the microbial flora stimulates the growth of candida population. Non invasive yeast cells undergo the morphological transition and develop hyphae what allow them to penetrate the host cells. Studies on the formation of germ tubes led to discovery of several regulatory pathways that trigger the morphological transition as it is depicted in Figure 2.1 [Brown & Gow, 1999, Biswas et al., 2007]. Nutrient availability is a strong inducer for the fungus' phenotypic transition via regulation of the Tor signaling pathway [Bastidas et al., 2009]. Sparse nutritional conditions lead to inactivation of the protein kinase Tor1 (Figure 2.1). Tor1 is a negative regulator of Bcr1 and Efg1 TFs, hence inactivation of Tor1 results in an increased activity of the two TFs that positively regulate the expression of adhesin genes, such as *ALS1, ALS3, ECE1, HWP1.* All these genes are hyhpae specific and phenotypic transition takes place. Development of hyphae is important in the fungal infection cycle since germ tubes enhance the adhesion to epithe-

lial cells. However, it has been observed that the fungi attach with different strength to different epithelial cells types. The strength of the fungal invasion, and the associated damage it does to the host, also change between epithelial cells types [Dalle et al., 2010].

Once hyphae attach to the epithelium they start to penetrate the host tissue. This activates an inflammatory response via release of pro-inflammatory molecules, such as IL8 cytokines, that play a role of in the recruitment of phagocytic cells, e.g., macrophages, neutrophils and dendritic cells, to the place of infection (Figure 2.3, (2)). The fungal cell wall is the most exposed part that has to be recognized by the host. The proteome of the fungal cell wall changes depending on the environmental conditions, but there are specific recognition mechanisms that allow the host to target the pathogen. The surface of host immune cells is filled with pattern-recognition receptors (PRRs) able to attach to pathogen-associated molecular patterns (PAMPs) expressed by the fungal cell wall. In other words, PAMPs are microbial signatures that are conserved among the pathogenic species. For each PAMP present on the surface of *C. albicans* there is a specific PRR that recognizes it, but the expression of PRRs can vary among the phagocytic cells [Netea et al., 2008]. As it is depicted in Figure 2.3, (3), specific PRRs are being activated upon contact with specific PAMPs. Within the phagocytic cells signaling pathways are stimulated due to the activation of the PRRs, and this results in the cytokines induction by these cells. The cytokines enhance the activity of host immune system response, and increase the rate of fungal clearance. Toll like receptors (TLRs) constitute a class of PRRs that is considered to be a key weapon of the innate and adaptive immune system. TLRs are also found on the surface of oral epithelial cells. Especially TLR4 type is being activated by *C. albicans*, and when neutrophils are present, the TLR4 receptors are even more pronounced protecting the epithelium from fungal invasion [Weindl et al., 2007].

A type of phagocytic cells, the dendritic cells (DCs), connect an innate immune response with an adaptive immune response because of the activation of T-Cells and B-Cells (Figure 2.4). After engulfment of *C. albicans* DCs present an antigen of the pathogen which is recognized by T_H-Cells (Figure 2.4, (3)). T_H-Cells are activated what leads to a productions of IL 17 cytokines. This molecules play a role in the recruitment of phagocytic cells, e.g., neutrophils (Figure 2.4, (4)). In immunocompetent host there is no need to activate the adaptive immune system since the innate immune system is able to prevent the fungal invasion. Therefore, the fungi are able to penetrate the tissue only in individuals with compromised immune system, or when barriers are breached.

There are two possibilities for *C. albicans* to enter the bloodstream, i.e., either by penetrating gastrointestinal mucosa or when there is a cut, e.g., due to intravascular catheter installation. From the bloodstream, the fungus disseminates to different body parts [Mavor et al., 2005]. In the bloodstream, fungus is exposed to new environmental conditions, new pH, nutrient, and it has to adapt to these changes. Both serum and

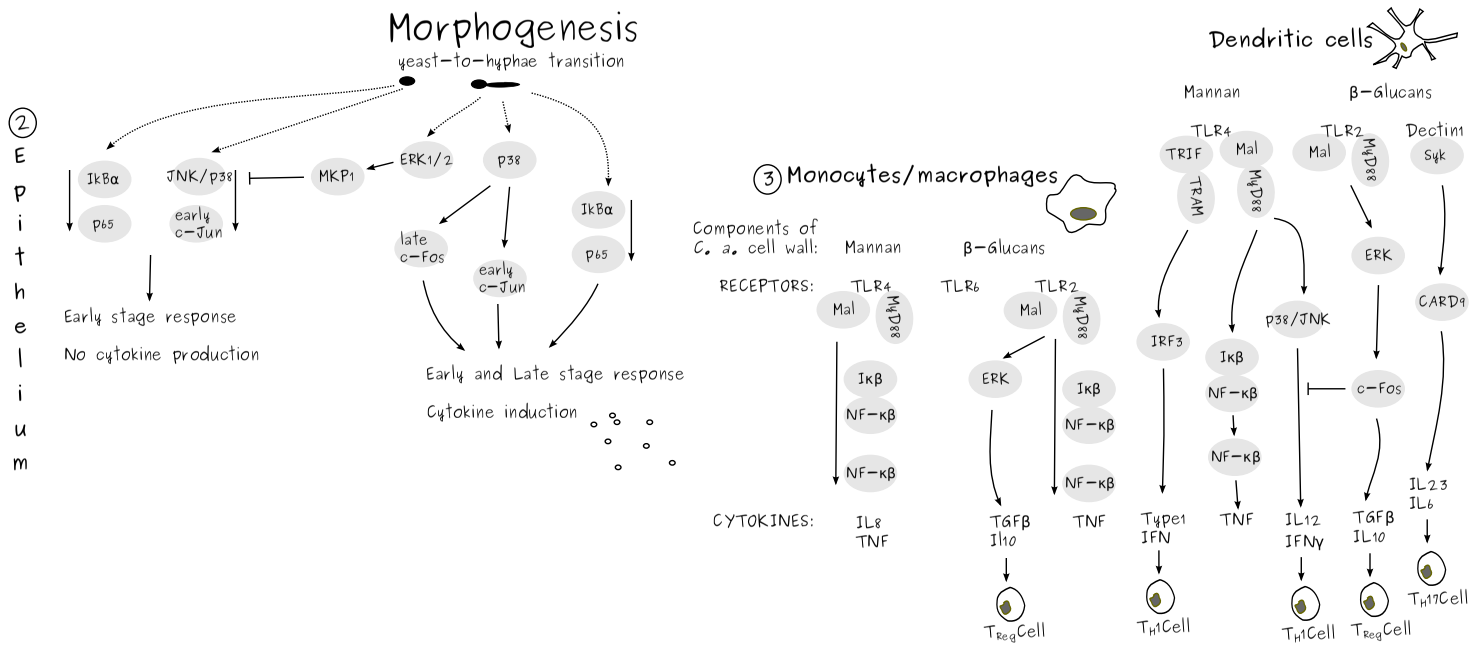

Figure 2.3.: Signaling pathways activated on the host side upon sensing the fungi. Yeast to hyphae transition triggers activation of pathways in an epithelium (2; based on [Netea & Kullberg, 2010]). Cytokines secretion by the epithelium causes phagocytic cells recruitment to the site of the infection. Upon contact with *C. albicans* cell wall, different signaling pathways are activated in immune cells (3; adapted from [Netea et al., 2008]).

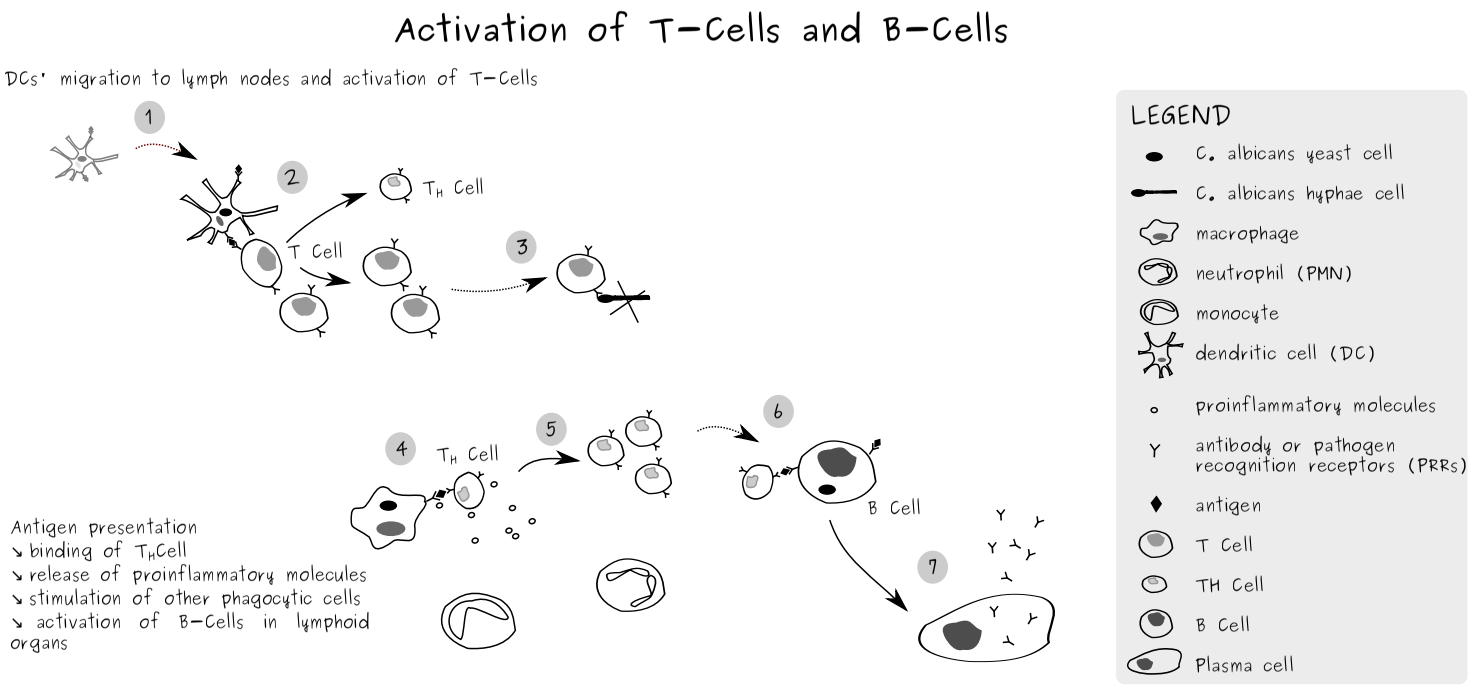

Figure 2.4.: Activation of T-Cells and B-Cells. (1) Dendritic cells (DCs) engulf the pathogen and migrate to lymph nodes with an antigen present on their surface. (2) Next, DCs activate specific T-Cells, i.e., with the proper receptor. Some of the activated T-Cells proliferate and produce specific T_H-Cells, i.e., with the correct antigen-recognizing receptor. (3) Other migrate to the site of infected tissue and destroy the pathogen. (4) T_H-Cells upregulate immune response via e.g., binding antigens presented by macrophages. Activation of T_H-Cells results in proinflammatory cytokine production, e.g., IL17, and enhanced recruitment of phagocytic cells. (5) Active T_H-Cells replicate, migrate toward lymph nodes and (6) bind the antigens presented by B-Cells. (7) The B-Cell matures to plasma cell, which is producing the specific antibodies. These antibodies bind the surface of the pathogen and additionally stimulate processes like: activation of complement, enhanced phagocytosis and enhanced inflammation.

glucose stimulate the activation of pathways that lead to hyphae development, i.e., Ras1-Cph1 and Ras1-Efg1 signaling pathways (See Figure 2.1). Hyphae are sensed by the cells from the innate immune system, and hence the fungi must again activate strategies in order to escape the host attack. For example, candida cells secrete aspartic proteases (Saps), molecules that make the surface of candida cells more proteolytic. This in turn facilitates the penetration of the host tissues and degrades the host defense. Hyphae are able to attach to the endothelium, and the most efficient appear to be hyphae with germ tubes of a length in the range between 3–7μm [Wilson & Hube, 2010]. Hyphae that successfully attach to the endothelial cells, induce their own endocytosis, a strategy that facilitates the fungal dissemination to the host internal organs.

In conclusion, the biology and the dynamics of these processes are only partially understood. It is not clear how the host attributes, and the virulence factors of the fungi, result in the fungal pathogenic activity. The cycle of fungal infection is a complex system, unlikely to be represented within one mathematical framework. Therefore, in this thesis I focus on an early stage of infection, colonization of the epithelial cells. I analyze the fungal dynamics by looking at the interactions from different angles, and also by considering different time scales.

2.4. Systems biology of fungal infection

Host-pathogen interactions are described by two complex systems, both exhibiting non linear dynamics that simultaneously influence each other. Therefore, the outcome of perturbations in those processes, e.g., due to a change of the environmental conditions, can not be predicted. To overcome this problem, mathematical models are developed. Computational approaches have to be applied in order two study dynamics of host and pathogen, both in isolation and when they interact.

Microbiologists want to capture the dependencies between and within genomes', proteomes', and metabolomes' members. To fight the pathogen, we need to understand the dynamics of changes that occur on the molecular level in the presence of various physical and chemical stimuli, drugs, and multiple combinations of any of them. In order to facilitate the analysis, computational techniques are applied. Consequently, a strategy based on developing mathematical models gave foundation to the field of systems biology. Systems biologists aim at developing models that could capture the entire complexity of the biology of the cell, including spatial and dynamic distribution of the inner content. These detailed models, sometimes referred to as systeome models, will potentially find application in a development of new treatment strategies and in a design of novel drugs. A priori, systeome models would serve for making predictions on how a disease will develop, e.g., fungal invasion, and which strategies are the best to fight the microbe. Mathematical modeling of a pathogen dissemination within a host in its entire complexity is currently an issue due to a number of reasons, e.g., limitations in the experimental procedures, or computer power necessary for running computational

models. Therefore, currently all mathematical models are based on assumptions and have number of boundaries, hence providing us only with an approximation of the processes. By testing in the experiments the model's predictions we can assess the validity of the assumptions and whether the boundaries have to be shifted. In order to parameterize the models of host-pathogen interactions, experiments would need to be devoted to the generation of time-dependent measurements under conditions relevant to those encountered *in vivo* at different stages of infection. At the pathogen level, it has to be considered how the fungus adapts to new niches, how it tunes metabolic processes, or how the fungal morphogenesis helps the pathogen to colonize the host. At the host level, it has to be analyzed how the host responds to the invading fungi, for instance, by developing a fever, or by activating the immune response. Thus, models need highly detailed data describing the host-pathogen interactions, not only regarding the harmless commensal state, but also when the pathogen causes damage to the host leading to a disease.

In summary, systems biology of fungal infection can be seen as a model-based strategy that aims at the understanding how the two systems influence each other. The power of such models is in their predictive nature, that can help in a design of a drug treatment by calculating drug's efficiency, or predicting microbial resistance to the drug. Host-pathogen interactions are complex. Understanding the functionality of either host or pathogen as a single system is not sufficient to understand what would happen in case the two are facing each other. At this point we could ask:

- Do the host and the pathogen communicate?
- Are the two organisms aware of each other?
- Do they fight against the other one or only try to establish a commensal state?

In the following chapters I address these questions. As first, I explore molecular mechanisms activated in the pathogenic fungi upon heat shock stress. Then, by using agent-based modeling technique, I investigate the dynamics of the fungal population when exposed to the activity of the phagocytic cells. The potential effect of various doses of a drug treatment on fungal population is also sketched. In the last chapter of the thesis, I propose two mathematical models, both placed in a context of pairwise interactions of the fungal cells. In these models, the host affects the outcome of communication in the microbial population, and it can, e.g., force the cells to compete with each other. The models differ in the assumptions and the granularity levels, but all of them incline to think about the underlying principles of the host-pathogen interactions.

3. Modeling heat shock response in *Candida albicans*

This chapter is based on:

Leach MD, Tyc KM, Brown AJP & Klipp E: "Modelling the Regulation of Thermal Adaptation in Candida albicans, a Major Fungal Pathogen of Humans".

PLoS ONE (2012). Joint first authorship.

The experimental data presented in this chapter has been done by Leach MD and published in the reference given above.

In this chapter I present precise and comprehensive description of dynamic heat shock response (HSR) in *Candida albicans*. Along with a description of the relevance of HSR in *C. albicans* to fungal infection the study provides the community with a tool that can be used to study response to thermal challenge and adaption in other eukaryotes. I present here a scheme of molecular wiring activated upon heat stress and hence, a possible mechanistic solution to the logic behind the experimental observations. The model was reduced to the minimum including only the conserved heat shock transcription factor Hsf1 and the target gene *HSP90* along with its product, the chaperone Hsp90. The model structure is centered around the assumption that the Hsf1 phosphorylation is correlated with the accumulation of non-native proteins in the presence of heat shock. It is due to the fact that the proteins compete with Hsf1 for Hsp90 binding. In turn, free Hsf1 is being phosphorylated and becomes transcriptionally active. The model presented in this chapter, implies that there should be an additional mechanism that controls phosphorylation levels of the Hsf1. The resulting simulations of the model show that the lone dissociation of Hsf1 from the complex Hsf1Hsp90 is not enough to cause Hsf1 phosphorylation and there must be an additional level of regulation that controls the activity of the Hsf1's, yet unknown, kinase K*.

3.1. Introduction

All eukaryotic cells, from yeast to human, respond to thermal changes in a similar fashion. Cells given a heat stress increase the production rate of proteases and molecular chaperones that allow the survival of the cell and establish a cell's homeostasis. Cells have to assure proper protein synthesis, their folding and maturation, trafficking and other.

Accumulation of nonnative, misfolded or aggregated proteins is a natural consequence of the heat stress and molecular chaperones are important to assure protein repair and recovery of the cell. However, the heat stress is only one of the stimuli that activates the general heat shock stress response [Morimoto, 1998]. In other organisms, for instance, in *Saccharomyces cerevisiae*, *Drosophila melanogaster* and *Xenopus* , it was found that thermal upshift is not the only stimuli that causes phosphorylation of the heat shock transcription factor (HSTF) [Ali et al., 1998, Ananthan et al., 1986]. Pharmacological inhibition of heat shock proteins' function or any treatment resulting in protein unfolding have a similar effect. Heat stimulates the activation of HSTF, a protein conserved throughout the kingdom. Activated HSTF binds to the heat shock elements (HSEs) present on the promoter of the heat shock family genes (Figure 3.1). This in turn induces

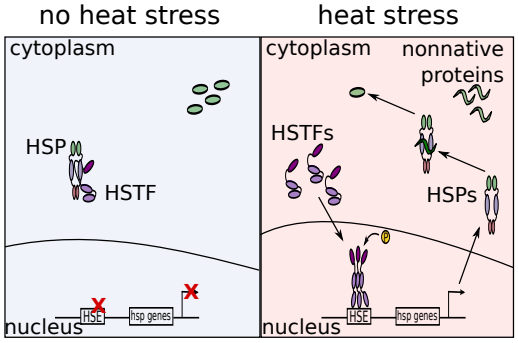

Figure 3.1.: Heat shock response. Schematic representation of the molecular mechanism activated in the cell. (Left) Adapted cells, no stress conditions. (Right) Elevated ambient temperature. HSTF binds HSE present on the promoter of HSP genes that causes the production of new HSPs. These bind nonnative proteins and protect them from the damaging stress.

production of vast range of heat shock proteins. Increased production of these molecular chaperones protects the cell from damaging effect of the heat stress. This is achieved via binding other proteins and blocking their denaturation and helping to fold them properly. Eventually chaperones downregulate HSTF activity, e.g., in *S. cerevisiae* or in HeLa cells the chaperone Hsp70 is considered to be a major repressor of HSTF activity [Rieger et al., 2005]. Other chaperones, e.g., Hsp90 can also be considered as many Hsp90-related processes are *de facto* Hsp70 dependent [Werner-Washburne et al., 1987]. In fact, in this study focus is given on how the molecular chaperone Hsp90 contributes to the regulation of HSTF.

The yeast *C. albicans*, a normal habitant of the human microflora [Odds, 1984] can cause mucosal infections (*thrush*) and establish life threatening systemic infections in debilitating patients. Although the fungus is obligately associated with warm blooded animals, it has retained the general heat shock response [Nicholls et al., 2009]. Similar to *S. cerevisiae*, *C. albicans* HSR is mediated by HSTF called Hsf1 [Nicholls et al., 2011]. The heat shock response has gained attention for many reasons. Chaperones control

the state of proteins and assist their repair if needed but also exhibit negative control over processes like aging or apoptosis. Temperature, along with other stimuli, is a strong inducer of hyphae development in *C. albicans*. Hyphae development in turn is necessary during the host invasion and infection process. On the other hand, activation of Hsf1 is compulsory for fungal virulence [Nicholls et al., 2011]. It is thus medically relevant to understand what are both antagonists and agonists of Hsf1 in *C. albicans* in order to avoid activation of Hsf1 even if it is very abrupt and transient one. HSPs are interesting to study because they influence interactions between these medically important pathogens and their human host, e.g., the molecular chaperone Hsp90 is immunogenic. Moreover, antibodies against Hsp90 have potential applications as a novel antifungal therapy [Matthews et al., 2003].

It is assumed that, in human cells, heat stress transcription factor named with HSF1 (mHsf1) exists in a monomeric state in non stressed conditions. mHsf1 either resides within a complex with Hsp70 or interacts with Hsp70 and this inhibits its transcriptional activity [Morimoto, 1993]. Damaged proteins which accumulate either during the thermal insult or upon other chemical stresses compete with mHsf1 for binding with Hsp70. Release of mHsf1 from the complex causes its instant trimerization and then phosphorylation and transcriptional activity follows. Active mHsf1 induces HSP family genes. New molecular chaperones allow cells to adapt to the stressful conditions by binding proteins of bad quality. When the situation is finally under control, chaperones start to downregulate the activity of mHsf1 by binding again to it. In yeast the mechanism of heat stress response is very similar. Stress causes accumulation of the non-native proteins, yeast Hsf1 becomes phosphorylated and heat shock genes are induced [Nicholls et al., 2009].

Fungal infections, especially those caused by *C. albicans*, are a striking medical problem. Nevertheless there are not many mathematical models available that describing biological processes in the fungi. Although there is a mathematical model describing Hsp70 interactions with mHsf1 in mammalian cells [Rieger et al., 2005], it was not possible to find a mathematical model that places Hsp90 and Hsf1 interactions at the heart of the heat induced stress response. As a consequence, experimental data for *C. albicans* heat stress response were supported with a mathematical model which is presented in this chapter. The model describes molecular interactions upon different strengths of the heat stress. Dissection of the experimental data, through a thorough analysis of the mathematical model and its experimental validation, helps to better understand the underlying molecular properties of the system. As the system develops in time the dynamics become non-linear and hence have to be supported with computational simulations. Set of experimentally determined time course data was used to parameterize the model. Next the model was used for making predictions that were also verified experimentally. It has been observed that the system adapts perfectly to the heat stress, it exhibits transient molecular memory and acquired thermotolerance. It is protected from the instant thermal upshifts when pretreated with mild shock. The system will exhibit a general heat shock response even for slow continuous temperature upshifts following

adaptation to a mild heat shock. Taken together, a experimentally verified model is presented that describes the molecular mechanism activated during a heat shock in the human fungal pathogen. The predictions of the model are discussed that describe the situations medically relevant but experimentally not tractable.

3.2. Development of the mathematical model

Heat shock stress initiates the expression of heat shock family genes that is necessary for the adaption to heat challenge [Morimoto, 1993]. In *C. albicans* it results in rapid and transient activation of the heat shock transcription factor Hsf1 (via phosphorylation [Nicholls et al., 2009]) and in induction of specific genes with heat shock elements (HSE) in their promoters, in particular the induction of HSP90 gene. Pharmacological or genetical disruption of the functionality of Hsp90 proteins completely deprives *C. albicans* cells from the ability to adapt to thermal shock [Brown & Leach, 2011]. This observation justifies why Hsp90 is considered to be a key component necessary for downregulation of the Hsf1 activity in the model of thermal adaptation in the fungus. The model was constructed based on the assumption that the chaperone Hsp90 can be present in the cell in three forms: (1) a free form, (2) complexed with transcription factor Hsf1 or (3) complexed with other nonnative proteins. The latter assumption is made on the basis that molecular chaperones participate in the proper synthesis and folding of many proteins [Goldberg, 2003, Young et al., 2004]. Moreover, it is hypothesized that heat shock response can be in fact initiated by damaged proteins that bind Hsp90, what in turn caused Hsp90 dissociation from Hsf1 transcription factor [Sharp et al., 1999]. Free Hsf1 becomes phosphorylated (by some yet unknown protein kinase; this process could be, for instance, govern by a protein kinase C [Sharp et al., 1999]) and becomes transcriptionally activate leading to the induction of the HSP90 gene. Activated Hsf1 binds characteristic HSEs present on the promoters of heat shock family genes, including HSP90. In human cells Hsp90 is a major repressor of mHsf1 activity and reduction of Hsp90, but not Hsp70, strongly activates mHsf1 [Zou et al., 1998, Hegde et al., 1995]. These observations allowed for the construction of the model based on the assumption, that Hsp90 is the major repressor of Hsf1 in *C. albicans*.

The model is consists of a set of ordinary differential equations (ODEs). Time course experimental data are used to find a set of parameters that allows us to generate the desired behavior of the model. The presented simulations qualitatively match the results of the experiments. Furthermore, a sensitivity analysis was performed that and a discussion proceeds of the crucial parameters that govern the overall dynamics in the model. The model is then used to analyze the impact of sequential heat shocks and stepwise heat shocks on the dynamics of phosphorylated Hsf1. Finally, predictions of the model are validated experimentally and discussed.

3.2.1. Structure of the model

A decision was made to construct a model with a low-granularity level. As such, the chaperone Hsp90 either interacts with Hsf1 or it interacts with other client and nonnative proteins, which are indistinguishable molecules in the model. Two forms of Hs1 are included, as it can be present in a phosphorylated state, Hsf1P which is then transcriptionally active, and unphosphorylated Hsf1, which is then inactive. The model accounts for a production of new Hsp90 proteins. In total the molecular chaperone Hsp90 is present in three forms (1) coupled with Hsf1 (Hsf1Hsp90) (2) coupled with nonnative proteins ($\mathrm{Hsp90_{Complex}}$) and (3) free Hsp90. These assumptions are based on the fact that in mammalian cells damaged proteins bind Hsp90 and cause its dissociation from mHsf1 [Sharp et al., 1999, Young et al., 2004]. Moreover, chaperones are necessary to assure proper proteins' folding [Goldberg, 2003]. The structure of the model is presented in Figure 3.2. It is assumed that Hsf1 constantly associates with and dissociates from

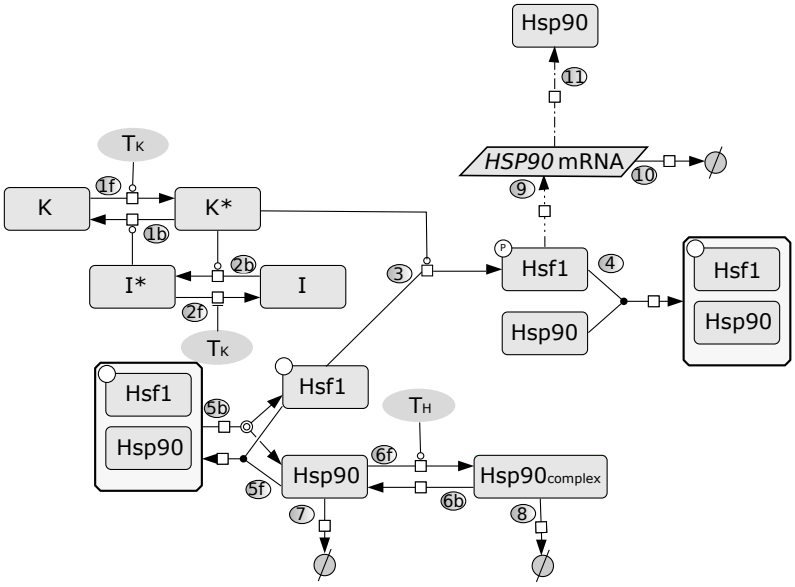

Figure 3.2.: Molecular wiring in the model of thermal adaption in *C. albicans*. Each arrow-ended line in the scheme represents either chemical reaction or mass flow. Positive regulation in the model is depicted with the lines ended with circles and negative regulation with the blind-ended lines. Transcription (9) and translation (11) of HSP90 gene are both represented by dashed lines. $\mathrm{Hsp90_{Complex}}$ represents complexes with vast range of client or unfolded proteins. The unknown protein kinase acting on Hsf1 is included, both in its inactive and active form, K and $\mathrm{K^*}$ respectively. Also active $\mathbf{I}^*$ and inactive **I** form of $\mathrm{K^*}$'s protein phosphatase (leading to $\mathrm{K^*}$ deactivation) is considered. See text for detailed description. I refer in the main text to the numbers in circles when I describe the respective process.

Hsp90 (5_f, 5_b). In the presence of heat shock, which is expressed by the parameter $\mathrm{T_H}$ in the diagram, Hsp90 is recruited for binding with other misfolded proteins (6_f). Hsp90

can also dissociate from these complexes (6_b). Both Hsp90 and $\text{Hsp90}_{\text{Complex}}$ can be degraded (7, 8 respectively). Both degrading processes are not additionally regulated in the model upon thermal insult application. However, there is an indirect regulation. The structure of the model implies that due to an increased $\text{Hsp90}_{\text{Complex}}$ formation the equilibrium shifts and promotes Hsf1 dissociation from Hsp90. Hence, this process increases Hsp90 degradation. Upon heat shock, which is this time expressed by the parameter T_K in the diagram, the unknown Hsf1 kinase K is activated, K^* (1_f) and it activates its own inhibitor **I** (2_b). Active **I** deactivates K^* ($\mathbf{I}^*$, 1_b). Activity of **I** is negatively regulated by the heat shock (2_f). **I** is again an unknown molecule in this model. This module regulates the activity of the kinase K, which is necessary to phosphorylate Hsf1, Hsf1P (3). Activated Hsf1 induces the production of new Hsp90 proteins (9). Newly formed Hsp90 molecules (11), together with the Hsp90 already present in the cell, repress the activity of Hsf1P leading to its dephosphorylation (4). This is a negative regulation of Hsf1 by Hsp90. In the model, a *HSP90*mRNA degradation is included as well (10).

3.2.2. Model formulation and model analysis

A set of ordinary differential equations (ODEs) is used to construct a mathematical model of heat stress adaptation in *C. albicans*. The ODE model describes dynamics of the model state variables whose parameters are determined basing on the time course experimental data. At the end, time response control coefficients are investigated, a type of sensitivity analysis technique that can be used to identify key parameters in the model which are responsible for the overall dynamics. In Table 3.1 I store all the notations that are used throughout. Initial values were determined along with other parameters in the model in the parameter estimation task.

Name	Short description	Value [a.u.]
K	Inactive kinase	$K_0 = 1 \times 10^{-2}$
K^*	Active kinase	$K_0^* = 1 \times 10^{-6}$
I	Inactive inhibitor	$I_0 = 3.56 \times 10^{0}$
I^*	Active inhibitor	$I_0^* = 1 \times 10^{-10}$
Hsf1	Heat shock transcription factor	$Hsf1_0 = 2.05 \times 10^{-4}$
Hsp90	Heat shock protein	$Hsp90_0 = 3.67 \times 10^{-1}$
Hsf1P	Phosphorylated Hsf1	$Hsf1P_0 = 1 \times 10^{-8}$
Hsf1Hsp90	Hsp90 coupled with Hsf1	$Hsf1Hsp90_0 = 1 \times 10^{-2}$
Hsp90Complex	Hsp90 bound to unfolded proteins	$Hsp90_{Complex_0} = 5.02 \times 10^{-1}$
*HSP90*mRNA	mRNA	$HSP90\text{mRNA}_0 = 3.53 \times 10^{-1}$

Table 3.1.: State variables in the model with initial values. Initial conditions were estimated together with other model's parameters during the parameter estimation. For this purpose time course experimental data presented later in Figure 3.6b and Figure 3.7b were used.

Restrictions in the model

Heat stress is implemented in the model as activation of the protein kinase K which then triggers Hsf1 phosphorylation. Activation of K is triggered via changes in parameter T_K. During the heat shock, denatured or misfolded proteins accumulate and bind Hsp90. Very likely this eventoccurrs at a rate different from T_K. Therefore a parameter T_H is included which describes the process of Hsp90 sequestration. When simulating the heat shock, both T_K and T_H are varied simultaneously. Their numerical values are determined based on the dynamical behavior of the system whose parameters are fitted to the experimental data.

In the mathematical model of heat stress adaption the events represented by the parameters T_K and T_H are of equal importance. Neither of the events alone is sufficient to cause Hsf1 phosphorylation (Figure 3.3). If we, for instance, block the activation of an unknown kinase K and then we apply a heat stress, there is no phosphorylation of Hsf1 observed in the model, a proxy for Hsf1 transcriptional activity, Figure 3.3a. The same holds for the formation of Hsp90 complexes with unfolded proteins. If there is no Hsp90 sequestration for binding damaged proteins it also results in no phosphorylation of Hsf1 (Figure 3.3b).

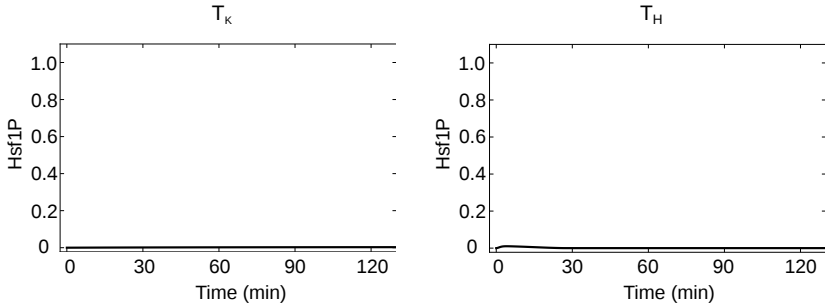

(a) Blocked activity of Hsf1's unknown kinase K prevents Hsf1 from being phosphorylated.

(b) No Hsp90 sequestration for complexing with its client or unfolded proteins preclude Hsf1 from being phosphorylated.

Figure 3.3.: T_K and T_H parameters trigger cells' stress response. Both processes, activation of the Hsf1's kinase and Hsp90 binding of unfolded proteins are required for Hsf1 phosphorylation in the model.

Following assumptions were made when constructing the model:

- constant concentration of the transcription factor $[\text{Hsf1}]_{\text{TOTAL}} = [\text{Hsf1Hsp90}] + [\text{Hsf1}] + [\text{Hsf1P}]$;
- the system to be in a homeostatic state before temperature upshift, which allowed us to set the model to a steady state in unstressed conditions and thus reduce the number of parameters that had to be estimated;

- following relation: $Hsf1Hsp90_0 < Hsp90_0 < Hsp90_{Complex_0}$;
- and also the amount of inactive kinase to be close to the amount of Hsf1 coupled with Hsp90, $K_0 \approx Hsf1Hsp90_0$.

Along with these assumptions it is proposed that Hsp90 is a key molecule responsible for the downregulation of phosphorylated Hsf1 during the thermal insults in *C. albicans*. The structure of the model is consistent with this idea as any disruption in Hsp90 production, or in proper chaperone's activity, deprives the cells from the ability to adapt to temperature upshifts (Figure 3.4).

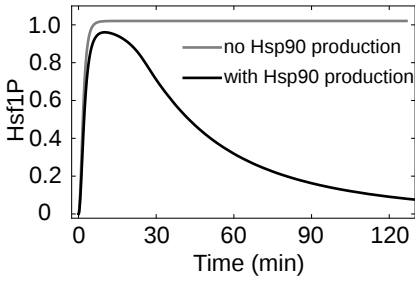

Figure 3.4.: Hsp90 controls Hsf1P levels. Hsp90 is necessary to downregulate Hsf1 activity in the model. (Solid black line) The model with Hsp90 production is able to adapt to thermal shift. (Solid grey line) The model with completely blocked production of Hsp90 implemented is not able to adapt to thermal shock and Hsf1P levels stay high.

Description of the model in mathematical terms

The proposed wiring in the molecular mechanism is described by a set of ordinary differential equations and the reaction kinetics are modeled using mass action and Michaelis-Menten equations (see Tables in Appendix A). Initially, there were twenty-two unknown parameters in the model but the assumption on homeostatic state reduced this number to fifteen. Furthermore, there is no database for *C. albicans* or any *Candida* species with information of molecules copy number per cell, that would allow us to better approximate the model's initial conditions. Hence, they were estimated along with other parameters using the tool COPASI [Hoops et al., 2006] and its inbuilt Evolutionary Programming task that minimizes the sum of square roots of the distance between experimental data points and model simulation results. During the estimation task the initial levels of Hsf1, Hsf1P, K^*, I and I^* were assumed to be insignificant. The model equations, the kinetic rate laws and parameters values are given in Appendix A.

Sensitivity analysis.

In order to understand the contribution of individual reaction parameters to the system's dynamics sensitivity analysis was performed. This technique facilitates the understand-

ing of action of the mathematical model and directly points at the set of most important parameters in the considered dynamical system. In other words we obtain information on which parameters govern the dynamics of the system. Metabolic control analysis (MCA) is the classical approach to study sensitivity of the model. In general, sensitivity analysis shows the differences in steady state concentrations of different state variables in the model upon infinitesimally small changes in the individual reactions, e.g., changes in parameters values, initial state variables or reaction enzymes concentrations. MCA was initially developed to investigate the metabolic networks but with time it has also found applications in sensitivity analysis of signaling pathways or gene regulatory networks. Using MCA, we can only look at influence of single parameter's small change on the steady state concentrations of state variables. Here, the aim was to look at the single parameter perturbations and their influence on networks dynamics. It was interesting to look at the deviations along the entire trajectory of a considered state variable rather then effect of the perturbations on a steady state. An approach developed specifically for such purpose was used, it is called time-varying response coefficients (RCs). Similar to MCA, when analyzing RCs of state variables we can see which reactions or parameters influence systems' dynamics the most. As first I use a formula for non-scaled response coefficients following the mathematical description [Ingalls & Sauro, 2003]:

$$R_p^S(t) = \frac{\partial S(t,p)}{\partial p}\bigg|_{p=p_0} \quad \text{with} \quad p = p_0 \cup q_0.$$

In the above formula p_0 is the set of all the parameters in the model and q_0 is the set of initial conditions, S are the state variables. $R_p^S(\cdot)$ is a matrix of a dimension $(\#S \times \#p)$. Below I present a single row from this matrix, namely $R_p^{\mathrm{Hsf1P}}(t)$ which represents the deviations in the dynamics of phosphorylated Hsf1 upon perturbations in the model's parameters. The nominal trajectory, is set to be the time course of phosphorylated Hsf1 simulated with the model for the 42°C heat shock. Following the scheme, I analyze the effect of perturbing each of the parameters from the set p. The analysis is restricted to the time scale of 120 minute which is the same as in the experimental setup. A positive value of $R_{p_i}^{\mathrm{Hsf1P}}(t)$ corresponds to the increase in the levels of phosphorylated Hsf1 upon infinitesimally small increase in p_i. A negative value $R_{p_i}^{\mathrm{Hsf1P}}(t)$ indicates a decrease in the Hsf1P while the parameter's p_i value increases.

In order to be able to compare all the RCs, as next I used scaled RCs which are dimensionless. They were derived according to the formula [Ingalls & Sauro, 2003]:

$$\tilde{R}_p^S(t) = (D^S(\cdot))^{-1} \cdot R_p^S(\cdot) \cdot D^P = \frac{\partial \ln S(\cdot)}{\partial \ln p}.$$

Each $D^X = \mathrm{diag}X$ in the above formula is a diagonal matrix constructed from the coefficients of the vector X. The RCs calculated with respect to the logarithms of the state variables allow us to look at the relative responses and, hence, direct comparison of the RCs for all of the parameters.

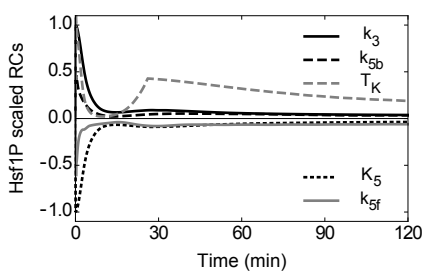

(a) Early response coefficients

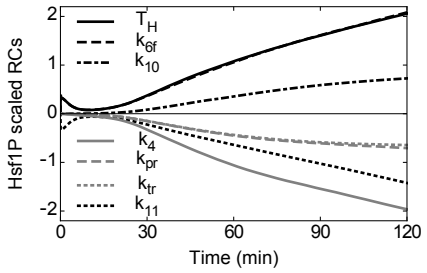

(b) Late response coefficients

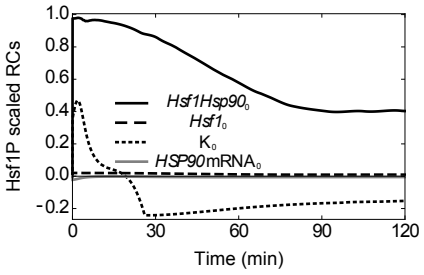

(c) Response coefficients w.r.t. initial conditions

Figure 3.5.: Time varying response coefficients. In the figure, only selected time-varying response coefficients for phosphorylated Hsf1 at 42°C are presented. The response coefficients which are not presented here have only a negligible effect on the phosphorylated Hsf1 dynamics. (a) Early response coefficients. According to their name, they influence the Hsf1P dynamics solely on a short time scale with respect to the scale considered. Here it is within the first 10 minute of the system response to the stress imposed. Infinitesimal perturbation of the indicated parameters will not influence the dynamics of the thermal adaption on a long term. (b) Late response coefficients which influence phosphorylated Hsf1 dynamics starting from 15 minute after stress is applied, leading to significant differences in the phosphorylated Hsf1 concentration at 120 minute time point. For instance, the parameter T_H has a positive RC at 120 minute, which means that an increment in its numerical value will result in higher levels of phosphorylated Hsf1 at 120 minute. (c) Response coefficients calculated for the initial concentrations. An increased amount of initial Hsf1Hsp90 complexes will increase Hsf1 phosphorylation levels throughout the thermal adaptation time scale considered in the model.

In Figure 3.5 selected non-zero RCs are presented. As it was expected, even infinitesimally small perturbations in the phosphorylation reaction (reaction 3) result in the deviations in the phosphorylated Hsf1 from the nominal trajectory. Hence, $R_{k_3}^{\mathrm{Hsf1P}}(t)$ is a positive RC that shows the most effect in the first minutes of the simulation. The value of $R_{k_3}^{\mathrm{Hsf1P}}(t)$ at the time point 120 minutes is zero which means, by the time 120 minutes the Hsf1P nominal trajectory and the perturbed one overlap. Therefore the $R_{k_3}^{\mathrm{Hsf1P}}(t)$ RC is classified as an early and positive RC (Figure 3.5a). From the analysis of the reaction of Hsp90 association with Hsf1P which basically governs Hsf1P dephosphorylation (parameter k_4) we observe a negative value of $R_{k_4}^{\mathrm{Hsf1P}}(t)$ at the time point $t = 120$ minutes. Moreover, $R_{k_4}^{\mathrm{Hsf1P}}(t)$ is a negatively valued and constantly decreasing function during the simulation, with a significant decrease starting from about 15 minutes after application of the stress. This classifies the $R_{k_4}^{\mathrm{Hsf1P}}(t)$ as a late RC (Figure 3.5b). Any increase in the parameter k_4 value results in lower levels of Hsf1 phosphorylation throughout the time scale considered. It was natural to assume that an increase in the initial levels of Hsf1 would result in higher levels of Hsf1 phosphorylation. Interestingly, $R_{Hsf1_0}^{\mathrm{Hsf1P}}(t)$ has little effect on the final outcome in the thermal adaptation process (Figure 3.5c). Similar result held for $R_{Hsp90_0}^{\mathrm{Hsf1P}}(t)$ but it is not presented in the (Figure 3.5).

In the model, some of the state variables are degraded, i.e., Hsp90 protein and $\mathrm{Hsp90}_{\mathrm{Complex}}$ as well as *HSP90*mRNA. These degradation reactions are not directly regulated by the thermal up shift. However, the increased rate of formation of the complex Hsp90 with other proteins, due to temperature change, promotes Hsp90 degradation. Sensitivity analysis showed that, in the model, Hsp90 protein turnover has little impact on Hsf1P dynamics. However, complex formation between Hsp90 and unfolded proteins influences Hsp90 protein degradation indirectly and thereby effects Hsf1 phosphorylation (parameter $\mathrm{T_H}$, k_{6f}, Figure 3.5b). This implies that the indirectly increased degradation of Hsp90, via shift of the mass balance, also influences Hsf1P levels. The *HSP90*mRNA degradation has less impact on Hsf1P and only some time after the application of the stress (parameter k_{10}, Figure 3.5b).

In summary, negative regulation of Hsf1P via binding to Hsp90 (k_4), formation of Hsp90 complexes with other proteins ($\mathrm{T_H}$, k_{6f}) or production of Hsp90 (k_{11}, k_{tr}) are the processes in the model that influence the most the dynamics of Hsf1 phosphorylation. Remaining parameters have only a minor effect, for instance, *HSP90*mRNA processing (k_{10}, k_{pr}). Parameters not presented here have negligible effect on the levels of phosphorylated Hsf1 within the considered time scale.

3.2.3. Data and dynamics of the model

The structure of the model is based on knowledge on the molecular mode of action of heat shock response in other organisms [Rieger et al., 2005, Morimoto, 1993, Ali et al., 1998, Morimoto, 1998]. The mathematical model is supported with kinetic data experimentally determined for Hsf1 phosphorylation levels for both 30°C to 37°C and 30°C to 42°C heat shocks (Figure 3.6). The activation of Hsf1 is absolutely necessary to induce heat

shock family genes [Nicholls et al., 2009]. Hence, also the dynamics of *HSP90*mRNA followed again during both 30°C to 37°C and 30°C to 42°C heat shocks (Figure 3.7).

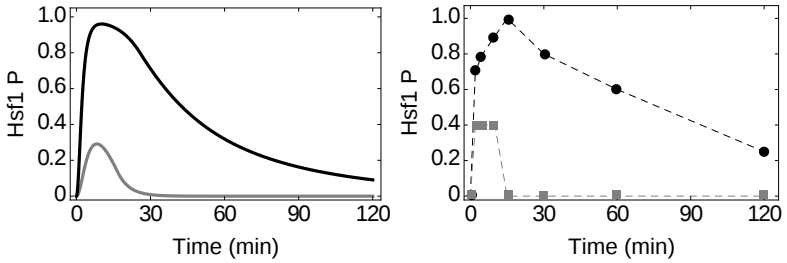

(a) Model simulations **(b)** Experimental data

Figure 3.6.: Temporal changes in Hsf1 phosphorylation levels upon exposure to the heat shock. Model simulations and experimental observations are confronted. (a) Simulated time course of Hsf1 phosphorylation levels during 30°C-37°C and 30°C-42°C heat shocks (grey and black solid lines respectively). (b) Representation of the experimentally determined phosphorylated Hsf1 levels during 30°C-37°C and 30°C-42°C heat shocks (grey dots and black dots respectively).

Experimental data indicate rapid and transient phosphorylation of Hsf1 during both 30°C to 37°C and 30°C to 42°C heat shocks. Phosphorylation of the Hsf1 is much prolonged and reach higher levels when cells are experiencing severe stress (Figure 3.6b, black). Nevertheless, the cells adapt to both thermal upshifts and eventually the heat shock response becomes completely downregulated. Downregulation of the heat shock rsponse is viewed here as a loss of Hsf1 phosphorylation levels. Experimental data for *HSP90*mRNA induction in both stresses were also collected. Exposure of the cells to 30°C-37°C heat shock resulted in three-fold *HSP90*mRNA increase relative to the control (Figure 3.7c). In line with higher Hsf1 phosphorylation, a 30°C-42°C heat shock caused stronger *HSP90*mRNA induction (Figure 3.7b, black line).

Parameters of the model were determined using these kinetic data. Despite of minimal structure of the model it satisfactory reproduces the dynamics of phosphorylated Hsf1 levels and *HSP90*mRNA induction in both considered ambient temperatures (Figures 3.6, 3.7). In order to reduce the model complexity to minimum some of the processes were excluded from the consideration, for instance, the Hsf1 production.

Constant total concentration of Hsf1

Experimental results obtained for this study indicate that the candida cells are able to adapt to the thermal challenge. Hsf1 is rapidly phosphorylated and then it is gradually dephosphorylated down to the levels which are not detectable in the experiments. Previous studies revealed that *C. albicans* cultures grown in different temperatures differ in total Hsf1 levels [Nicholls et al., 2009]. In all cases examined the trend was that the total

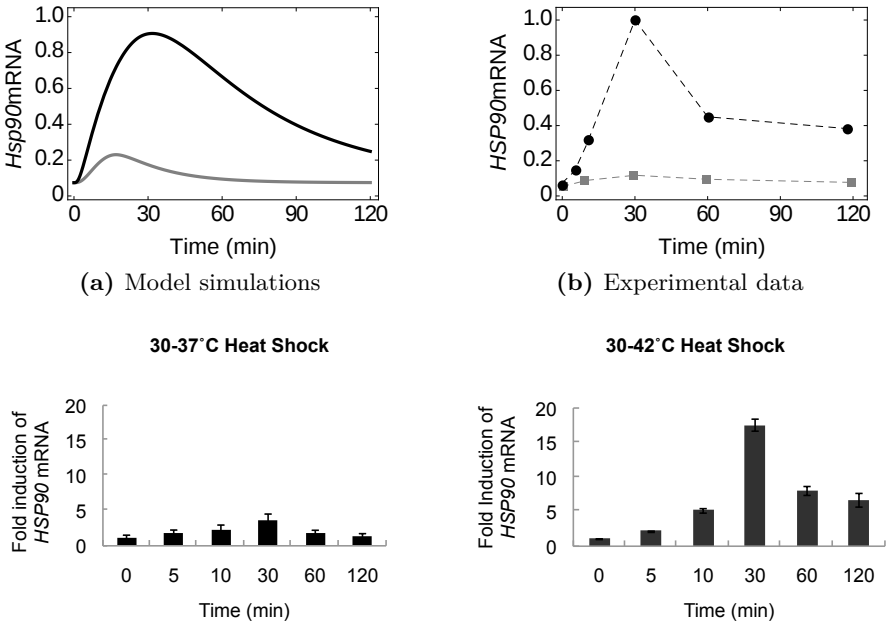

(a) Model simulations **(b)** Experimental data

(c) Experimental raw data **(d)** Experimental raw data

Figure 3.7.: Temporal changes in *HSP90*mRNA levels upon exposure to the heat shock. Model simulations and experimental observations are confronted. (a) Simulated time course of *HSP90*mRNA induction during 30°C-37°C and 30°C-42°C heat shocks (grey and black solid lines respectively). (b) Representation of the experimentally determined *HSP90*mRNA levels during 30°C-37°C and 30°C-42°C heat shocks (grey dots and black dots respectively). (c,d) Figures adapted from [Leach et al., 2012]. Experimental raw data for *HSP90*mRNA fold induction relative to the control (*ACT1*mRNA) in both heat stresses.

amount of Hsf1 in the cells increases with the growth temperature and no phosphorylation of Hsf1 is detected in steady state cultures. In this study only a 120 minute time scale was examined for the analysis of thermal adaptation's dynamics. This corresponds to a maximum of two generations of cells. An increased cells numbers could be a source of increased total Hsf1 levels in the experimental results. Thus in the following I check how the theoretical increase in Hsf1 levels would impact the dynamics of the model if it was included (Figure 3.8). To do that, I double the amount of the total Hsf1 in the mathematical model after 120 minute of 42°C thermal shock application. Interestingly, such operation does not drastically change the simulated dynamics of phosphorylated Hsf1 and also in such scenario Hsf1 activity is going to be downregulated to zero (not shown in the Figure 3.8).

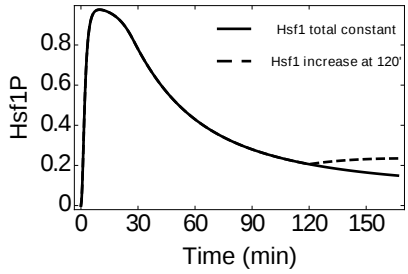

Figure 3.8.: Variations in the total amount of Hsf1 in the model. (Solid line) Dynamics of Hsf1 phosphorylation in 30°C-42°C heat shock when not considering changes in the total Hsf1 concentration. (Dashed line) A rapid increase in total amount of Hsf1 in the model at 120 minute time point after application of 30°C-42°C thermal shock.

Perfect adaptation to thermal insults

The experimental data in combination with the mathematical model argue that heat shock response exhibits perfect adaptation. It is based on the system's behavior where even if the stimuli remains present, the activity of the key molecule in the system, which is here considered to be phosphorylated Hsf1, becomes eventually downregulated to basal levels. This would explain why the authors in the study [Nicholls et al., 2009] observed an increase of total Hsf1 amount in the cells along with an increase of growth temperatures, ranging from 15°C to 40°C, but they have never observed phosphorylated Hsf1 in any of the growth temperatures after cells have adapted to it. The model presented in this chapter implies that for each of the growth temperature tested in the study there must be a rapid Hsf1 phosphorylation. However, this is always a transient activation which is going to be downregulated to the basal levels after the cells have adapted to the thermal insult.

Sequential heat shocks

For some organisms exposure to a mild stress results in an increased resistance to a severe stress, which might also be of other type. In this context, application of the severe stress, without pretreatment, would normally lead to a death of the organism. As an example, *C. albicans* is protected by high oxidative stress when previously subjected to a mild heat shock and the cells' resistance results in about two fold survival increase [Enjalbert et al., 2003, Gonzalez-Parraga et al., 2010]. Similarly, an exposure of *C. albicans* to a mild heat shock increases cellular resistance when afterwards subjected to a severe heat shock [Arguelles, 1997]. Such increased resistance is referred to by acquired thermotolerance. Systems that display acquired thermotolerance were also observed in other organisms, e.g., in mammalian cells [Li et al., 1982a, Li et al., 1982b], *Drosophila* cells [Petersen & Mitchell, 1981] or baker's yeast *S. cere-*

visiae [McAlister & Finkelstein, 1980]. In this study an increased *C. albicans* cells resistance is viewed as kinetic changes in the molecular system activated during the stress that prepare pretreated cells to extreme situations. In the mathematical model of heat shock adaption the occurrence of acquired thermotolerance is investigated by looking at the dynamics of phosphorylated Hsf1. An acquired thermotolerance may also be a tran-

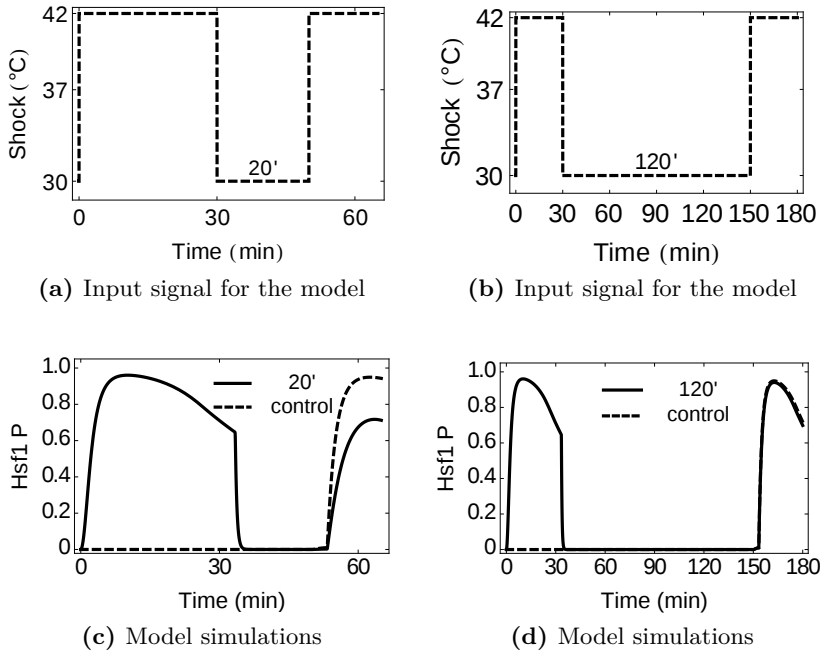

(a) Input signal for the model **(b)** Input signal for the model

(c) Model simulations **(d)** Model simulations

Figure 3.9.: Sequential heat shocks. Predicted behavior of the system during second 30°C to 42°C heat shock pretreated with 30 minutes of the same heat shock strength with two various recovery time intervals of 20 minute and 120 minute. The model predictions were experimentally tested by western blotting of extracted phosphorylated Hsf1 at different time points during the second heat shock. (a,b) Schematic representation for the thermal insult with 20 minute and 120 minute recovery time respectively. (c) Simulations of the model for the input with 20 minute recovery time. Solid black line corresponds to the situation were cells undergo two consecutive shocks. Dashed black line corresponds to the system with no prior heat shock treatment. These are control cells used for comparing relative changes in Hsf1 phosphorylation when subjected to a second heat stress. (d) Simulations of the model for the input with 120 minute recovery time. Solid black line corresponds to the situation were cells are pretreated with 30 minute 30°C to 42°C heat shock. Dashed black line corresponds to the system with no prior heat shock treatment.

sient effect of the cells' pretreatment and as such it is referred to in terms of molecular "memory". In Figure 3.9 it is analyzed whether the system exhibits a molecular memory by separating two heat shocks of the same strength by giving the cells either 20 minutes or 120 minutes for recovery. The mathematical model predicts that in *C. albicans* the

aqcuired thermotolerance correlates with lower phosphorylation levels of Hsf1 during the second heat shock. The model was used to simulate the scenario were cells are exposed

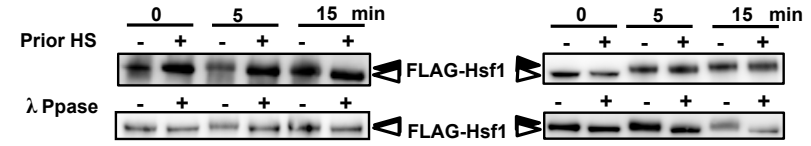

(e) Experimental data

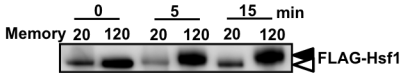

(f) Samples' comparison

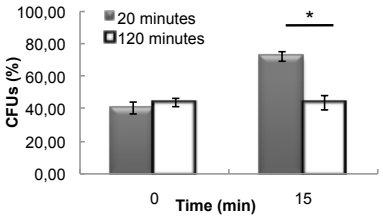

(g) Cell viabilities

Figure 3.9.: Sequential heat shocks, Figure continues. Figures adapted from [Leach et al., 2012]. (e) Exponentially growing cells in 30°C were subjected to 42°C heat for 30 minutes. Afterwards they were placed back at 30°C for 20 minutes (Left) and 120 minutes (Right) prior to a replacement into 42°C heat shock. During the second heat shock proteins were extracted and Hsf1 phosphorylation levels were measured by western blotting (upper panel). Included are lambda phosphatase (λ Ppase) controls (lower panel) to assess Hsf1 phosphorylation changes in the second heat stress. In the upper left panel we observe a band shift and λPpase controls in the lower left panel only assure that these shifts are indeed due to phosphorylation. The λPpase detaches the phosphate groups from proteins it is run on. Again shift differences in the λPpase controls indicate reduced phosphorylation during the second stress. In the upper right panel we do not observe any band shifts and also additional control (λ Ppase, lower right panel) displays no band shifts and hence the conclusion of equally phosphorylated Hsf1 in both conditions. (f) Samples from the experiments with 20 and 120 minute intervals between subsequent heat shocks compared along side. Much more intense bands in samples that were given 120 minute recovery time can be seen. These indicate stronger Hsf1 phosphorylation when 120 minute break is given and hence, in conclusion a loss of molecular memory is observed. (g) Acquired thermotolerance corresponds to increased resistance upon exposure to a second stress. Cells that are given 20 minutes recovery time (grey bars) exhibit increased cellular resistance to a second heat stress (compare 0 with 15 minute time point in the presence of the second heat stress). The feature is lost when cells recover for 120 minute (white bars).

to 30°C to 42°C heat shock for 30 minute. Next they are being placed back into 30°C for either 20 minute or 120 minute and after that time again 30°C to 42°C heat stress is applied. Always phosphorylated Hsf1 dynamics in the model are followed in order to later claim whether the model develops thermotolerance or not. It is seen that 20

minute pause before second heat stress application results in a lower phosphorylation of Hsf1 in the second stress with respect to the control cells that experienced the stress only a single time (Figure 3.9c). This prediction was later tested experimentally (Figure 3.9e). Interestingly 120 minute break between two stresses results in a complete loss of the molecular "memory" in the system (Figure 3.9d). During the second stress the model behaves as it would be experiencing the stress for the very first time. There are no differences in the dynamics of phosphorylated Hsf1 simulated for this scenario (Figure 3.9d). This prediction was again verified experimentally (Figure 3.9e).

The system displayed acquired thermotolerance and it was further tested experimentally by looking at the cell viabilities (Figure 3.9g). There was a significant increase in cell viabilities for cells that have experienced prior heat shock and were given 20 minute recovery time (grey bars in Figure 3.9g). This resistance is however lost when 120 minutes are given for the recovery time (white bars in Figure 3.9g). Viability loss could be caused by many factors, trehalose decrease [Arguelles, 1997] or heat shock proteins decrease included. Nevertheless, these observations argue that *C. albicans* develops thermotolerance but the molecular memory in the system is a transient feature that is lost after 120 minutes.

Stepwise temperature upshifts

The natural primary host response to fungal infection is an induction of fever. Thus, as first the dynamics of thermal adaptation in the fungus upon exposure to stepwise temperature upshifts are analyzed that could also be verified experimentally. Cells grown at 30°C where subjected to a 42°C heat shock after 30 minutes preparation phase at 37°C (Figure 3.10).
Cells are able to adapt to an exposure to 37°C thermal insult in less than 30 minutes (Figure 3.10c) and yet the model predicted that cells would again have to adapt to the second instant temperature upshift from 37°C to 42°C (Figure 3.10b). Second heat shock would still cause rapid and transient phosphorylation of Hsf1 until adaptation to new ambient temperature is established. These predictions were verified experimentally. Experimental observations confirmed again there was a rapid and transient phosphorylation of Hsf1 to the 30°C to 37°C thermal challenge and no phosphorylated Hsf1 was detected 20 minutes after exposure to the heat. The second heat shock again resulted in the rapid increase of Hsf1 phosphorylation level followed by its gradual decrease.

Naturally next step is to simulate a situation that is more relevant to *in vivo* situations. The fever development in patients is a process of continuous temperature increase rather than a discrete upshift. Therefore, now I present the simulations of the model where the effect of temperature on the model behavior is driven by a continuous slow temperature increase from 37°C to 42°C over a period of 20 minute, 60 minute, 90 minute and 180 minute (Figure 3.11a). In all the tested scenarios we can observe a transient phosphorylation of Hsf1 (Figure 3.11b, perfect adaptation in all cases is seen but exceeds the presented time scale). As a consequence, we can hypothesize that a tran-

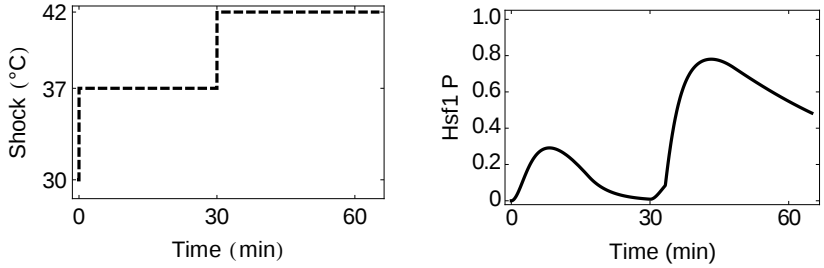

(a) Input signal for the model **(b)** Model simulations

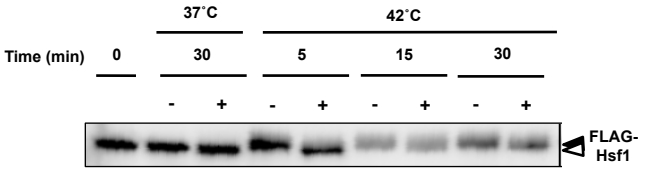

(c) Experimental observations

Figure 3.10.: Stepwise heat shocks. (a) Schematic representation for the thermal insults. (b) Simulations of the model when experiencing the thermal challenge as indicated in (a). (c) Figure adapted from [Leach et al., 2012]. Included are lambda phosphatase controls to assure adaptation by 30 minutes of the first heat stress and rapid Hsf1 phosphorylation in the second heat stress. (-) Samples from not stressed cells. (+) Samples from cells that experienced heat stress. For instance, for 30 minute point both (-) and (+) samples are level that assures that in the cells treated with 37°C there is no Hsf1 phosphorylation at 30 minute time point.

sient phosphorylation of Hsf1 that follows thermal adaptation would always take place even when considering *in vivo* systems. It is in line with a mouse model of systemic *Candidiasis*, where Hsf1 activation is absolutely necessary for the full virulence of the microbe [Nicholls et al., 2011].

3.2.4. Rejected models

Before the final version of the model was established (presented in Figure 3.2) other model structures were considered. However, model simulations, predictions and litera-

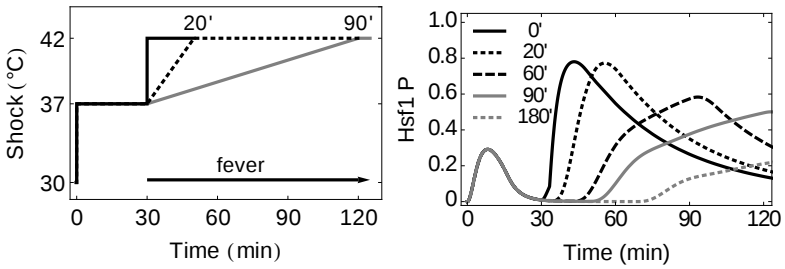

(a) Input signal for the model **(b)** Model simulations

Figure 3.11.: Slow temperature increase. Model driven predictions to continuous temperature increase from 37°C to 42°C over a period of 20 minute, 60 minute, 90 minute and 180 minute after 30 minute 30°C to 37°C heat stress. (a) Scenario for the ambient temperature. We first let the system adapt to a 30°C to 37°C heat stress and then simulate slow thermal increase up to 42°C. (b) Simulations of the model. Hsf1 becomes phosphorylated in all the scenarios tested and systems displays perfect adaptation to thermal insults in all of the conditions (not shown in the figure).

ture gradually led us to include or exclude specific steps. Below, I discuss the workflow shortly as it provides us with an example of how the modeling process work (see also Figure 1.1).

Model 1.

Model 1 (Figure 3.12) was the very first representation of molecular mechanism describing heat shock response in *C. albicans*. The most important differences with the final model, which is presented in Figure 3.2, are: (i) the state variable R^* for ribosomal activity and (ii) two distinguishable Hsf1Hsp90 complexes. Two distinct Hsf1Hsp90 complexes, one from before application of the stress (Hsf1Hsp90) and one that is formed after the stress was applied (Hsf1Hsp90:st). In principle, Hsf1Hsp90:st represents the complexes where the Hsf1 that binds Hsp90 after the heat shock application stays for some time in this complex as it is not immediately ready for its re-phosphorylation (reaction 9 in the model 1). The remaining part of the model 1 shares the description of the final model presented in Figure 3.2.

Three forms of Hsp90 are considered: (i) the free form Hsp90, (ii) in a complex with unfolded proteins $\text{Hsp90}_{\text{Complex}}$ and (iii) in a complex with a heat shock transcription factor Hsf1Hsp90. Hsf1 constantly associates and dissociates from the complex with Hsp90 (5). At elevated temperature protein kinases K are activated (1p) and bind free transcription factor forming a complex Hsf:K^* (2) and causing phosphorylation of Hsf1 (3). The transcriptional activity of Hsf1P can be repressed by binding the chaperone Hsp90 and forming a complex Hsf1Hsp90:st (4). This inactive complex can be then restored in the pool of Hsf1Hsp90 (9). The restoration process, according to

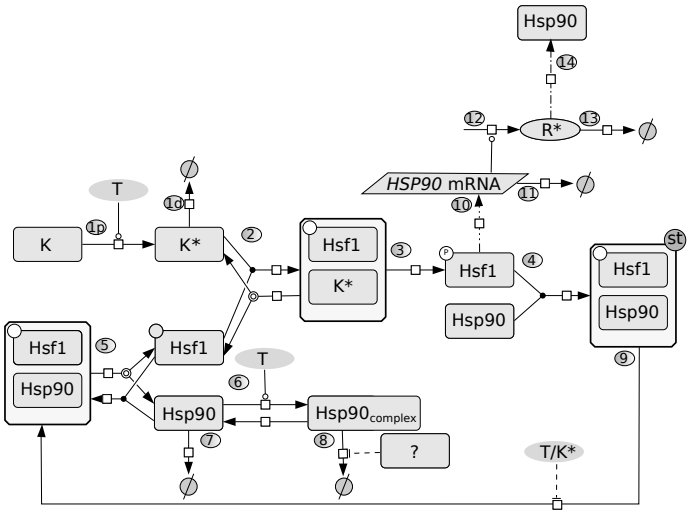

Figure 3.12.: Model 1. Molecular wiring in the model 1 of thermal adaption in *C. albicans*. Lines ended with circles indicate positive regulations and blind-ended lines negative regulations. Hsp90Complex represents complexes with unfolded proteins. Included is unknown Hsf1's protein kinase, in both its inactive and active form K and K^*. Reaction 9 in the scheme is indicates the time needed for Hsf1 before it is again functional and transcriptionally active. Reaction 8 describes heat regulated Hsp90 degradation. R^* in the diagram represents ribosomal activity responsible for Hsp90 translation from *HSP90*mRNA.

the mathematical model, is negatively controlled by the heat shock. The Hsf1P induces the transcription of *HSP90*mRNA (10). The *HSP90*mRNA is also degraded (11). R^* indicates the ribosome's activity. In the presence of *HSP90*mRNA the ribosomal activity increases (12) and produces Hsp90 (14). Afterwards it is inactivated (13) and Hsp90 is also degraded (7). During the heat shock, Hsp90 together with other proteins from the family of heat shock proteins binds unfolded proteins and protects them (6). Here $\mathrm{Hsp90_{Complex}}$ is the pool of Hsp90 in a complex with other misfolded proteins. Hsp90 can also dissociate from these complexes. There is degradation of the $\mathrm{Hsp90_{Complex}}$ included (8).

The model described here was able to reproduce the dynamics of the experimental time course data presented in Figure 3.6b and in Figure 3.7b. The model 1 predicted a molecular memory in the system. The simulations indicated that this memory is lost when120 minutes is given for the system as a recovery time before application of the second 30°C to 42°C heat shock (see Figure 3.13d). Another predictions of the model was that it develops resistance to a second instant shock when no recovery time is in between, a stepwise heat shock. In other words, the system is protected from instant shift to a higher temperature when pretreated with 30°C to 37°C 30 minute heat shock (Figure 3.14). However, experiments did not confirm this prediction. Even

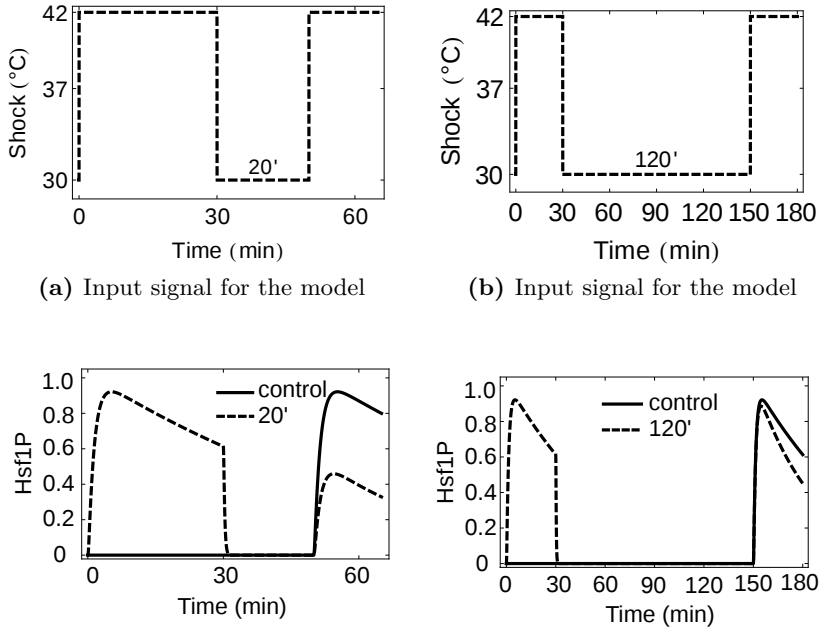

(a) Input signal for the model **(b)** Input signal for the model

(c) 20 minute pause **(d)** 120 minute pause

Figure 3.13.: Sequential heat shocks. (a, b) Schematic representation for the thermal insult with different recovery times. (c, d) Simulations of the model for the scenario in (a, b) respectively. (Dashed lines) Cells are experiencing the heat shock twice. (Black lines) System with no prior heat shock treatment.

though the experimental data confirmed there is, to some extent, a protection from second immediate more severe heat shock (Figure 3.10c), this acquired thermotolerance would still result in Hsf1 phosphorylation, which is in contrary to no phosphorylation at all displayed by the model 1 (Figure 3.14). Because of this experimental result, the structure of the model 1 had to be revised what led us to the structure of the model 2.

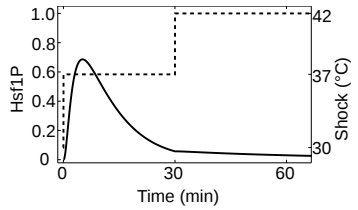

Figure 3.14.: Stepwise heat shock. Simulation of the model when the system is experiencing thermal challenge as indicated by dashed line. The system is protected from the second instant thermal insult since no phosphorylation of Hsf1 is observed in 42°C. Based on this simulation the model structure was consequently rejected.

Model 2.

Rejection of the model 1 (Figure 3.12) led us to the schematic structure of the model 2 presented in Figure 3.15.

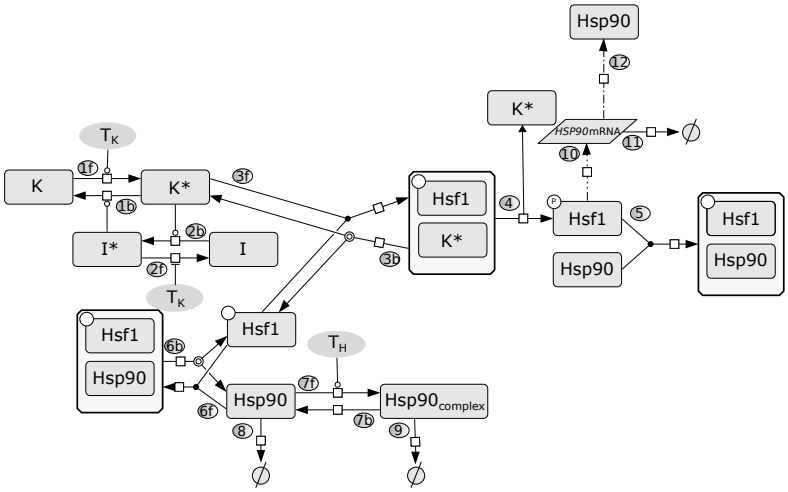

Figure 3.15.: Model 2. Molecular wiring in the model 2 of thermal adaption in *C. albicans*. Each arrow-ended line in the scheme represents either chemical reaction or mass flow. Positive regulation in the model is depicted with the lines ended with circles and negative regulation with the blind-ended lines. Hsp90Complex represents complexes with vast range of client and/or unfolded proteins. In addition to already presented in the model 1 (Figure 3.12) unknown Hsf1's protein kinase (inactive and active form K and K^*) we include active I and inactive I^* form of K's protein phosphatase (leading to K^* deactivation).

As first, ribosomal activity was excluded from the model (R^* in Figure 3.12). Also, instead of regulating Hsp90 degradation rate upon heat stress a decision was made to regulate kinase K activity via inclusion of an unknown protein - I - along with its active state - I^* - that together control the levels of K^*. The whole module is dependent on the heat stress. The possibility was excluded that the Hsf1Hsp90 complexes which can be formed before and after the stress application differ structurally. Therefore, they are indistinguishable in the model 2 and hence, reaction 9 in the model 1 was deleted (Figure 3.12).

Model 2 exhibits a very much similar qualitative dynamical behavior when compared with the final version of the model previously discussed in this chapter (Figure 3.2). Model 2 responds in similar fashion to stepwise heat shock as well as when subjected to sequential heat shocks. It does display molecular memory and also here, the memory effect is lost when 120 minute pause is given between two subsequent 30°C to 42°C heat shocks (not presented). However, we decided on the model presented in Figure 3.2 as it further reduces the complexity of the model structure due to exclusion of the Hsf1 complex with its active kinase K^* that catalyses Hsf1 phosphorylation. In the final

model, we substituted three mass action reactions (reaction 3_f, 3_b and 4 in the model 2 (Figure 3.15)) with a single Michaelis-Menten reaction (reaction 3 in model (Figure 3.2)). Hence we also decreased the number of unknown parameters by one. The equations of the model 2, kinetic rate laws and parameters values are given in Appendix A at the end of the thesis.

3.3. Discussion

A fundamental feature allowing eukaryotic cells to survive in the fluctuating environment is their ability to adapt to these fluctuations. Among other stress responses typical to eukaryotic cells, *C. albicans* has also retained heat shock response. The core of this response involves the activation of heat shock transcription factor that induces genes from the family of heat shock proteins. These chaperones are important in the cell as they are able to protect vast range of proteins from denaturation. Hence, it is important for the cell to produce more chaperones that are ready to protect the inner content of the cell in the presence of heat stress. The study presented in this chapter is one of the first attempts to use the systems biology approach to understand heat induced stress response in a human fungal pathogen.

An existing model of heat shock response in mammalian cells could potentially serve as a tool for our study [Rieger et al., 2005]. It did not however include Hsp90, although it was reported that Hsp90 represses mHsf1 activity in mammalian cells [Zou et al., 1998]. Also in *S. cerevisiae*, fully functionally Hsp90 is necessary to downregulate heat induced response of the cell [Duina et al., 1998]. Taking into account these published evidences model is centered around the assumption that Hsp90 is a key molecule responsible for *C. albicans* adaptation to heat stress. While proposing the model structure, the possibility that there might be other factors that regulate heat stress response can not be excluded. Novelty of the mathematical model presented here is in the inclusion of a module with kinase and phosphatase acting on Hsf1. Not much is known about these two and also no signaling pathway with Hsf1 as a final effector is known to the community. Experimental data indicate complete dephosphorylation of Hsf1 within ten minutes after replacement of the cells back to 30°C. In the model, following shift from 42°C to 30°C, Hsf1 activity downregulation is governed by Hsp90 which are no longer sequestered for binding nonnative proteins. It appears that downregulation of the Hsf1's kinase activity is not essential at this point. However, downregulation of this active kinase, K^*, is required for the memory effect in the system. Taken together, it can be argued for an activity of some, yet unidentified, phosphatase during the process. Interestingly K activity is not the only variable in the model responsible for the feature of acquired thermotolerance. As experimentally verified, given 20 minute pause between the two sequential strong heat shocks, simulations show phosphorylation of Hsf1 but to a smaller degree compared to the cells that have experienced the shock only once. Giving 120 minute recovery time for the cells is enough for them to lose the acquired thermotolerance. This

leads us to the conclusion that 120 minute is enough for the whole protein degradation and secretion machinery to reestablish the initial homeostatic state in the cell. If we block Hsp90 degradation in the model, the system will lose the property of acquired thermotolerance and there will be no Hsf1 phosphorylation observed upon application of the second heat shock. Taken together, both the unknown phosphatase and Hsp90 are necessary for this phenomenon.

The model of heat stress adaptation predicted several features in the system with fine accuracy:

- Memory effect upon sequential heat shocks which is lost when 120 minutes are given to the system as a recovery time.
- The system shows lower phosphorylation levels of Hsf1 upon experiencing severe heat stress when pretreated with a mild heat shock.
- Simulating slow continuous temperature upshifts always lead to transient activation of Hsf1.

Each of the conditions tested resulted in perfect adaptation of the system. This is consistent with the data that there is no phosphorylation observed in cells that have adapted to the growth temperature [Nicholls et al., 2009] and that Hsf1 activation is required for fungal pathogenic activity [Nicholls et al., 2011].

The mathematical model presented in this chapter is one of the first attempts to model heat shock response in *C. albicans*, the most frequent isolate responsible for majority of human fungal infections. The model will serve as a starting point for studying heat shock response in this human pathogen when increasing its granularity level or when including modules that Hsf1 might interfere with, for instance, metabolic module or other genes induced by Hsf1. It can also serve as a platform for studying heat shock response in other organisms also in mammalian cells.

4. Agent based modeling approach applied to study *Candida albicans* interactions with epithelial cells

This Chapter is based on:

Tyc KM, Klipp E (2011) Modeling Dissemination of Pathogenic Fungi within a Host: A Cartoon for the Interactions of Two Complex Systems.

J Comput Sci Syst Biol S1:001. doi:10.4172/jcsb.S1-001

Interactions of the pathogenic species with the human host are subject of intensive investigation. Opportunistic pathogen species attack their host only when host's conditions have changed. The aim is to understand how the pathogens are recognizing these changes and what processes enable them to infect the host. Via infection the host activates its immune response in order to combat the dangerous species. This is facilitated by a special class of pattern recognition receptors (PRR) present on the surface of the immune cells, which are activated in response to pathogen-associated molecular patterns (PAMPs) [Netea et al., 2008]. Such a view on host-pathogen interactions exhibits very high granularity level. Hence, by zooming-out from that we can capture the general dependencies of the two agents. In order to establish an infection, pathogens have to cross several natural host barriers, each time facing changes in the environmental conditions. Microbes not only have to adapt to the new niche but they also have to respond to a number of host defense responses (temperature upshift due to fever, oxidative stress induced by phagocytic cells, etc.). The pathogenic fungus *Candida albicans* survives because it is able to adapt to variety of conditions. Survival is additionally increased due to fungus' ability to modulate host responses, that enable the pathogen to evade the immune response.

Mathematical models of microbial interactions with the host are of interest to pharmaceutical companies, as they may provide tools for testing diverse drug treatment strategies and predict the results of their application. However, a model, to serve as a tool for medical applications must be of high granularity level and be supported with a large amount of experimental data. The biology of candida infection is not yet completely understood and because the fungus is normally studied in laboratory conditions, we are often away from conditions experienced in nature. Some studies are based on samples taken from patients that suffer from fungal infections. However, by detaching

the pathogen from the host niche we lose a view on mutual dependences in their entire complexity. Modulations in pathogen gene expression patterns are no longer reflecting the situation *in vivo*, i.e., when performing experiments we usually look at one condition, whereas pathogens residing within the host must cope with a multitude of stresses simultaneously. For this reason mathematical models are useful to address this aspect.

In this chapter I apply a method used for studying emergent phenomena. By studying interactions of single cells I investigate biological aspects of the fungus *C. albicans* leading to certain patterns observed in the population. The model presented in this chapter can serve as a tool to investigate host-pathogen interactions. I will start from the description of the pathogen interactions with its human host. I will especially focus on the interactions with the human epithelial cells (which are first to be colonized and lead to *thrush*). Next, I will provide a description of the agent based modeling technique, a practical application and the results.

4.1. Introduction

The yeast *C. albicans* is a normal habitant of the human microflora. The microbe can be present both in yeast and hyphae morphological states, while it is residing in its host without causing any harm. To avoid unnecessary immune response and maintain homeostasis the host has to be able to distinguish between commensal and pathogenic states of the fungus. The colonization of mucosal niche by the fungi is facilitated by a morphological switch and an increased rate of proliferation. The hyphae morphological state is specifically sensed by the epithelium leading to secretion of a group of cytokines by the epithelial cells. This pro-inflammatory response is positively correlated with fungal burden [Moyes et al., 2010]. In more detail, epithelial cells recognize the hyphae form by activating the NF-κB pathway and a biphasic MAPK pathway. Activation of the latter is dependent on the fungal burden and results in an induction of the pro-inflammatory response. Epithelial cells were observed to activate neutrophils (PMNs) which avoid the fungal invasion [Weindl et al., 2007]. On the other side however, immune cells are approaching the pathogen and eliminating it via phagocytosis [Behnsen et al., 2007]. Thus, the whole system is composed of multiple cell types that interact with each other.

The development of mucosal *thrush* can be studied by looking at the dynamics of fungi populations colonizing the epithelial layer. Due to the fact, that the spatial distribution of the cells greatly affects the dynamics of the population growth I decided to apply here a computational method known as agent based model (ABM). Each ABM, as the name suggests, is composed of autonomous agents. This mathematical formalism is increasingly being used to study biological system, where interacting agents infer the systems dynamics. The ABM technique not only allows for testing the rules that define global patterns we seek to understand but it also facilitates inclusion of such processes like ability of an agent to learn or adapt. Agents can also have a memory feature.

With ODE models we can tackle the temporal behavior of diverse signaling pathways

or regulatory networks. While studying molecular pathways with ABM, it is possible to analyze an effect of spatial distribution of molecules in the cell on the systems' dynamics [Hsieh et al., 2010, Pogson et al., 2006, Pogson et al., 2008]. Recently it has been also applied to study a metabolic reaction [Klann et al., 2011]. ABM technique is applied to study systems where multiple interacting cells establish the system's dynamics. It has found applications to study functionality of the immune response [Folcik et al., 2011], granuloma formation [Segovia-Juarez et al., 2004, Warrender et al., 2006], immunotherapy strategies and tumor progression [Pappalardo et al., 2011], drug resistance in bacterial populations [Dugatkin et al., 2008], bacterial chemotaxis [Miller et al., 2010], fungal morphogenesis (this chapter and [Thorne et al., 2007]). It is applied to study social epidemiology [El-Sayed et al., 2012], social behavior (examples in [Elliott & Kiel, 2002]), financial markets, and many others.

The agent-based models are build from modules that form a system of interacting autonomous agents. Such modular structure is an advantage for ABM as we can easily manipulate the granularity level of the investigated system. We can add new agents at any time or change the agents' behavior without modifying the rules of other agents.

The agent-based modeling approach applied to host-pathogen interactions can help us to understand the rules defining cellular interactions and how the environment influences these interactions. By means of ABM we can gain intuition on the studied system and thus plan the experiments appropriately. Emerging live imaging is a bridge between this type of mathematical formalism and biological systems.

4.2. Development of the mathematical model

I have constructed a model, where fungi cells interact with each other and with PMNs from their surrounding. Simulations of this model reflect the process of colonization of the epithelial cells. The model presented in this chapter was constructed basing on the literature and personal communication with the expert's knowledge.

C. albicans feeds on surrounding microflora or dead tissue. In the model I include only two morphological states of the fungi: yeast and hyphae form. It is known that nutrient starvation is a strong signal for initiation of the hyphae development [Biswas et al., 2007]. Hence, in the model a transition between the two morphological states is triggered by the nutrient availability. Hyphae cells are crucial in the invasion of the epithelial cells, which causes the damage [Phan et al., 2000, Wächtler et al., 2011] and stimulates the pro-inflammatory response. Different cytokines are released and act as chemo-attractants for the recruitment of the phagocytic cells to the site of infected tissues. It was shown that PMNs are efficient in killing hyphae [Urban et al., 2006, Wozniok et al., 2008] and are attracted by the hyphae to greater extend than by the yeast [Jacobsen et al., 2012].

I use the ABM formalism to put the above considerations into a single mathematical framework. The freely available tool NetLogo [Wilensky, 1999] is used here for that purpose. Although there were no experimental data available for this project, ranges for

some parameters could have been based on the published evidences. The study presented in this chapter is purely qualitative. Basing on the model results I analyze the impact of hypothetical drug treatment on the population growth and discuss the results.

4.2.1. Structure of the model

In the model fungal cells live on the epithelium and feed on nutrient present there. In order to avoid complete exploitation of the nutrients I include some constant restoration rate in the model. It is also assumed that *C. albicans* cells are interacting with each other and PMNs. PMNs are recruited to the site of infection via signaling molecules released by the epithelium. In addition, following assumptions are made.

- The fungus can alternate between two phenotypic states: (1) It can grow in a yeast form and proliferate (2) but it can also switch morphology and develop germ tubes leading to a hyphae cell development. The morphological transition is governed in the model by a nutritional signal and it is activated when nutrient availability drops below a certain threshold.
- All agents in the model live in a two dimensional world. The world is divided into a grid of patches. Each patch has a certain amount of nutrient the fungus can feed on and its depletion is a starvation signal for the fungus, which is a strong signal inducing morphological switch. Nutrient restoration is allowed.
- In the model, only the hyphae form can cause actual damage to the host. In other words, epithelial cells will respond only to the hyphal form and depending on total hyphae load the strength of pro-inflammatory response can change.
- Nevertheless, hyphae with too long germ tube are considered not to be able to cause damage and are called inactive. Although the germ tube length is not explicitly visualized, there is a parameter included that stores the information of how old the fungal cells are and hence indicate the length of the germ tube.

The model has four predefined sets of agents: yeast, hyphae (active and inactive) and PMNs as it is presented in the Figure 4.1. I assume only the active hyphal form to be dangerous to the host while the inactive form is considered to be harmless.

Figure 4.1.: Agents in the model. Yeast (red), active hyphae (grey) and inactive hyphae (yellow), PMNs (blue). Each agent is an autonomous entity. Its action is explicitly defined by a set of rules strictly associated with each cell type and these are summarized in Appendix B.

On the other side, the host is capable of sensing the dangerous form of the fungus and the epithelium can release a special type of molecules to the environment. These molecules,

called cytokines, act as chemo-attractants to PMNs, which are recruited to the site of infection upon sensing intensity of the cytokine gradient. Hyphae cells present on the epithelium cause damage and the inflammation is induced.

4.2.2. Model formulation

The code of the model is given in Appendix B at the end of the thesis. Parameters are stored separately in Table B.1 and also given in Appendix B.

I started from the development of a minimal model where occurrence of one event initiates another. Hence, we begin with nutrient consumption by yeast cells, which eventually will lead to a drop of nutrient supply below a threshold necessary to trigger hyphae development. Hyphae will induce a pro-inflammatory response upon contact with the epithelial cells. Inflammation leads to the recruitment of PMNs to the system which will kill both types of fungal cells, with an increased specificity toward hyphae cell type. The inflammation in the model is seen in the simulation (Figure 4.2) by a release of green scales appearing gradually around the world. The lighter it gets the more damage occurs at the given spot.

4.2.3. Dynamics of the model

The work presented here is a qualitative study but the model itself can be used for validation of the rules that govern dynamics of considered cell types. There are a number of parameters that together account for the system's dynamics. The crucial parameters are: initial fungal load, expansion of the pro-inflammatory response gradient and as a consequence, the PMNs' chemotaxis. Moreover, I had to incorporate a parameter that corresponds to the efficiency of the fungi phagocytosis and to the way how the PMNs are approaching the pathogen. The PMNs' movement is directed toward hyphae cell type with random deviations from the track in the range $-\frac{\pi}{4}$ rad to $\frac{\pi}{4}$ rad. Below I present the simulation results of the model.

I begin with the analysis of the system when no treatment is applied. I look at four different time points: 0, 400, 500 and 1500 and present the respective snapshots of the simulation in Figure 4.2. Our first observation is that for a given parameter set (see Appendix B) population grows and this process can not be blocked by the activity of PMNs. Moreover, the population of colonizing fungi tends to gather together (see Figure 4.2d) rather than equally distributes over the world. Colonies of *Candida* cells are forming that consist of both cell types as well as both active and inactive hyphae. This could correspond to a development of *thrush*, where immune cells are not able to control the fungi population growth. In order to treat the infection, we would naturally apply appropriate medical treatment. In the following I will test the impact of a hypothetical anti fungal drug on the population growth.

The function of the drug considered here is a reduction of the proliferation rate of the yeast cell type. In other words, by decreasing the fitness of the fungi we increase the

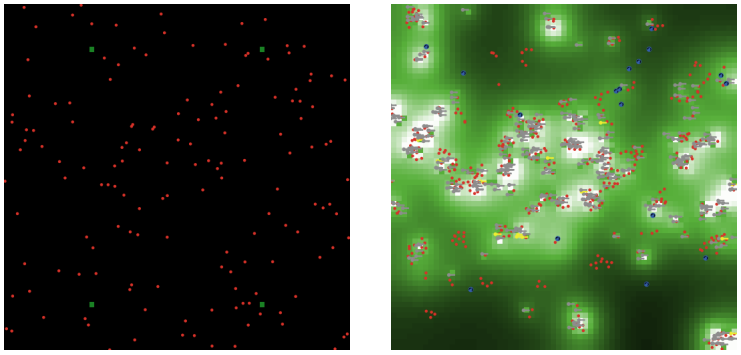

(a) $t = 0$ **(b)** $t = 400$

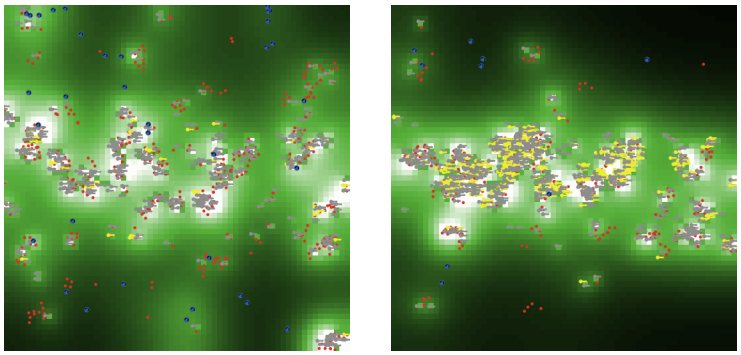

(c) $t = 500$ **(d)** $t = 1500$

Figure 4.2.: Simulation of the model. Arbitrary time units. **(a)** The simulation of the model begins with a pure yeast population (red spots). The four patches marked in green are the portals for PMNs entry to the system. **(b, c, d)** Hyphal cells (gray spots) invade the yeast population and induce an inflammatory response indicated by different scales of green around the world. PMNs are recruited to the system, upon sensing the gradient, to phagocytize the colonizing fungi (blue spots). Yellow spots are the inactive hyphal cells that do not contribute to the inflammatory response.

effort for producing new fungal cells. As previously, I look at the same four different time points: 0, 400, 500 and 1500 and present the respective snapshots of the simulation in Figure 4.3. This time however, the system is challenged with a high dose of a drug, which is supplied at the time point $t = 400$. Based on Figure 4.3 we come to the conclusion that high doses of the drug ultimately clear the infection as no pro-inflammatory response is present at the end of simulation. Although the colonization of the epithelial cells is blocked, yeast cells are not completely gone. Some portion of yeast cells remain in the system (Figure 4.3d). The simple prediction of the model is that via decreasing the fungal fitness, we can in theory block the infection progress. Nevertheless, the drug application will not clear the fungi completely and the treatment would have to continue. Otherwise it would result in recurrent fungal invasion.

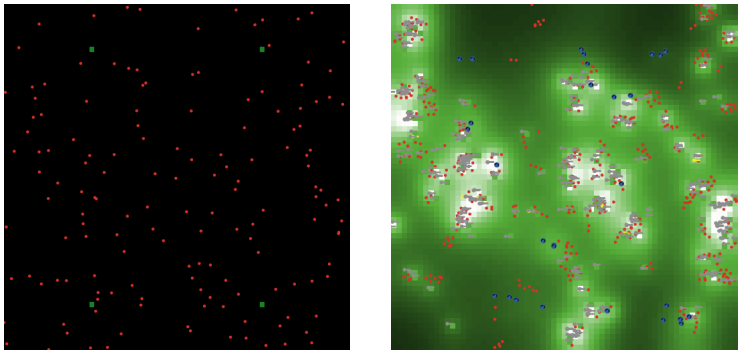

(a) $t = 0$ **(b)** $t = 400$; drug application

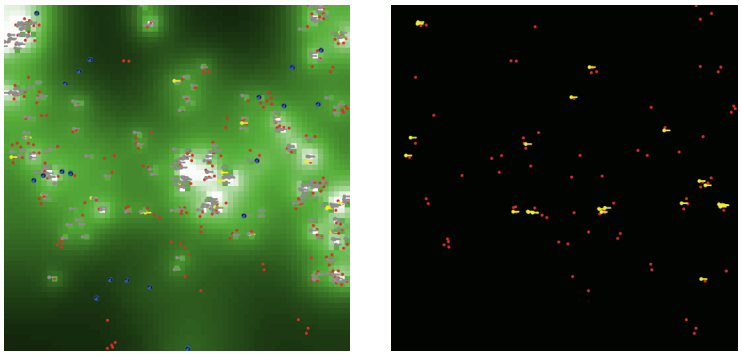

(c) $t = 500$ **(d)** $t = 1500$

Figure 4.3.: Simulation of the model when high-dose of a drug is applied. Arbitrary time units. **(a)** The simulation of the model begins with a pure yeast population (red spots). The four patches marked in green are the portals for PMNs entry to the system. **(b)** At time $t = 400$ I apply a high dose of a drug. **(c)** Already 100 time units after drug application we observe the results of the drug treatment, which triggers a significant decrease in hyphae cells number. **(d)** At the end no active hyphae are present and only yeast cells survive. Some inactive hyphae also can be found.

The simulation results can also be stored as time courses of different cell type numbers throughout the simulation time. To better see the impact of drug application on population dynamics I present the results of both simulations types, untreated and treated, in Figure 4.4. It is now clear that high-dose of a drug applied significantly reduces the population size but the yeast form is sustained.

Next I present to what extent the efficiency of the drug, i.e., its dosage, influences the dynamics of the studied system. Although high-dose of a drug successfully blocks the infections, it might not be an optimal solution for the treatment, due to potential side effects. On the other side, the application of a lower dose of the drug does not clear the fungi. Although through low drug dose application we are able initially to reduce the population size, the population will eventually adapt to the treatment and start again

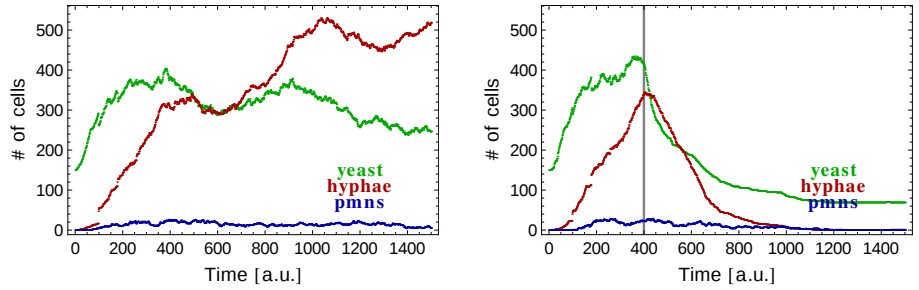

(a) No drug treatment is given

(b) At $t = 400$ a high dose of drug is applied

Figure 4.4.: Comparison of total cells numbers from two simulation types. **(a)** No drug treatment steps are taken. The fungi population size increases and the colonization of an epithelium is successful as the PMNs are not able to block it. **(b)** High dose of the drug blocks the process of colonization. Hyphae cells go extinct but yeast cells stay and reach a steady state.

to grow. This also results in sustained inflammatory response. Additional steps would have to be taken to clear the infection. See Figure 4.5 for illustration.

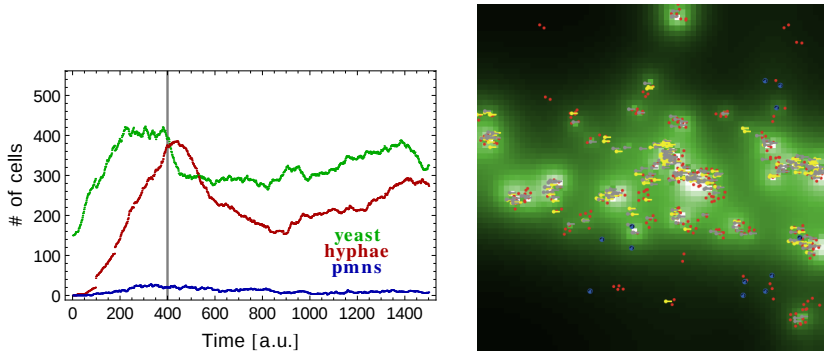

(a) At $t = 400$ a low dose of drug is applied

(b) $t = 1500$

Figure 4.5.: Low dose drug treatment. **(a)** The total population size can be kept on a certain lower level compared to Figure 4.4a. Application of low dose drug initially decreases the fungal population size. With time the population recovers and we again observe increase in number of yeast and hyphae cells. **(b)** The infection is not successfully treated as at the end of simulation we still observe the inflammation (green gradient around the world).

Model analysis

Some of the parameters that govern the model dynamics introduce stochastic processes in the system. These parameters account for both recruitment and movement of PMNs.

Also a switch from the yeast state to the hyphae state is partially influenced by the probability to make this decision.

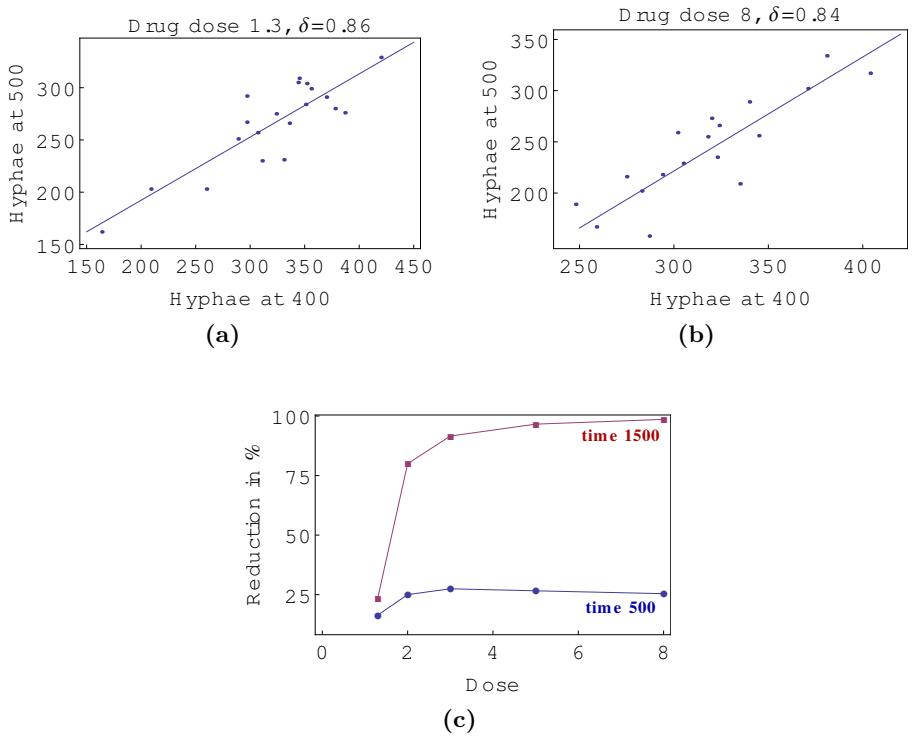

Figure 4.6.: Influence of drug treatments on hyphae burden. Presented are simulation results from twenty repeats. Compared are results for both low and high drug doses and shortly after the drug application. Treatment is always given at time point $t = 400$ and counts are made at time point $t = 500$ (upper panel) and also for $t = 1500$ (bottom panel). **(a)** Impact of a low dose drug treatment on a hyphae load 100 time points after drug application. We see a good correlation between twenty independent simulation results. **(b)** Impact of a high dose drug treatment on a hyphae load 100 time points after its application. We see a good correlation between twenty independent simulation results. **(c)** Blue: efficiency of different drug doses on a short time scale, i.e., 100 time points after its application. Efficiency is reflected as reduction in hyphae burden. Red: efficiency of different drug doses on a long time scale. Depending wether we look at a short time scale or a long time scale, a drug dosage governing the maximal efficiency of a treatment shifts from a dose 3 to about 6 respectively; it can be seen as plateaux are reached in (c) close to these values.

I compare the relative efficiency of a drug treatment with both low (Figure 4.6a) and high dose (Figure 4.6b) and whether by repeating the simulations we obtain significantly diverse results. The drug is always applied at the model time point $t = 400$. I plot the results on a scatter plot, with hyphae cells numbers at time point $t = 400$ plotted against hyphae cells numbers at time point $t = 500$. We observe high correlations

between results from twenty repeats of model simulations (Figure 4.6). As revealed by the Figure 4.6c we observe a saturation effect of the drug dosage on fungi treatment. After reaching a certain threshold there is no improvement in drug efficiency along with increased dose applied. The drug dose threshold increases though if we are looking at immediate treatment results or if we look at the long term treatment. This rather not intuitive result brings us to the conclusion that increased drug dose not always helps the host to recover faster from fungal infection.

4.3. Discussion

Diverse computational techniques are being developed to study biological systems. One they have in common is that all of them focus on how to represent formally interactions on different levels, for instance molecular or cellular level, and how these interactions evolve to a specific function. The main goal of this study was to establish a model of cellular interactions. Fungi population interacting with PMNs can evolve and colonize the epithelium leading to the development of *thrush*. When no experimental data are available, the agent based modeling approach becomes very practical. The rules governing activity of the agents can be constructed based on general information. For instance, the fact that hyphae development is triggered by sparse nutritional conditions can be implemented in a way that the yeast to hyphae switch occurs whenever the amount of the nutrient on a patch drops below a set threshold. Therefore, we do not have to include any regulatory pathways activated within the yeast cells which result in germ tube formation. Also, a single simple rule in the model triggers hyphae induced inflammation. Inflammatory response is proportional to the burden of active hyphae at given spot. Using ODE models we would have to pay more attention to the velocities of all of these events. The other downside of using ODE models for modeling population dynamics is that their simulations represent the average of an observed trend. In other words, any deviations in behavior between different cells of the same type are smoothed. Taking these into account ABMs facilitate implementation of the following features: (1) agent's memory; (2) learning processes or (3) adaptation processes. These were not tested in the model but it will be certainly a starting point in the follow-up studies, to see how the emergent phenomena are influenced by each of the three features. Another feature of ABM approach is in its facile inclusion of any other cell types. Thus, the extension of the system is always plausible without causing too many technical problems. For comparison, ODE models do not have this advantage as we would have to modify all of the equations appropriately. Apart from handling interactions of many cell types, ABMs also allow for stochastic simulations. As we have seen, stochastic elements in the model presented in this chapter do not influence significantly the population dynamics (Figure 4.6). It is important to highlight at this point, that the parameter estimation in ABMs is a non-trivial problem. However, some parameters can be obtained via experimental measurements and than used in the model; a so called bottom-up systems biology ap-

proach (see §1.2.1). For instance, we can measure the doubling time of fungi population or the time necessary to switch between different morphological states. Applying live imaging we can approximate the phagocytosis rates. The ABM approach itself can be used to study the rules that define the activity of the agents leading to global patterns being observed. Moreover, in the presented simulations it is always assumed that the applied drug is not degraded. Thus, the model can be further elaborated and used for simulating other scenarios, if we allow the drug to be degraded. We could study how different times of drug activity influence fungi population. Hence, we could propose optimal intervals between subsequent drug application and optimal dosage of the drug.

We come to the conclusion that ABMs allow for the analysis on the population-level and finding out how the interactions of autonomous pre-programmed agents establish systems dynamics. The state of the fungus, fungal load, pro-inflammatory response, chemotaxis of the PMNs (along with random movement implemented) describe all together the systems' dynamics. By studying this parameters we can get insights into our better understanding of why certain interactions types have been established and how these are reflecting the efficiency of the PMNs in fungal clearance.

Summing up, ABM approach shares advantages and disadvantages with rule based modeling (for its application see for instance [Kühn, 2010]). The approach allows for the implementation of simple if - then rules, which can be derived directly from natural language. Also, more cell types can be considerably handled by the user as behavior of each type is implemented separately. The downside of the approach lies in the lack of computational methods to parameterize the model from experimental data. There are also no tools existing for automatized analysis of the system. Nevertheless, ABMs have found application in broad areas: social sciences, market analysis and in medical application. ABMs can serve as educational tools and, in particular, NetLogo used here, provides very nice visual interface displaying simulation results of the model.

5. Other approaches for studying *Candida albicans* interactions with its human host

5.1. Introduction

Human microflora is a habitat for a number of species able to cause a disease to its host under certain circumstances. In the immunocompetent host, *Candida albicans* is a benign member of the human microflora, but any interference into established host-*C. albicans* interactions may result in fungal infection. The interactions of the fungus with its host can be seen in various distinct ways. One is a scenario where fungi respond to the state of its host in a manner presented in Figure 5.1. In this context, the fungi and the host are constantly influencing each other. In the second scenario, whatever host or pathogen is doing, the characteristic of their responses can fall into one of the three groups: (i) attack the opponent - A; (ii) activate defense strategies - D; (iii) cure itself - C (Figure 5.1, bottom). Such mechanisms could be considered on a single cell level. However, we know that fungal burden influences the strength of host response [Moyes et al., 2010]. Environmental conditions impose phenotypic variability in the fungal population, which can be observed throughout the infection process. The fact that distinct phenotypes can be present at the same time, although every population's member experiences the same environmental conditions argues for social behavior and cell-cell communication within microbial population - a phenomenon termed with 'sociomicrobiology' [Parsek & Greenberg, 2005]. Different social behaviors can establish, which are necessary for communication and cooperation among the members of the group. The cooperative types of interactions in the fungal population may lead to form multicellular bodies with features that are not possible to be expressed by single cells [Bassler & Losick, 2006]. On the other end, whenever individuals interact, a conflict and competition may arise since microbes are all fighting for common resources.

In this chapter, I apply principles of game theory to study interdependencies between members of fungal populations. I analyze interactions among fungal cells in the context of evolutionary games and examine whether cooperation or competition between different cells types takes place. In general, we could assume that cooperation among members of the group establishes in order to produce novel forms of common good, e.g., a public good or a new organism. In contrary to the cooperation, competition favors the stronger individual, what not necessarily has to be the best for the population. The survival of the fittest individuals could also be seen as having a destructive impact on the population on a long time scale, since the competition between different individuals will force the

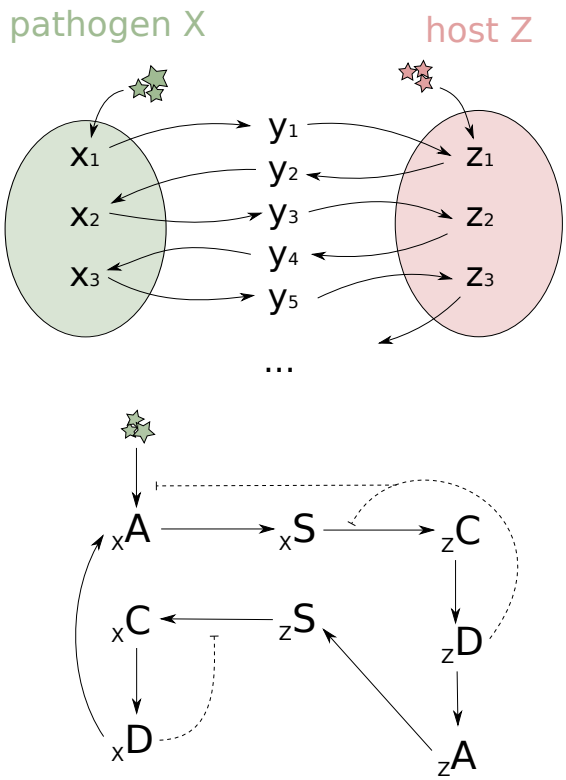

Figure 5.1.: Host-pathogen interactions. (Top) In one scenario, host and pathogen are constantly responding to each other's action. (Bottom) More sophisticated interactions, where both systems respond to an attack (A) of each other, but also incorporate strategies, like defense strategies (D) to reduce the negative action of the opponent, and activate mechanisms to cure itself (C stands for overall harm caused by the opponent).

competitors to occupy distinct niche eventually. Therefore, different mechanisms have evolved in order to allow for cooperative behavior in the population, and thus, allowing for the coexistence of different species. The evolution of mechanisms that can lead to cooperation in the population are reviewed in [Nowak, 2006].

In microbial populations, cooperation occurs whenever one strain helps the other to survive. It does not necessarily imply that the help is mutual. Cooperation can be induced by different means. For example, a population of wild type yeast *S. cerevisiae* cooperates with another genetically modified *S. cerevisiae* strain having nothing in return [Gore et al., 2009]. The cooperation is established due to ability of the WT strain to produce an enzyme invertase. The enzyme is necessary for budding yeast to grow on sucrose, which first has to be hydrolyzed. A mutated strain called a cheater, which does not produce the invertase, takes an advantage of WT and consumes its products. Because of that, mutants are able to survive and also invade the population.

Another type of cooperation, the self-destructive cooperation, occurs in the population of *Salmonella typhimurium* [Ackermann et al., 2008]. This bacterial pathogen is limited in its ability to colonize the gut due to the presence of other microbes in the microflora. However, *S. typhimurium* can invade the gut tissue due to its phenotypic variability. The gut invasion triggers the inflammatory response that in turn results in the removal of competing microbes from the gut microflora. The *S. typhimurium* cells that invaded the tissue will die due to activity of the innate immune system, but the remaining *S. typhimurium* cells will succeed in gut colonization. Hence, such type of cooperation in a microbial population is termed self-destructive cooperation.

Different types of interactions may establish in microbial communities, and depending on whether the interacting species benefit from them or not, interactions can be classified as mutualism, commensalism, amenalism or parasitism [Faust & Raes, 2012]. In the next two section I interpret the microbial interactions as games in a pairwise context, where each of the two players has a number of strategies to play. See Figure 5.2 for an illustration of the following concept. If we know the payoff matrix of the game, then a cooperation can be seen as a condition where one player changes its current strategy to increase its own payoff, but by doing so it simultaneously increases the payoff of the opponent. Competition in turn, would be seen as a situation where the player changes its current strategy to increase its own payoff, but by doing so it simultaneously decreases the payoff of the opponent. Here, a cooperative interaction would correspond to a mutualism, and a competitive interaction to a parasitism as it is discussed in [Faust & Raes, 2012].

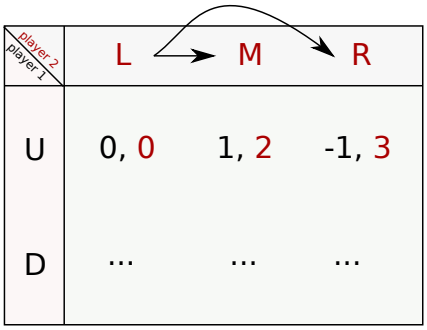

Figure 5.2.: Accessing cooperative and competitive strategies from the payoff matrix. Player 2 by changing its strategy from L (left) to M (middle) increases its own payoff but also the payoff of the player 1 playing strategy U (up), i.e., the strategy M cooperates with the strategy U. On the other side, player 2 when choosing strategy R (right) instead, increases its own payoff but the same time decreases the payoff of player 1 playing U, i.e., strategy R competes with strategy U.

In the next section I give a mathematical description for evolutionary dynamics, a method I use for assessing types of interactions between yeast cells basing solely on mathematical analysis of the experimental data. In any case, interactions between cells are viewed in a pairwise context. Analysis of a mathematical model describing evolution-

ary dynamics in a yeast population, which is parameterized basing on the data published in [Gore et al., 2009], indicates the types of cells' interactions in the population what is in a great agreement with explanations provided by the authors. After this introduction to the method and its practical application I use the technique to analyze the dynamics of *C. albicans* population profile, and then provide with hypothesis why certain types of interactions may occur in candida population.

5.2. Evolutionary games in microbial populations

5.2.1. Model formulation

Let us consider a game with two players, where each of them has two strategies, s_1 and s_2, to play. The payoff matrix of such a game stores the players' gains for choosing particular strategy. In a growing population consisting of two replicating strains, we will consider pairwise interactions between individuals that affect the population profile, i.e., proportions of each cell type. Replication rates of the two strains are tuned with respect to the current population profile. Such adjustment of the replication rates defines evolutionary games. Evolutionary stable state (ESS) is a population profile that establishes at the end, with the property that no mutant strategy can invade the population, and hence, change its final profile (see [Webb, 2007]). If we link the strategies from two-persons game with the two strains in the population, and thus, the players' gains with the corresponding proliferation rates assigning them the same numerical values, then the Nash equilibrium (§1.3.3) of the two-persons game and ESS of the corresponding population are the same [Webb, 2007]. In such a case the payoff matrix of the two-persons game and the matrix that couples replication rates are the same. In general, a payoff matrix defines a type of game, and a matrix of replication rates establishes population profile dynamics. Therefore, I will use a term 'game dynamics interactions' to highlight what specific type of game is corresponding to the matrix of replication rates in the given population.

From the derivation given in [Webb, 2007] I recall below a replicator equation. In the next section I will use the equation to analyze different game dynamics interactions that may establish in fungal populations. It is assumed that there are two different cell types, s_1 and s_2, and both can proliferate. There might be some fluctuations in the size of population with some birth rate $\mathcal{B}$ and death rate $\mathcal{D}$, which are independent of the game, and hence of the population profile. The total population size is given by

$$N = n_1 + n_2,$$

where n_i is the number of individuals in the state s_i, $i \in \{1, 2\}$. The proportions of individuals in each of the states are given by

$$x_i = \frac{n_i}{N}. \tag{5.1}$$

Thus the vector $\mathbf{x} = (x_1, x_2)$ is the population profile with $x_1 + x_2 = 1$. The dynamics of the system are described by the following set of ODEs:

$$\begin{aligned} \dot{n}_1 = &\ (\underbrace{\mathcal{B} - \mathcal{D}}_{\alpha})n_1 + n_1\pi(s_1, \mathbf{x}) \\ \dot{n}_2 = &\ (\mathcal{B} - \mathcal{D})n_2 + n_2\pi(s_2, \mathbf{x}), \end{aligned} \tag{5.2}$$

where $\pi(s_i, \mathbf{x})$, $i \in \{1, 2\}$, are the average rates of replication for the type i that depend on the population profile $\mathbf{x}$. In general, a cell in state s_i can either meet a cell of its own type or of the other type, and hence, its proliferation rate π will vary accordingly. We can define each of the proliferation rates by the following equation

$$\pi(s_i, \mathbf{x}) = \pi(s_i, s_1)x_1 + \pi(s_i, s_2)(1 - x_1).$$

It means, cell s_1 has a probability x_1 to meet s_1, and it proliferates proportional to the rate $\pi(s_1, s_1)$ but at the same time there is a probability $x_2 = 1 - x_1$ that it will meet cell type s_2, and that it will proliferate proportional to the rate $\pi(s_1, s_2)$ in this case. The total population size changes with the rate

$$\dot{N} = \sum_{i=1}^{2} \dot{n}_i = (\alpha + \overline{\pi}(\mathbf{x}))N, \tag{5.3}$$

with $\alpha = \mathcal{B} - \mathcal{D}$ and $\overline{\pi}(\mathbf{x})$ defined as an average growth given by the equation

$$\overline{\pi}(\mathbf{x}) = \sum_{i=1}^{2} x_i\pi(s_i, \mathbf{x}).$$

From Equation 5.3 we observe that depending on the value of α the population size either growths exponentially or follows an exponential decay. For the purpose of next section, I will derive now an equation that allows us to look at dynamical changes of the population profile. From Equation 5.1 we derive

$$\dot{n}_i = \dot{x}_i N + x_i \dot{N},$$

and hence,

$$\begin{aligned} \dot{x}_1 &= \frac{\dot{n}_1}{N} - x_1\frac{\dot{N}}{N} \\ &= \underbrace{\frac{n_1}{N}}_{x_1}(\alpha + \pi(s_1, \mathbf{x})) - x_1(\alpha + \overline{\pi}(\mathbf{x})) \\ &= (\pi(s_1, \mathbf{x}) - \overline{\pi}(\mathbf{x}))x_1 \end{aligned}$$

and simple calculations lead to the final formula

$$\dot{x}_1 = x_1(1 - x_1)(\pi(s_1, \mathbf{x}) - \pi(s_2, \mathbf{x})). \tag{5.4}$$

The equation 5.4 models the temporal changes in the proportion of cells of type s_1 in the entire population. The contribution of the cell type s_1 to the population profile is affected by the average proliferation rates $\pi(s_i, \mathbf{x})$. Furthermore, since

$$x_1 + x_2 = 1$$

the dynamic fractional change of the other cell type s_2 is given by

$$\dot{x}_2 = -\dot{x}_1.$$

5.2.2. Analysis of the system

In the previous section we have derived the following equation

$$\dot{x} = x(1 - x)(\pi(s_1, \mathbf{x}) - \pi(s_2, \mathbf{x})) = f(x). \tag{5.5}$$

It has three steady state solutions and their stability is dependent on the parameter values (Figure 5.3). For simplicity I set

$$\begin{aligned} a &= \pi(s_1, s_1) \\ b &= \pi(s_1, s_2) \\ c &= \pi(s_2, s_1) \\ d &= \pi(s_2, s_2). \end{aligned} \tag{5.6}$$

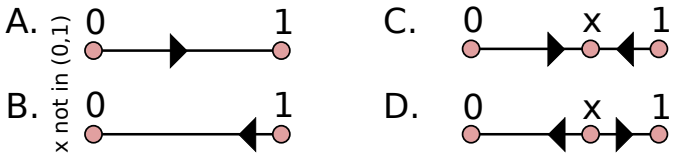

Figure 5.3.: Parameters value determine stability of population profile. Consistent with previous section, either strain s_2 completely takes over the population, i.e., $x = 0$; or strain s_1 is only present, i.e., $x = 1$; or both strains types will coexist, i.e., $x \in (0, 1)$. In (A, B, C) initial proportions of different strains do not affect the ESS. (A) ESS is 1. (B) ESS is 0. (C) Both strains will coexist and ESS establishes for $\hat{x}_3 \in (0, 1)$. (D) Since both 0 and 1 are stable steady states, a bi-stability in the system occurs and in this case, the final ESS depends on the initial conditions.

The steady state solutions take the form

$$\hat{x}_1 = 0 \quad \text{and} \quad \hat{x}_2 = 1 \quad \text{and} \quad \hat{x}_3 = -\frac{b-d}{a-b-c+d}. \tag{5.7}$$

A steady state $\hat{x}_i$ is stable whenever $f'(\hat{x}_i) < 0$ is satisfied, and hence,

$$f'(\hat{x}_1) = b - d \quad \text{and} \quad f'(\hat{x}_2) = c - a \quad \text{and} \quad f'(\hat{x}_3) = -\frac{(c-a)(b-d)}{a-b-c+d}.$$

5.2.3. From population dynamics to games

Through the example presented in this section I aim to shed light on how using the method described in §5.2.1 we can identify the types of interactions in microbial populations. For that purpose I base the discussion on the work of [Gore et al., 2009]. By engineering *S. cerevisiae* cells the authors are able to establish a game in the system. They constructed a mutant strain which fails to produce the enzyme invertase that is necessary for the yeast to feed on sucrose. Both wild type (WT) and mutant strains compete for common nutrient resources when they grow together on a sucrose media. The WT strain, later in the text referred to as a cooperator, is able to feed on sucrose and proliferate because its invertase hydrolyzes the sugar, and hence facilitates uptake of the glucose. The mutant strain is still able to grow on this medium as it utilizes the glucose produced by the cooperator cells. Since the mutant cell does not contribute to the public good it is named by the authors as a cheater strain. Depending on the conditions in the system either both cell types survive or one of them will go extinct. I study the dynamics of the system using the replicator equation (Equation 5.4). This model describes the temporal evolution of each strain in the population. The parameters that govern the system's dynamics, in theory, indicate how fast each of the strains replicates. I start from a description of the payoff matrix for a two-players game (see Figure 5.4).

		cell 2	
		cooperator	**cheater**
cell 1	**cooperator**	***E, E***	***E - C, E_d***
	cheater	***E_d, E - C***	***0, 0***

Figure 5.4.: Payoff matrix of a game between two cells. Each cell has two strategies to follow: either to cooperate or to cheat.

The produced enzyme accounts for the public good that is being exploited by both cell types. Let us first look at the interactions of both cell types, restricting ourselves to the case where exactly two cells are playing. When two cheater cells are on a sucrose

medium, then they will not grow as no invertase will be produced. Hence, the fitness of the two is set to 0. When both cells living together are cooperators, then they equally utilize the public good and there are no costs involved. Their fitness is set to E. When only one cell will cooperate, then the cooperator cell gains the payoff E but also pays a cost C as part of its product is used by the cheater cell. The cheater cell has a fitness E_d in this case.

The WT strain used by the authors is a histidine auxotroph. It means that by varying the histidine concentration in the medium, the authors control the payoff matrix. By limiting the histidine concentration they slow down growth of the cooperators and hence, increase the 'cost-of-cooperation' increasing the parameter C in the payoff matrix in Figure 5.4. From now on I focus on a conceptual mathematical analysis of the population data derived from the data published in [Gore et al., 2009] and presented in Figure 5.5.

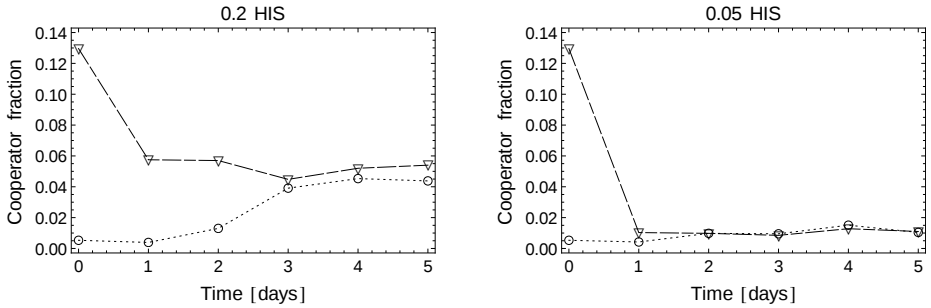

Figure 5.5.: Time dependent fraction of cooperator strain in two different histidine concentration in the medium. The figures are adapted from the data communicated by Gore, J. and published in [Gore et al., 2009]. Considered are populations with low, about 0.5%, initial portion of cooperator cells (circles) and high, about 13%, initial portion of cooperator cells (triangles).

The payoff matrix in Figure 5.4 takes now a more general form which is given in Figure 5.6. Since only C (see Figure 5.4) is manipulated when histidine concentration is varied, it means that in both conditions, i.e., 0.2 and 0.05 histidine concentration, only the payoff of a cooperator cell when coexisting with a cheater cell, will change. All the remaining parameters are fixed. This means we alternate between parameters ur_1 and ur_2 when considering two different histidine concentrations in the medium (see Figure 5.6). In more detail, I consider the fitness of two cooperator cells not to be influenced by the histidine concentration when living together. The same holds for two cheater cells. The fitness of the cheater cell, when living together with a cooperator cell is also considered not to be influenced by the histidine concentration (the cheater cell would always attempt to consume the same amount of the public good). However, the fitness of the cooperator cell varies and the lower the histidine concentration the more it is exploited by the cheater cell.

I use the data presented in Figure 5.5 for estimation of the parameters in the replicator

0.2 HIS	cell 2: cooperate L	cell 2: cheat R1
cell 1: cooperate U	*ul, ul*	*ur_1, dl*
cell 1: cheat D	*dl, ur_1*	*0, 0*

0.05 HIS	cell 2: cooperate L	cell 2: cheat R2
cell 1: cooperate U	*ul, ul*	*ur_2, dl*
cell 1: cheat D	*dl, ur_2*	*0, 0*

Figure 5.6.: Payoff matrices of a game between two cells. Cells have two strategies to follow; they can either cooperate or cheat. By varying histidine concentration we manipulate the parameters ur_1 and ur_2.

equation, that I recall below.

$$\dot{x} = x(1-x)(\pi(s_1, \mathbf{x}) - \pi(s_2, \mathbf{x})).$$

In this formula, x is the fraction of cooperator cells in the population, s_1 is the strategy to cooperate and s_2 is the strategy to cheat. Moreover,

$$\pi(s_1, \mathbf{x}) = ul \cdot x + ur_1 \cdot (1-x),$$

and

$$\pi(s_2, \mathbf{x}) = dl \cdot x + dr_1 \cdot (1-x).$$

For both 0.2 and 0.05 histidine concentration, the model was fitted solely to data with low initial fraction of cooperator cells in the population, i.e., about 0.5% (Figure 5.7). The simulations reflecting the high initial fraction, i.e., 13% of the cooperative strain are predictions of the model.

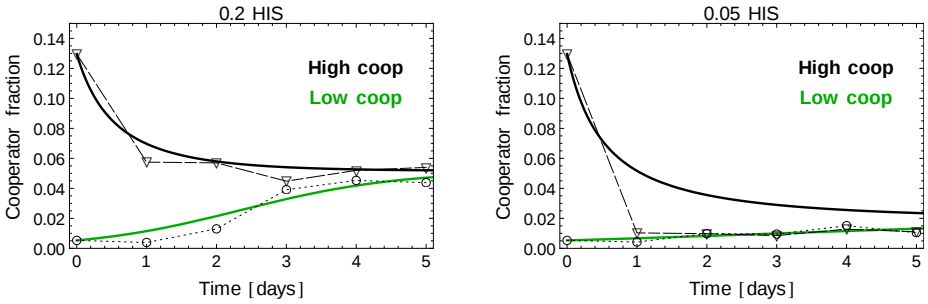

Figure 5.7.: Simulations for one set of parameters. $dl = 17$, $ul = 0.0041$, $ur_1 = 0.92$, $ur_2 = 0.34$. The model is fitted to a low initial fraction of cooperator cells of 0.53% (green lines). Simulations for high initial fraction of cooperator cells are the model predictions (black lines). Circles and triangles are the experimental data points.

I estimate the parameters of the model using the tool COPASI and its inbuilt Evo-

lutionary Programming task [Hoops et al., 2006]. I run the parameter estimation task 1000 times setting the ranges for a parameter search space between 10^{-4} and 10^{4}. Only the fits with RSS (see §1.4.1) lower than 9.8^{-5} are considered for the analysis. All together there are four parameters that have to be estimated: dl, ul, ur_1 and ur_2. Let us assign to $\mathcal{T} = [0, 1, 2, 3]$ a tuple $\mathcal{K} = [dl, ul, ur_1\, ur_2]$, i.e., we assign to the first element of $\mathcal{T}$, which is 0 a numerical value of dl, to 1 a value of ul, etc. In the text below I call a motif, an ordered tuple $\mathcal{T}_M$ whose assigned elements form an increasing sequence. For example, the parameters used for generating simulation presented in Figure 5.7 form the tuple $\mathcal{K} = [17, 0.0041, 0.92, 0.34]$ that corresponds to the tuple $\mathcal{T}_M = [1, 3, 2, 0]$ (see also Figure 5.8). For each resulting parameter estimation set I construct its corresponding $\mathcal{T}_M$. In total 998 out of 1000 parameter sets were accepted. I store 998 of $\mathcal{T}_M$'s and I look how often the motifs repeat. There are $4! = 24$ possibilities for distinct $\mathcal{T}_M$ to appear.

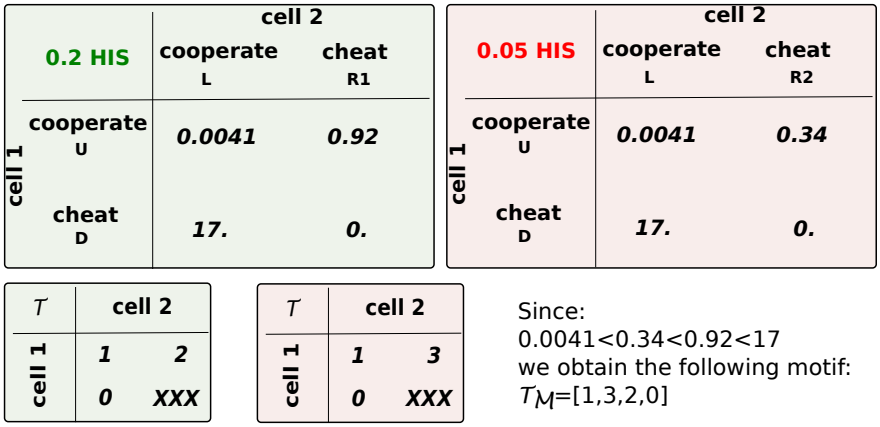

Figure 5.8.: Construction of $\mathcal{T}_M$ tuple. Payoff matrices, for both histidine concentrations, are based on the parameters values from Figure 5.7. By ordering the entries of payoff matrices (top panel) from min to max value we permutate the entries of the matrices in the bottom panel respectively.

Looking at Figure 5.9 we see that only three motifs keep appearing, i.e., $\mathcal{T}_M = [1, 3, 2, 0]$, $\mathcal{T}_M = [3, 2, 1, 0]$ and $\mathcal{T}_M = [3, 1, 2, 0]$. A first result coming from the analysis of the motifs is that cooperator cell is doing better of interacting with a cheater cell in the 0.2 histidine concentration. This can be seen as in all cases $ur_1 > ur_2$, in other words, the element 2 proceeds the element 3 in each of the $\mathcal{T}_M$'s (see also Figure 5.8 for help). These results are in line with authors' point, that via a decrease in histidine concentration we increase the cost-of-cooperation, and hence, the fitness of a cooperative cell, when confronted with a cheater cell, is decreased. In all cases, the cheater cells are the fittest as each time dl has the highest numerical value (0 is the last element in each of the $\mathcal{T}_M$'s). This also can be explained due to the fact that cheater cells always take advantage of the cooperative strain, giving nothing in return.

Analysis of $\mathcal{T}_M = [1, 3, 2, 0]$

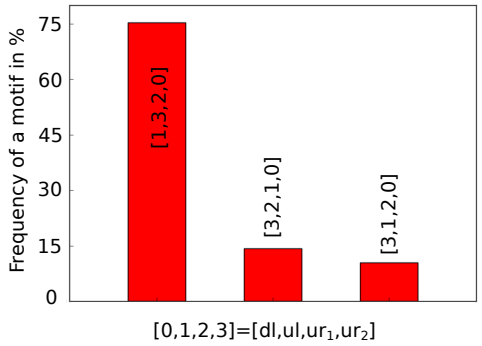

Figure 5.9.: Frequency of motifs explaining experimental data. Analyzed are 998 accepted out of 1000 parameter sets. Each column represents how frequently a given motif appears.

The motif $\mathcal{T}_M = [1, 3, 2, 0]$ indicates that the following holds:

$$ul < ur_2 < ur_1 < dl.$$

Because $ul < ur_1$, we can conclude that a cooperative cell has higher payoff when confronted with a cheater cell. Moreover, since $ur_2 < ur_1$, we see that decreasing the histidine concentration there are associated costs for cooperator cells as their fitness decreases from ur_1 to ur_2. The relation is conserved in all of the three motifs. I plot all of the numerical values for estimated parameters for the motif $\mathcal{T}_M = [1, 3, 2, 0]$ in Figure 5.10. Since the motif $\mathcal{T}_M = [1, 3, 2, 0]$ is the most frequently appearing in the parameter estimation results, and $ul < ur_2 < ur_1$ holds, one could think about the public good also in the way described below. Even though the public good, i.e., generated glucose, is consumed by cheater cells that do not contribute to its production, the presence of cheater cells might stimulate its higher production by cooperative strain. According to Figure 5.2, the cheater cells would ironically become "cooperative strain", in the sense that they induce the production of the public good. On the other side, in the work [Gore et al., 2009] the authors point out that in this system, invertase expression in WT cells can be repressed by glucose, and hence, WT cells exhibit higher production of the enzyme, only when competing against cheater cells.

Analysis of $\mathcal{T}_M = [3, 2, 1, 0]$

Considering the motif $\mathcal{T}_M = [3, 2, 1, 0]$ we conclude that the following must hold:

$$ur_2 < ur_1 < ul < dl.$$

The fitnesses ur_1 and ur_2 of a cooperative cell when confronted with a cheater cell are decreased compared to ul. The motif points out that in both 0.2 and 0.05 histidine

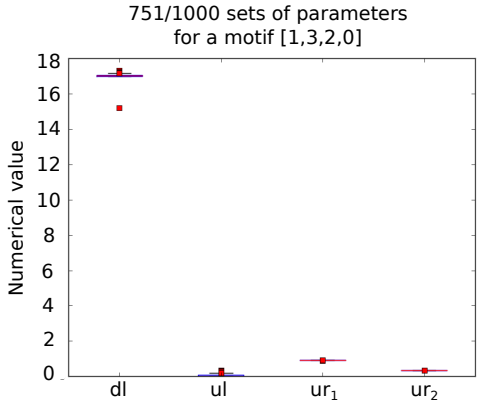

Figure 5.10.: Parameters values for the motif $\mathcal{T}_M = [1, 3, 2, 0]$. 751 out of 1000 estimated parameters are plotted. There is a consistency in their numerical values between different parameter estimation results.

concentration we deal with a snowdrift game dynamics interactions as the inequalities in the matrix from Figure 5.6 fulfill the necessary condition: $dr_i < ur_i < ul < dl$, for $i \in \{1, 2\}$ (see §1.3.3).

In conclusion, basing solely on the mathematical analysis of the parameter estimation results from the population data, i.e., by looking at the motifs $\mathcal{T}_M$, it was possible to derive conclusions similar to the ones provided by authors in [Gore et al., 2009]. In a broader view, as long as the assumption on pairwise interactions can be made, the analysis of the model described here could be applied to microbial communities in search for the strains with specific types of interactions. Types of interactions would be interpreted basing on Figure 5.2.

We can extend the analysis of the motifs by comparing the average advantages from being the cooperative strain and from being the cheater strain. The advantages are expressed with the formulae:

$$\pi(s_1, \mathbf{x}) = ul \cdot x + ur_1 \cdot (1 - x), \quad \text{i.e., an average advantage for being a cooperator}$$

and

$$\pi(s_2, \mathbf{x}) = dl \cdot x + dr_1 \cdot (1 - x), \quad \text{i.e., an average advantage for being a cheater.}$$

From Figure 5.11 we see that, when the system initially contains high proportion of a cooperative strain, the fitness of cheater cells subpopulation will be decreased, while the fraction of cooperative strain decreases (Figure 5.7, both histidine concentrations). On the other side, when initial fraction of the cooperative strain is low the average fitness of the cheater strain subpopulation will be increased along the increment of cooperative cells fraction in both histidine concentrations considered (see Figure 5.12 and Figure 5.7).

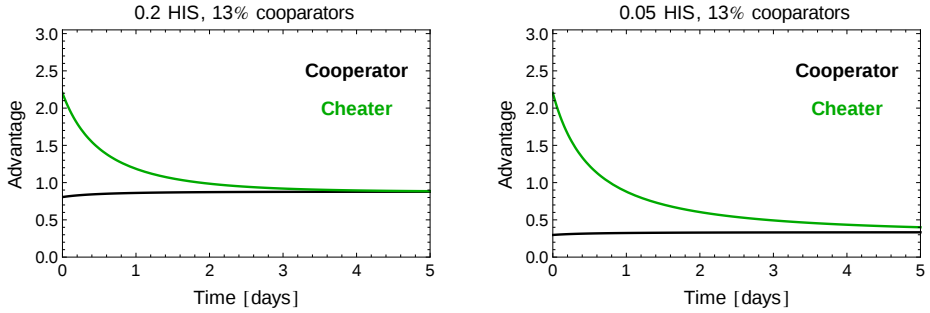

Figure 5.11.: Advantages for populations of cooperator and cheater cells. When starting from high initial fraction of cooperative cells, we will decrease the fitness of cheater cells subpopulation over time. Cooperative cells are always less fit than cheater cells.

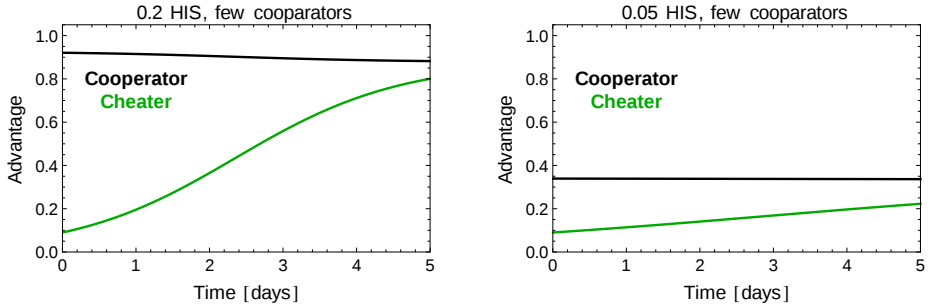

Figure 5.12.: Advantages for populations of cooperator and cheater cells. When starting from low initial fraction of cooperative cells (0.53%), we will increase the fitness of cheater cells subpopulation over time. Cooperative cells are always more fit than cheater cells.

We have to keep in mind the following: few cooperative cells in the population impose low concentration of glucose in the medium the cells could feed on. Hence, even a slight increase in cooperative strain proportion, and consequently more glucose gathered, will instantly be milked by cheater cells. The simulation results support the authors' hypothesis, that a cooperative strain is more advantageous when it constitutes only a small fraction of the population. As suggested in [Gore et al., 2009], it is due to the fact, that when only a small fraction of cooperative cells is present, they are more likely to consume the glucose that they are producing. This is captured in the model's simulations and if we compare the initial advantage of the population, i.e., at time $t = 0$ from Figure 5.11 and Figure 5.12, we see that independently of the histidine concentration, always when starting with low cooperative cells content, this subpopulation is doing better off than the cheater cells.

Discussion

As it was many times stressed, in this section I used the published data and only describe a possible mathematical analyses of these. The presented here example can serve us as a crash course into application of evolutionary games to biological data. We can infer mutual dependencies that arise between different cell types by studying the temporal evolution of the population profile. The analysis can be facilitated when we apply techniques that describe such evolutionary dynamics, here in particular the replicator equation. Assuming that we have the time dependent fractional changes of different strains in the population, as it was the case in [Gore et al., 2009], we can estimate the parameters of the replicator equation that can be used to reconstruct the corresponding payoff matrix (Figure 5.2). In turn, the content of the payoff matrix reveals the type of game that is being played. We have seen that in the example presented here only three distinct $\mathcal{T}_M$ motifs appeared. Yet, in each case it was correctly extracted, that a decrease in histidine concentration increases the cost-of-cooperation, and hence, the fitness of the cooperative cell. We also observed that a low initial fraction of the cooperative cells is advantageous for this subpopulation as their fitness is higher than the fitness of cheater cells subpopulation.

The model itself, although very simple, was able to capture all the hypotheses posed by the authors. The type of the played game was also correctly predicted. I believe this approach can be applied to study more complex microbial structures. One of the most reasonable applications of this approach would be the investigation of systems where it remains unclear, which strain is the cooperator. Similarly we can shed light on couples which represent competitive behavior. Assessing experimentally solely the fractional time evolution of the subpopulation such question can be easily investigated by this method. From the reconstructed payoff matrix we can identify such couples. And once we know where to look for, the method can be applied to direct the experiments.

5.3. Game theoretic model of *Candida albicans* yeasts and hyphae interactions

This section is based on:

Tyc KM, Kühn C, Wilson D & Klipp E: "Assessing the advantage of morphological changes in Candida albicans: a game theoretical study".

In preparation.

5.3.1. Introduction

The ability to express various virulence factors (VFs) in human pathogens allows the microbes to invade the host and spread to different body organs. In at-risk patients some pathogenic species undergo a phenotypic transition, that often indicates the initiation of a disease. For *Candida albicans*, one of the most crucial VF is its ability to form germ tubes and become true hyphae. The model presented in this section considers pairwise interactions among the cells from candida population and how these influence the population profile. First, I introduce a game theoretical model with two players, where each has two strategies to choose: either exist as a yeast cell or exist as a hyphae cell. As next, I consider a growing candida population. I investigate how the pairwise interactions among the candida cells affect the growth rates of both yeast and hyphae subpopulations. In this context, depending on morphotypes of the two players different proliferation rates will apply to each of them. In the model, the outcome of the interactions is influenced by the immune status of the host and nutritional conditions. Moreover, yeast and hyphae subpopulations' growth rates are affected by the current yeast/hyphae ratio. Depending on the model's parameters, the population profile can fall into one of the three groups: (i) yeast cells are favored and a pure yeast population is observed, (ii) hyphae are advantageous and pure hyphae population establishes, (iii) both morphological forms coexist. It is considered that yeast cells favor dissemination [Jacobsen et al., 2012] whereas hyphae cells are necessary for invasion and to cause a tissue damage [Wächtler et al., 2011]. Hyphae can penetrate both epithelial and endothelial cells and by doing so they pave a way for yeast cells and facilitate their dissemination. The coexistence of both forms is thus possible and observed in the model for some parameter ranges. Distinct population profiles that are observed are results of the type of interactions between the microbes. As such we can distinguish between cooperative and competitive behavior. Inspired by the model simulations the conclusion can be made, that cooperation between two phenotypically distinct cells might be necessary for the invasion and dissemination, that also leads to a higher fungal burden. A competitive behavior would then occur during the colonization of a specific niche. I apply the replicator equation described in §5.2.1 to study the effect of microbial interactions on the population profile and relate these to fungal infection. Finally, using a game

theoretic nomenclature, the results of the model will allow us to conclude that the game that defines the type of interactions between the cells shifts from a Snowdrift game to a Prisoners' dilemma during the infection process.

5.3.2. Biological background

The yeast *C. albicans* is an opportunistic human pathogen. It causes most of fungal infections ranging from benign *thrush* to life-threatening systemic diseases at some group of patients. The powerful feature of the fungus is its ability to grow in distinct forms among which yeast and hyphae are the most extensively studied. Yeast to hyphae morphological transitions, and an increased fungal burden, are often associated with an initiation of fungal infection. Both events can be induced by the host's immunodeficiency or disruption of its bacterial flora, e.g. due to antibacterial drug treatment. Formation of germ tubes can be stimulated by the nutrient availability and many other signals [Phan et al., 2000]. *C. albicans* feeds on nutrients provided by the host, the microflora or dead tissue. By developing hyphae, the fungus is able to penetrate the host's tissues and access the nutrients from the inside of the host cells. I note here that only hyphal cells can cause a tissue damage [Wächtler et al., 2011]. Since starvation is known to be a strong inducer for the germ tube formation ([Biswas et al., 2007]) in the model it will be a driving force for the phenotypic transition in the candida population. In the mathematical model I also assume that the outcome of the fungal interactions is influenced by the status of the host immune system. I consider the activity of phagocytic cells, neutrophils (PMNs), to be the major determinant of the outcome of those interactions. A number of studies support this choice. For instance, as reported in [Lionakis et al., 2011], in a mouse model of invasive candidiasis PMNs are the most widely recruited leukocytes to all the tissues, except for the brain, infected by *Candida*, i.e., spleen, liver or kidney. Moreover, it has been shown that PMNs successfully kill *C. albicans* [Urban et al., 2006, Wozniok et al., 2008] and that they are more attracted by *C. albicans* hyphal cells [Wozniok et al., 2008, Jacobsen et al., 2012]. Also neutropenic patients are more susceptible to candidemia [Koh et al., 2008].

5.3.3. Two-player game

I employ the game theoretic formalism to later study the impact of nutrient availability and host immune system status on the phenotypic variability in a candida population. Interactions within a microbial population are understood in a pairwise context. I begin with a simple view and consider a game with two players, i.e., two cells, where each cell can choose between two strategies, either act as a yeast (strategy y) or as a hyphae (strategy h). It is assumed that in healthy individuals mostly yeast cells are observed. This implies that in rich nutritional conditions and balanced microflora the yeast form is favored. I express the fitness l of a yeast cell, i.e., its proliferation rate and the payoff in the two-players game at the same time, with a S-shaped function, that ensures the

maximal payoff. It is expressed by the following equation

$$l(n) = \frac{v_y n^\sigma}{n^\sigma + K^\sigma} \quad \text{with} \quad k_y = K^\sigma, \tag{5.8}$$

with n reflecting nutritional conditions, σ the steepness of the curve, v_y maximal payoff given unlimited nutrient and K nutritional conditions necessary to receive half of the maximal payoff possible. In Figure 5.13 we see that the better are nutritional conditions the fitter are the yeast cells, i.e., their payoff $l(n)$ increases. Hyphal cells in contrary are

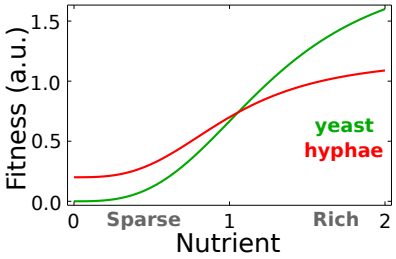

Figure 5.13.: Fitness profiles $l(n)$ and $d(n)$ for yeast and hypha respectively. For simulations following parameters values are considered: $\sigma = 3$, $v_y = k_y = 2$, $v_h = k_h = 1$, $i = 0.2$. Under rich nutritional conditions yeast form is favored (green line above red line). Hyphae are more advantageous in sparse nutritional conditions than yeast (red line above green line).

induced by a starvation signal, i.e., hyphae are favored in sparse nutritional conditions. The fitness d of the hyphal cells increases while nutritional conditions get better and it is defined by the following equation

$$d(n) = \frac{v_h n^\sigma}{n^\sigma + K_d^\sigma} + i \quad \text{with} \quad k_h = K_d^\sigma, \tag{5.9}$$

where $i > 0$ is a term that increases the hyphae fitness due to its ability to acquire nutrients from invaded host cells. Depending on the nutrient availability different cell types will perform better and it is determined by the above constructed functions describing $l(n)$ and $d(n)$ (Figure 5.13). In addition to nutrient availability, PMNs affect the outcome of the game and they are indirectly activated by hyphae, i.e., through a release of pro-inflammatory molecules by the epithelial cells. In total three situations may occur in the game, i.e., either two yeast cells play; or two hyphae cells; or one yeast and one hyphae (see Figure 5.14). The payoff matrix of this game can be justified by the following implications.

- The payoff for a hyphae is defined in Equation 5.9. Hyphae are exposed to a PMNs' phagocytic activity that establishes a cost for hyphal form. Since a hyphal cell can be killed I subtract a cost k from its payoff. The parameter k reflects the efficiency of PMNs. In general, the payoff for a hyphal cell, when playing against a yeast, is given by $\pi(h, y) = d(n) - k$.

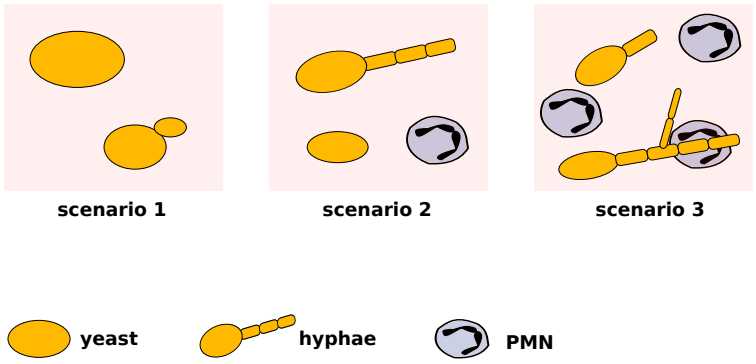

Figure 5.14.: Three scenarios may occur in the game. Either both cells will play yeast (left) or both will play hyphae (right) or one will choose yeast and the other hyphae (middle).

- The payoff for a yeast is defined in Equation 5.8. When a hyphae is around, also the yeast cell is exposed to the PMNs' activity and potentially can thus be killed. But since the attraction of PMNs toward a yeast form is lower than toward a hyphal form [Jacobsen et al., 2012] the payoff for yeast when playing against hyphae is set to $\pi(y,h) = l(n) - bk$, with $b \in (0,1)$.

- I consider each hyphae to contribute to the activation of the immune system. This increases the number of PMNs recruited to the system and thus increases the probability of killing the hyphae. Hence, in case both cells choose to play hyphae a payoff $\pi(h,h) = d(n) - 2k$ for each cell applies.

The payoff matrix of the game is given in Figure 5.15. From now on I fix the parameters values as it is easy to show that as long as the inequalities between numerical values in table-cells in Figure 5.15 are conserved the conclusions remain valid.

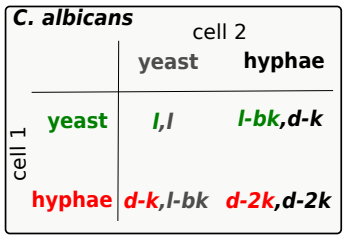

Figure 5.15.: Payoff matrix in steady nutritional conditions. Payoffs are color coded, cell 1 scores the first value, cell 2 the second value in each of the possible scenarios. Abbreviations $l := l(n)$ and $d := d(n)$.

Both nutritional conditions and phagocytic activity of PMNs are the external stimuli that can modify the outcome of the game. Depending on the strength of each of the signals different strategies combinations define Nash equilibrium, i.e., a scenario in which

no cell increases its payoff by deviating from its current strategy. In pure strategies, i.e., no randomization, a Nash equilibrium is when:

- both cells are yeast and $\pi(y, y) > \pi(h, y)$;
- both cells are hyphae and $\pi(h, h) > \pi(y, h)$;
- both yeast and hyphae coexist, and $\pi(y, h) > \pi(h, h) \,\&\, \pi(h, y) > \pi(y, y)$.

For fixed parameters values with only nutrient and PMNs effectivity being variable we can summarize the possible Nash equilibria as it is depicted in Figure 5.16.

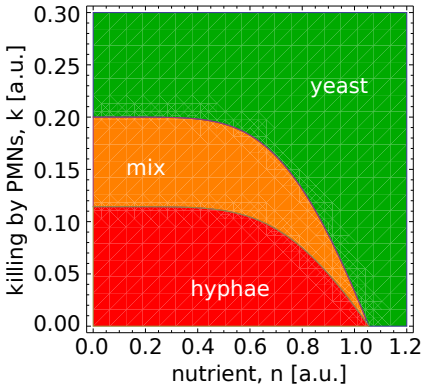

Figure 5.16.: Nash equilibrium (NE) in the game. Each cell's strategy choice is influenced by nutritional conditions and the PMNs' effectiveness, e.g., in rich nutritional conditions even if PMNs are compromised, both cells acquiring yeast form is a NE (green region and high n). In sparse nutritional conditions acquiring hyphae by both cells is a NE only when PMNs are compromised, i.e., low k (red region). (orange region) Coexisting both cell types establish a NE.

5.3.4. Interactions within a population

A game within a candida population in steady environment

In the discussion I refer to a yeast form as a benign form of the fungus and a hyphal form as its hostile form. In the following subsection it is assumed that candida population is composed of both of the forms. Depending on the environmental conditions one of the two forms becomes more advantageous, but only the harmful form is able to invade the host. The rates of proliferation of the two cells types change when external conditions vary. By studying the time evolution of the fungal subpopulations, i.e., proportions of yeast and hyphae, we can asses the game dynamics interactions in the system. The payoff matrix derived in Figure 5.15 will represent now the proliferations rates for interacting fungal cells (see §5.2.1 for explanation). Let x be the fraction of yeast cells in the

population whose time evolution is modeled with the replicator equation (see §5.2.1):

$$\begin{aligned} &\dot{x} = x(1-x)(\pi(y,\mathbf{x}) - \pi(h,\mathbf{x})), \text{ with} \\ &\pi(y,\mathbf{x}) = x\pi(y,y) + (1-x)\pi(y,h), \text{ and} \\ &\pi(h,\mathbf{x}) = x\pi(h,y) + (1-x)\pi(h,h). \end{aligned} \tag{5.10}$$

From the analysis in §5.2.2, for x^* considered a steady state of the above equation three scenarios are plausible:

- $x^* = 1$ is a stable steady state and only yeast cells are present in the population. In this case, the fungal population is non-invasive and hence, benign to the host;
- $x^* = 0$ is a stable steady state and only hyphae cells are present in the population. Here the fungal population is invasive and hostile to the host;
- $x^* \in (0,1)$ is a stable steady state and both cells types constitute the population. The fungal population is considered to be moderately hostile to the host in this case.

Adapting the parameter values that were considered in the two-players game (see Figure 5.13) the regions for resulting evolutionary stable states in candida population, i.e., stable x^*, correspond to those presented in Figure 5.16. As next, I analyze the impact of cooperation and competition between the microbes on the population profile.

Targeting yeast cells does not pay off to the host

The final population profile depends on nutritional conditions and phagocytic strength of the PMNs. In the model, it was assumed that the PMNs are less attracted by yeast cells than by hyphal cells. Thus, following questions arise:

- What is the advantage for the host from targeting hyphal cells to higher extent?
- Why the host does not control the fungal burden by targeting also the yeast cells?

The simulations of the model point out that an increase in ability to target yeast cells, and hence, their increased phagocytosis, would lead to a higher fraction of the hyphae cells in the population. Thus, the population would become more hostile to the host (see Figure 5.17).

Let us assume that the nutritional conditions n are fixed in the model. Then, there are ranges of parameter k values such that the coexistence of two phenotypic forms is plausible. For those parameters, the corresponding payoff matrix indicates Snowdrift game dynamics interactions. It is due to the ranking of the payoff values that, in this case, satisfy the following inequality:

$$\pi(h,h) < \pi(y,h) < \pi(y,y) < \pi(h,y).$$

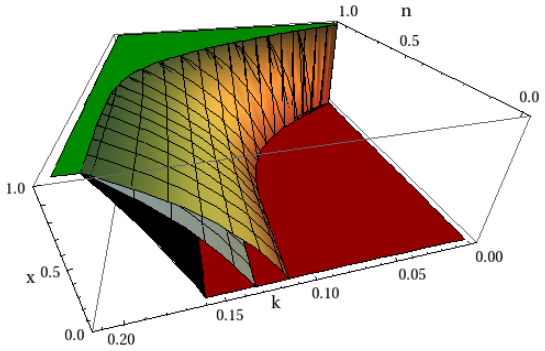

Figure 5.17.: Manipulations in PMNs phagocytic activity on yeast cells change the population profile. This is achieved by varying b in the following rate $\pi(y,h) = l(n) - bk$ where n is steady. By increasing the PMNs' attraction toward the yeast cells, i.e., increasing b, the hyphae cells become more pronounced in the population. (Green) Only yeast cells are present, $x = 1$. (Red) Only hyphal cells are present, $x = 0$. (Yellow through Grey to Black) $b = 0.25$, $b = 0.5$ and $b = 0.75$ respectively. The higher the value of b is, the lower is the fraction of yeast form.

In the model, the phagocytic activity of the PMNs influences the microbial interactions. As such, PMNs can exert either cooperative or competitive behavior on the microbes (see Figure 5.2). Cooperation between fungal cells will take place whenever the following relation is conserved:

$$\pi(y,y) < \pi(y,h) \,\&\, \pi(h,y). \tag{5.11}$$

In this case the presence of hyphae is good for the population of yeast cells as the fitness of yeast cell increases. On the other side, the fungi compete whenever the following relation is conserved:

$$\pi(y,h) < \pi(y,y) < \pi(h,y).$$

It means a hypha decreases fitness of the met yeast cell. By varying the parameter b in the payoff $\pi(y,h) = l(n) - bk$ we change the PMNs' phagocytic activity, and hence, we change the cost of cooperation between the cells. There is a critical value b^* that establishes a threshold for which the game dynamics interactions shift from a Snowdrift game dynamics to Prisonners' dilemma (Figure 5.18, left). To ease the manipulation of the yeast cells' fitness, the following is considered $\pi(y,h) = a \cdot l(n) - bk$. Also in this case, by varying the parameter a we can induce cooperation between the cells. There is a critical value a^* that determines the line between cooperation and competition between the cells (Figure 5.18, right). In general the population profile is not dependent on the initial fraction of yeast and hyphae. However, for some parameter values a bistability in the system may occur and only in this case the evolutionary stable state (ESS) depends on the initial yeast/hyphae ratio (Figure 5.19). Variations in PMNs specificity influence not only the population profile, but also the 'population response time' (PRT), i.e., time to reach half of the ESS (Figure 5.20). From Figure 5.20 we read

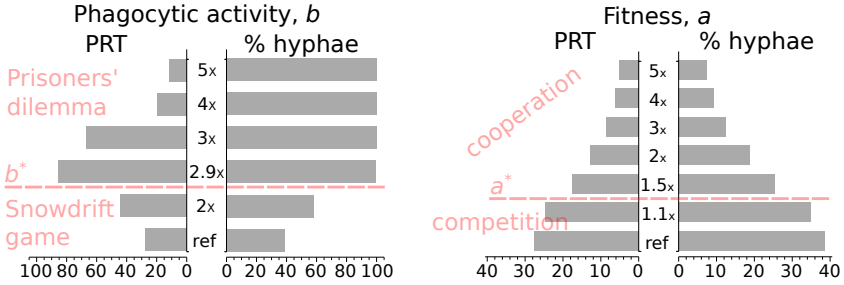

Figure 5.18.: Variations in PMNs' specificity and yeast cell fitness. The yeast proliferation rate $\pi(y,h) = a \cdot l(n) - bk$ is considered. Population response time, PRT, is the time point when 50% is reached from the initial yeast fraction to the ESS. (Left) The higher is b the more competitive are the cells. (Right) By increasing a we induce the cooperative behavior.

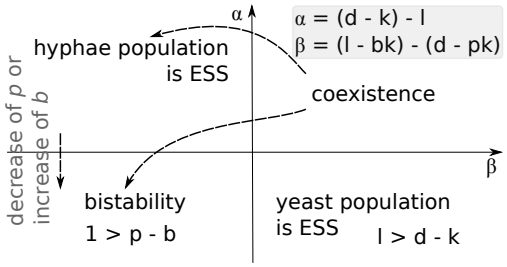

Figure 5.19.: Stability analysis of the population steady state. The differences between considered fitness values are given with $\alpha = \pi(h,y) - \pi(y,y)$, $\beta = \pi(y,h) - \pi(h,h)$. In quadrants I, II and IV the initial yeast/hyphae ratio does not influence the ESS. In theory immune response suppression, decrease of p in $\pi(h,h) = d - pk$, or loss of specificity, increase of b in $\pi(y,h) = l - bk$ can lead to a bi-stability in the system. In this case, i.e., for parameters in quadrant III, the initial yeast/hyphae ratio may change ESS.

that decreasing b - the attraction of PMNs toward yeast cells - we increase PRT. It means that the hyphae will need more time to outcompete the yeast cells (see also Figure 5.18, left, above b^* threshold). The critical value b^* of PMNs attraction toward yeast cells is the threshold that once passed results in a dramatic decrease of the PRT and an instant domination of hyphae in the fungal population (Figure 5.18). In this model the host status clearly affects the population profile what could be considered in addition to well established conditions for which hyphae development is triggered [Biswas et al., 2007, Whiteway & Bachewich, 2007, Shapiro & Cowen, 2010, Sudbery, 2011]. In conclusion, increased targeting and thus phagocytosis of the yeast cells would not payoff to the host as this could result in a development of a more hostile population.

Evolutionary models can be applied to study microbial populations that consist of cells that vary phenotypically. The dominance of one form or another is influenced by the external conditions. I assume that candida population although in some conditions might appear phenotypically homogenous, the genetic predisposition of the cells varies.

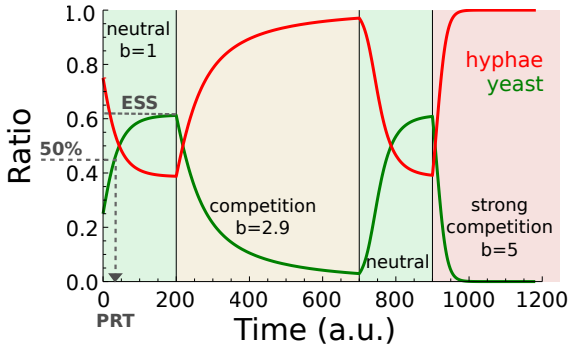

Figure 5.20.: Variation in time to reach the ESS. The yeast proliferation rate $\pi(y,h) = l(n) - bk$ is considered. Simulations are run for an initial yeast fraction of 0.25. Equal recognition of yeast and hyphae by the host, $b = 1$, is a point of reference and it corresponds to the region 'neutral'. For $b = 2.9$ the cells compete, for $b = 5$ a strong competition is assumed. In the green region yeast cells are favorable since their proportion increases (green line). Both forms will coexist and ESS for some value in $(0, 1)$ will establish. Population response time, PRT, is marked. With an increase of b, the cost of cooperation, the yeast cells fraction decreases.

In other words, when conditions change only part of the cells develop hyphae, i.e., those with predisposition. Such hyphae are persistent in the sense they will remain hyphae and give birth only to hyphae cells (also a new segment at the hyphal tip). Game dynamics interactions influence the proliferation rates of the cells types, and thus, fungal burden in the model.

Competition and host invasion

Competitive games are those where only one player can win, and in the candida population it would correspond to a situation where either pure yeast or pure hyphae is an ESS with given cell type as a winner. Obviously, the more we increase the cost of cooperation, which is the PMNs attraction toward yeast form, the more competitive the two forms become, i.e., their fitnesses $\pi(y,h)$ and $\pi(h,y)$ are more and more distant. For $\pi(y,h) < \pi(h,h)$ the yeast form becomes unsustainable and due to Prisoners' dilemma game dynamics interactions in the population hyphae will completely dominate the population. Although it would be more advantageous for the whole population to persist with the yeast form (see §1.3.3). Increasing the yeast benefit by changing environmental conditions via n (Figure 5.13), a cooperative behavior will be favored due to an increase of the fitness of both cell types. Consequently, yeast/hyphae fraction will increase in the population (similarly to the analysis in Figure 5.18, right).

The model developed here considers pairwise interactions in the fungal population that tune growth rates of both phenotypes. Such interactions could establish another level of communication for determining a balance in the microbial communities. In conclusion, external signals establish a difference between a cell's benefit and an associated cost

while interacting with another cell in the microbial population. In the abstract, if we relate the hyphae proportion to the severity of infection the above analysis indicates that cooperative behavior would be expected to occur in mild infections. The invasion of the host, accompanied by accumulation of hyphae, would then occur upon competitive game dynamics interactions. In some conditions pure hyphae population may establish what could be a result of Prisoners' dilemma game dynamics interactions. Although cooperative games dynamics interactions limit the fungal population capability to invade the host, due to reduced levels of hyphae, they allow the population to adapt to the external conditions more rapidly than competitive games (compare PRTs in Figure 5.18).

Model with nutrient consumption

So far I have analyzed the impact of PMNs activity and nutritional conditions on the population profile, and how these establish different interactions types between the cells, given that the nutrients are not being consumed. Now I look at how variations in these parameters affect the total fungal burden. I also allow for consumption of the nutrients in the system by the fungal cells and include a basal nutrient restoration rate (see Appendix C). The values that reflect proliferation rates (Figure 5.15) determine various game dynamics interactions in the population. Since the nutrients are utilized the fungal proliferation rates are changing over time (see Figure 5.21b). Whenever the following relation is conserved

$$\pi(h,h) < \pi(y,h) < \pi(y,y) < \pi(h,y) \tag{5.12}$$

a Game of chicken is being played (see §1.3.3). Considering that due to nutrient availability the proliferation rates change over time their corresponding time courses should be one above the other to fulfill Inequalities 5.12. In Figure 5.21b, starting from a time point about 7 the red line (payoff $\pi(h,h)$) is below the yellow line (payoff $\pi(y,h)$), which in turn is below the green line (payoff $\pi(y,y)$) and this one is below the orange line (payoff $\pi(h,y)$). Hence Inequality (5.12) is satisfied from the time point 7 on and Game of chicken dynamics are imposed on the system. As a result only hyphae form will be observed in the system since it is the only stable ESS. Competitive pairwise interactions dynamics are necessary for hyphae to dominate the fungal population. This will also result in severe infection followed by fungal invasion. On the other side, cooperative pairwise interactions result in a lower hyphae proportions (Figure 5.18, right), but such type of interactions leads to a higher fungal burden (Figure 5.21a).

In general, it is considered that the yeast cells favor dissemination into different body parts during the infection process [Jacobsen et al., 2012]. From the simulations of the model, the cooperation in the microbial population may establish in order to increase the size of a yeast form population (Figure 5.21a). On the other side, the coexistence of both forms is necessary for the dissemination as only hyphae are able to penetrate the epithelial cells what consequently allows the yeast cells to pass through. Hyphae

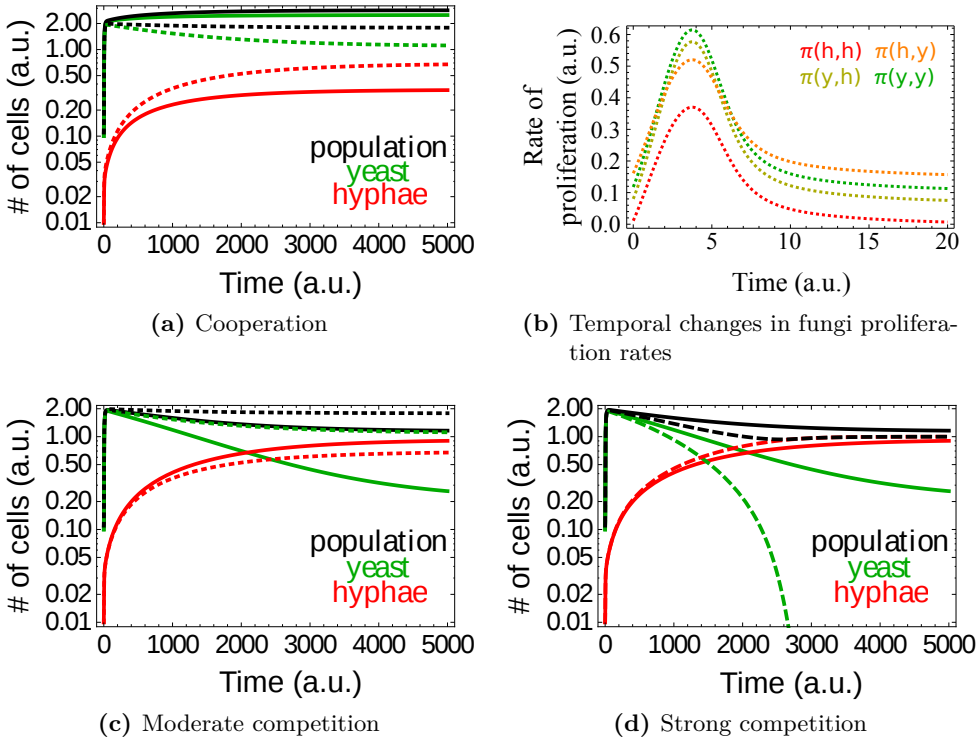

(a) Cooperation

(b) Temporal changes in fungi proliferation rates

(c) Moderate competition

(d) Strong competition

Figure 5.21.: The type of interaction influences the burden of the fungal subpopulations. In order to easily manipulate the yeast cell's fitness it is considered $\pi(y,h) = p_1 l(n) - p_2 bk$. By changing p_1 and p_2 either cooperation or competition between the cells will establish. In all cases dotted lines were determined for: $p_1 = p_2 = 1$; dashed lines $p_1 = 1$, $p_2 = 4$. **(a)** Solid lines were determined for $p_1 = 5$, $p_2 = 1$. By increasing yeast fitness, i.e., p_1, the cells are forced to cooperate. Total fungal burden increases (solid black line above dotted black line) but hyphae burden is decreased (red line below dotted red line). **(b)** Temporal changes in fungi proliferation rates influenced by nutrient consumption, $p_1 = p_2 = 1$. **(c)** Solid lines were determined for $p_1 = 1$, $p_2 = 2.9$. This enhances the competition between yeast and hyphae. The fungal burden is decreased (black solid line below black dotted line) but the population is more pathogenic (red solid line above red dotted line). **(d)** Strong competition allows for complete domination of hyphal cells - dashed green line drops drastically. The fungal burden is even more decreased when compared to **(c)** (dashed black below solid black line) but it is even more pathogenic (dashed red line above solid red line).

are also necessary in later stages in order to cross the endothelial cell layer. And again hyphae are important in order to facilitate an escape of the fungi from the vascular system. Since hyphal cells strongly activate the immune response, one role for yeast cells could be to maintain the high total population cells number without causing unwanted activation of the host immune response. In the final stages of infection, for instance

in the kidney, hyphal form is mainly observed [Lionakis et al., 2011], but according to the model presented here, a pure hyphae population can establish when both types of microbes are competing. This would imply that in the course of infection the types of interactions between fungal cells change from cooperative - necessary for crossing host barriers, to competitive - necessary for invading the organs. Summing up the above considerations it can be concluded that hyphal morphology exhibits 'double-crossing nature', in which the hyphae has a propensity to 'betray' the yeast once it has reached a desired niche.

Fungal infections are initiated by a colonization of the epithelial cells and an increased fungal growth rates. For the candidiasis to happen fungus has to cross the host barriers and hyphae are necessary at this point as they are able to penetrate the host cells. In the model presented in this section, hyphae fraction is being controlled by differentiable PMNs' attractions toward yeast and hyphae. Although higher attraction toward yeast cells would decrease the fungal burden (Figrue 5.21c and Figure 5.21d) such situation would lead to a development of fungal population that is more pathogenic and hence more competent to cross the host barriers. Hence, host's ability to distinguish between the two distinct fungi forms can be considered as its weapon that enables the host to control the possibly most benign population. In conclusion, we can postulate that the host would have no advantage from killing yeast cells more efficiently. Increased killing of yeast would result in more pathogenic fungal population and an increased risk of fungal invasion. Fungi cells have to cross two general host barriers: epithelial cells and then endothelial cells before they colonize the internal organs. There are few questions we can highlight at this point, for instance:

- Does the PMNs' specificity in targeting different fungal cells types vary at different stages?
- Do the PMNs' lose this specificity as the infection proceeds?

The simulations of the model indicate, that the answer to these question would depend on whether the yeast cells cause damage to the host at different stages of the infection or not.

There are cases reported with patients suffering from recurrent candidiasis. In the model developed in this section there are parameter ranges for which oscillations in the system can be observed. As such, e.g. when only 1% of the until now used nutrient restoration rate is applied, then damped oscillations in the fungal population will appear (Figure 5.22). By limiting the nutrient availability naturally the fungal burden will be decreased. This is seen in the simulations where fungal burden is decreased by two orders of magnitude when compared to the results in Figure 5.21.

5.3.5. Discussion

Systems where cooperativeness or competition between individuals occur are extensively studied. We seek the answer for a question what is a driving force for certain behav-

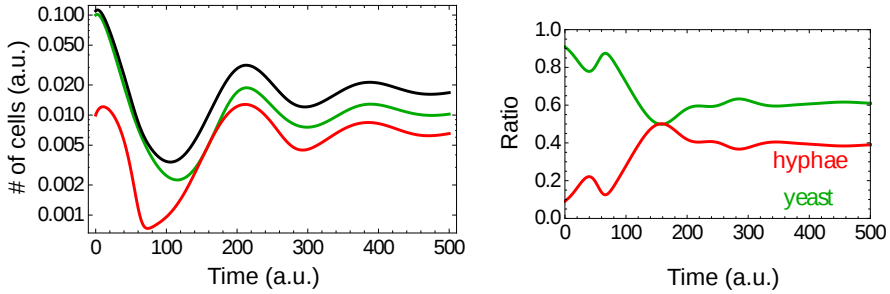

Figure 5.22.: Modifications in the nutrient restoration rate. Damped oscillations in the model can occur, for instance, by decreasing the so far used rate of nutrient restoration by a factor of 0.01. This also decreases the fungal burden by two orders of magnitude.

iors to establish in the population. The model of candida cells interactions presented above argues for a Snowdrift game dynamics interaction within fungal population that invades the host and this dynamics are induced by the host wealth. There are two main conclusions from the study.

- Two phenotypically distinct fungi cells will coexist when there is a low attraction of PMNs toward the yeast cells. This is also beneficial to the host since a less pathogenic population will establish.

- Strong PMNs' attraction toward yeast cells results in pure hyphae population and hence, more invasive. Increased targeting of the yeast cells may also lead to bistability in the system; the only case where the ESS will depend on the initial yeast/hyphae ratio.

The model simulations allow to partially answer the question: 'why the PMNs differentially recognize both fungal cells types?'. For example, an increased efficiency in targeting only hyphae keeps the invasive form on a low level even if this implies a higher fungal burden.

It has been reported that in a mouse model of systemic candidiasis, mainly hyphae cells are found in the kidney [Lionakis et al., 2011]. Basing on the analysis of the model's possible ESS it can be hypothesized that the microbial population evolves to a pure hyphae population due to, e.g. an increased cost of cooperation b in this internal organ. This would also imply, that the specificity of killing the hyphae cells by the host vanishes. In other words, hyphae-targeting rate can be considered to be specific for the niche in this case.

It is important to highlight that the model excludes the possibility of switching between the two forms. Instead, the fungal population consist of cells, where each cell has a predisposition to be either a yeast or a hyphae and their specific phenotype is only later determined by the external conditions. In other words I assume that the cells

vary, even if they may be not distinguishable beforehand when looking only at their current phenotype. Changes in the external world only favor one form more than the other and eventually cause the cells to express their 'concealed' phenotype. In theory, microbial populations could be composed of phenotypically distinct subpopulations with fluctuating advantages while the environment changes. This concept has been introduced in [Kumamoto & Pierce, 2011]. Lately, it has been hypothesized, that in terms of gene expression pattern, hyphae are different between distinct stages of the infection that also affects the host's ability to recognize the microbe and its capacity to activate defense mechanisms [Gow et al., 2012]. Because of that, the game dynamics interaction in the population vary as the infection progresses, and the respective two-persons game's payoff matrix is updated at each step. As already proposed in [Kumamoto & Pierce, 2011], also here in addition to environmental conditions, the host-pathogen interactions are tuned by presence of distinct phenotypes in the *C. albicans* population.

5.4. Phenotypic variability in microbial population: dynamics of the switch

Phenotypic changes of individuals in genetically homogenous populations are frequently observed [Avery, 2006]. Despite of living in the same environmental conditions some organisms carrying identical genetic information can display different phenotypes. The switch between distinct phenotypes can be induce by external conditions. In the previous section, section §5.3, it was assumed that a fungi population consists of cells of different phenotypes without a possibility to change it. New born cells were assumed to acquire the phenotype of the parental cell. In this section, I analyze how the assumption that the cells can change their phenotype influences the results obtained in the previous section. Investigated will be the advantage of the whole population from ability of the individuals to acquire different phenotypes. Among *Candida albicans* cells we can distinguish between yeast, hyphae and pseudohyphae cells types and different are isolated depending on the environmental conditions. In the mathematical model the external conditions are assumed to determine the proportions of the types of the cells which will be found in the fungal population. In theory, the fungus *C. albicans* would adjust the phenotype in order to increase its fitness in new environmental conditions. The dynamic model of switching in *Candida* population presented in this section implicates that under certain conditions the phenotypic variability takes place in order to increase the fitness of the whole population. In this section it is considered that the overall fungal burden determines the fitness of the population. In this context, the most fit population is the one with highest fungal burden.

5.4.1. Biological background

Interactions of the opportunistic pathogen *C. albicans* with its human host are complex. I have elaborated on this topic in §2.3. Here, only some aspects of the host-pathogen interactions are pointed out. Depending on the environmental conditions, the yeast can grow in distinct morphological states (as a yeast cell type, hyphae or pseudophypahe [Berman & Sudbery, 2002, Odds, 1998]). For modeling I consider only yeast and hyphae, also because these are the most extensively studied nowadays. Yeast and hyphae have different role during the commensalism and when infecting its host. For instance, the yeast form may facilitate dissemination [Jacobsen et al., 2012], while hyphae would be important for active epithelial penetration [Wachtler et al., 2012]. It is known that a starvation signal is a strong inducer of hyphae development [Biswas et al., 2007]. Hence, in the model the transition between yeast and hyphal states is governed by nutrient availability. Another important factor in the model that controls the phenotypic switch is the status of the host's immune system. It does not necessary mean that the host's status has a direct effect on the fungi phenotypic switch. Just like hyphae would indirectly activate the host's immune response, i.e., hyphae cells are sensed by the epithelium that secretes cytokines that stimulate the activation of the innate immune system

[Netea & Kullberg, 2010, Moyes et al., 2010]. The status of the host's immune system is included in the model and termed with 'immunity' in Figure 5.23.

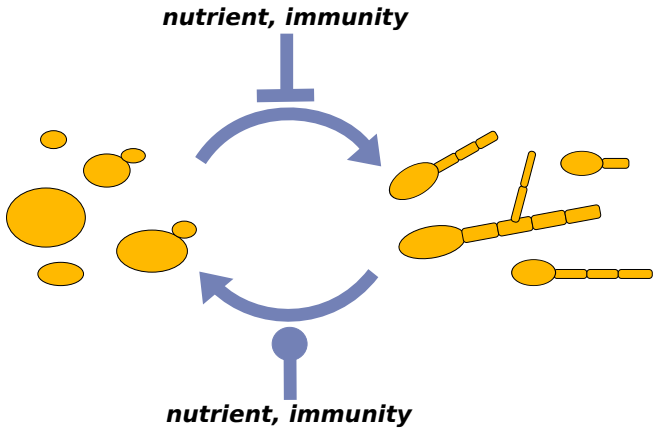

Figure 5.23.: Yeast to hyphae transition, master model. In the model the morphological transition is governed by nutrient availability and status of the host's immune system. The blind-ended line indicates the negative control over the switch under given conditions, while the dot-ended line expresses a positive control under specified conditions.

It is known that, immunocompromised patients are more susceptible to fungal infections and especially neutropenic patients are more likely to suffer from candidemia [Koh et al., 2008]. Therefore, it is justified to consider that the status of the host's immune system could control the phenotypic variability in the fungi population.

5.4.2. Model formulation

In this section I establish a dynamic mathematical model that describes how the pairwise fungal interactions influence the morphogenetic transition in microbial populations. The model is later used for investigation of how fluctuations in its parameters values, i.e., nutrient or status of the host's immune system, affect the fungal burden. I derive a formula that models the temporal contribution of each of the phenotypical forms in the population, i.e., yeast and hyphae fractions. Derivation of the mathematical model is largely based on the scheme presented in [Webb, 2007] and also in §5.2.1.

Each cell can live in one of the two different states s_1 and s_2, constantly switching back and forth between these states. I consider the evolution of switch in the population in a pairwise context, and thus, distinct switching rates will apply. There are fluctuations in the total size of population with some birth rate $\mathcal{B}$ and death rate $\mathcal{D}$ which are not affected by the fungal interactions in the population. It is assumed that a new born cell acquires the cell type of the parental cell. The total population size is given by

$$N = n_1 + n_2,$$

where n_1 is the number of individuals currently in the state s_1 and n_2 is the number of individuals in the state s_2. Proportions of individuals that are present in each of the states are given by

$$x_i = \frac{n_i}{N}. \tag{5.13}$$

Hence, the population profile is given by the vector $\mathbf{x} = (x_1, x_2)$. Individuals switch from s_1 to s_2 at average rate $\pi(s_1, \mathbf{x}) > 0$ decreasing the size of the subpopulation of the type s_1 and increasing the size of the subpopulation of the type s_2. Similar holds when cells switch from s_2 to s_1 at average rate $\pi(s_2, \mathbf{x}) > 0$. Hence, the system describing dynamics of switch from one type to another can be represented by the following set of ordinary differential equations

$$\begin{aligned} \dot{n}_1 = &\ (\underbrace{\mathcal{B}_1 - \mathcal{D}_1}_{\alpha_1})n_1 - n_1\pi(s_1, \mathbf{x}) + n_2\pi(s_2, \mathbf{x}) \\ \dot{n}_2 = &\ (\underbrace{\mathcal{B}_2 - \mathcal{D}_2}_{\alpha_2})n_2 + n_1\pi(s_1, \mathbf{x}) - n_2\pi(s_2, \mathbf{x}). \end{aligned} \tag{5.14}$$

In the above formulae $\pi(s_i, \mathbf{x})$ for $i = 1, 2$ are the average rates of switch for the type i and they depend on the proportions of each cell type due to pairwise interactions. We should consider that a cell in state s_i can either meet a cell of type s_1 with a probability x_1, or a cell of type s_2 with a probability x_2. Hence, the transition rates $\pi(s_i, \mathbf{x})$ between distinct morphological forms vary and are affected by the fractions x_1 and x_2. In particular, the transition $\pi(s_1, \mathbf{x})$ from the morphological form s_1 to s_2 is affected by the opponent s_j met what establishes the rate of switch $\tau(s_1, s_j)$ with a probability x_j, where $j \in \{1, 2\}$, and the following applies

$$\pi(s_1, \mathbf{x}) = \tau(s_1, s_1)x_1 + \tau(s_1, s_2)(1 - x_1).$$

Analogously for the second cell type we obtain

$$\pi(s_2, \mathbf{x}) = \tau(s_2, s_1)x_1 + \tau(s_2, s_2)(1 - x_1).$$

For $\alpha_1 = \alpha_2$, changes in the population size are given by

$$\dot{N} = \sum_{i=1}^{2} \dot{n}_i = \alpha_1 n_1 + \alpha_2 n_2 = \alpha N,$$

and thus, the population either follows exponential growth (for $\alpha > 0$) or declines exponentially (for $\alpha < 0$). As next, I derive a formula for temporal changes of the fractional contributions of each cell type in the population. From Equation 5.13 we obtain

$$\dot{n}_i = \dot{x}_i N + x_i \dot{N},$$

and hence,

$$\begin{aligned}\dot{x}_1 &= \frac{\dot{n}_1}{N} - x_1 \sum_{i=1}^{2} \frac{\alpha_i n_i}{N} \\ &= \frac{\alpha_1 n_1 - n_1 \pi(s_1, \mathbf{x}) + n_2 \pi(s_2, \mathbf{x})}{N} - x_1(\alpha_1 x_1 + \alpha_2 x_2) \\ &= x_1(\alpha_1 - \alpha_1 x_1 - \alpha_2 x_2) - x_1 \pi(s_1, \mathbf{x}) + x_2 \pi(s_2, \mathbf{x}).\end{aligned} \tag{5.15}$$

Taking into account that $x_1 + x_2 = 1$ the above formula simplifies to the following form

$$\dot{x}_1 = x_1(1 - x_1)(\alpha_1 - \alpha_2) - x_1 \pi(s_1, \mathbf{x}) + (1 - x_1)\pi(s_2, \mathbf{x}). \tag{5.16}$$

The time course of x_1 from Equation 5.16 follows the temporal changes in the proportions of cells of type s_1 in the population. These are influenced by the death and birth rates in both s_1 and s_2 subpopulations. Only in case $\alpha_1 = \alpha_2$ the proportional changes of both subpopulations over time are not affected by birth and death processes. Since $x_2 = 1 - x_1$ the temporal changes in the proportion of cells s_2 are given by $\dot{x}_2 = -\dot{x}_1$.

5.4.3. Analysis of the system

Let x be the fraction of s_1 type in the population. The equation derived in the previous section:

$$\dot{x} = x(1 - x)(\alpha_1 - \alpha_2) - x\pi(s_1, \mathbf{x}) + (1 - x)\pi(s_2, \mathbf{x}) = f(x) \tag{5.17}$$

has two possible steady state solutions. To ease stability analysis of these points let us consider:

$$\begin{aligned}\beta &= \alpha_1 - \alpha_2, \\ a &= \tau(s_1, s_1), \qquad b = \tau(s_1, s_2), \\ c &= \tau(s_2, s_1), \qquad d = \tau(s_2, s_2), \\ \delta &= b^2 + \beta^2 + 2\beta c + c^2 - 2b(\beta + c) + 4ad.\end{aligned} \tag{5.18}$$

For $f(x) = 0$ we obtain the following solutions

$$\hat{x}_1 = \frac{\beta - b + c - 2d + \sqrt{\delta}}{2(a - b + c - d + \beta)} \quad \text{and} \quad \hat{x}_2 = \frac{\beta - b + c - 2d - \sqrt{\delta}}{2(a - b + c - d + \beta)}. \tag{5.19}$$

Steady states' stability analysis reveals that the steady state $\hat{x}_1$ is a stable point and the other one, $\hat{x}_2$, is unstable. It is due to the fact that

$$f'(x_1) = -\sqrt{\delta} \quad \text{and} \quad f'(x_2) = \sqrt{\delta}, \quad \text{where} \quad \delta > 0. \tag{5.20}$$

The rates of switch from one form to the other one are expected to be positive thus also the values of the parameters a, b, c, d should be positive. x from the Equation 5.17 takes values in the range $[0, 1]$, and hence, the population profile will evolve either to 0, 1 or to some state $x \in (0, 1)$ independently of the initial conditions (Figure 5.24). In order

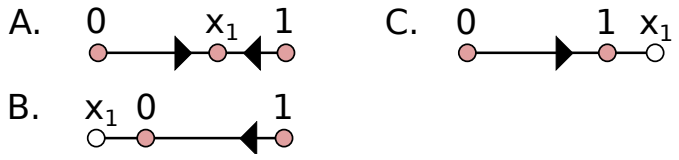

Figure 5.24.: Stability of the population's steady profile. (A) In case $\hat{x}_1 \in (0,1)$ both forms will coexist at steady state. (B) If $\hat{x}_1 < 0$ form s_1 will die out. (C) If $\hat{x}_1 > 1$ then only form s_1 will survive.

to represent graphically the dependencies between parameters' values and the resulting population profile, I set $a = 1$. The relative difference between the rates of switch d and $b - c$ change the population profile. They are compared for distinct values of β and presented in Figure 5.25.

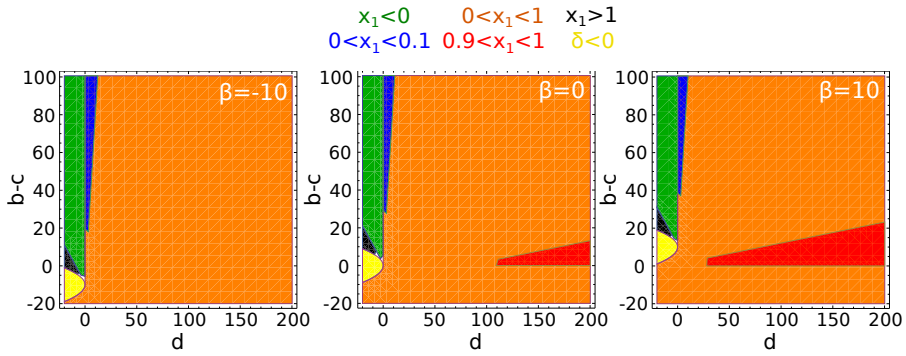

Figure 5.25.: Population profile for various β. x_1 is the final fraction of type s_1. The fractions of s_1 at steady state are color coded in the legend of the figure. The distance $b - c$ is the relative difference in a cell's rates to change from s_1 to s_2 and *vice versa*.

5.4.4. Model and Results

Model setup

The candida population consists of cells that are able to display different phenotypes depending on the environmental conditions. The cells are assumed to be able to exist in a yeast form and in a hyphae and they are constantly switching the phenotype. The phenotypical transition is additionally regulated by pairwise interactions between the individuals in the population (Figure 5.26). The interactions are dependent on the proportions of different cells' types. Discussed will be different cases on restrictions on the switch between the phenotypes. As first considered is the model in Figure 5.23 where the cells are able to switch both from yeast to hyphae (y2h) and from hyphae to yeast (h2y). Rates of switching are determined by nutrient availability and overall status of the host's immune system. It is assumed that under rich nutritional conditions yeast

form is the persistent one (Figure 5.27). In such case, it is unlikely that the yeast cells

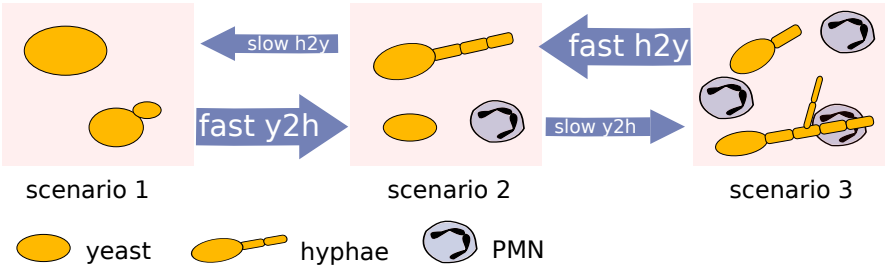

Figure 5.26.: Rates of switch are determined by the pairwise interactions. The switching dynamics are affected by the status of the immune system of the host. Considered are environmental conditions stimulating hyphae formation. In the scenario 1 the switch from yeast to hyphae (y2h) is relatively fast. Since the host's immune system is activated by the presence of hyphae, in the scenario 2 the y2h rate is down regulated. The more hyphae is present the stronger immune response, and hence, the switching rate from hyphae to yeast (h2y) is faster than in scenario 2.

will switch the phenotype and develop germ tubes, as it would only cause unnecessary activation of the host's immune system response. In contrary, under sparse nutritional conditions hyphal form becomes favorable and the yeast cells are prone to change their morphological state. The dependencies are illustrated in Figure 5.27 where the fungus' ability to trigger either y2h or h2y switch depends on nutrient. Based on Figure 5.27

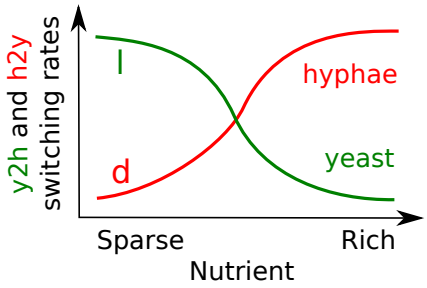

Figure 5.27.: Qualitative description of cell's transition to another phenotypic state. Rich nutrients favor yeast cell type and sparse nutrients govern the y2h switch at rate l. The h2y switch is governed at rate d. The worse are the nutritional conditions the higher is the y2h switching rate.

we can derive the switching rates for all scenarios presented in Figure 5.26. The status of the host's immune system k is now included. Parameter n indicates the nutritional conditions.

- In case two yeast cells are interacting the y2h switching rate is given by $\tau(y, y) = l(n)$. However, when a yeast cell communicates with a hyphal cell then the status

of the host's immune system k decreases the y2h switching rate. Hence, for the yeast cell the formula $\tau(y,h) = l(n) - b \cdot k$ will apply.

- It is assumed that the status of the host's immune system can potentially affect the h2y switching rate $d(n)$ and speed it up. Hence, when a hyphal cell communicates with a yeast cell then the h2y switching rate is set to $\tau(h,y) = d(n) + k$.
- The activation of the immune system response is considered to be dependent also on the hyphae burden. The more hyphae the more active is the immune system and consequently the faster will be the h2y switching rate. Hence, in the scenario where two hyphae are interacting a rate of switch $\tau(h,h) = d(n) + 2k$ for each hyphae is set.

The expressions for the y2h and h2y switching rates are collected in the matrix in Figure 5.28. In the model of switching the dynamics are governed by two functions l, d which are dependent on nutrient, and the host's status k. The analysis of the model presented in this section is focused solely on qualitative behavior (see Figure 5.27). Hence, I assume:

$$\begin{aligned} d(n) &= \frac{vn^\sigma}{n^\sigma + K^\sigma}, \\ l(n) &= 1 - d(n), \quad \text{where} \\ v &= 1,\ K = 0.1,\ \sigma = 4. \end{aligned} \tag{5.21}$$

As a consequence, different population profiles will establish when varying either nutrient availability n or the status of the host's immune system k. The relative contributions of yeast and hyphae in the population are calculated basing on the formula for x_1 given in Equation 5.19. I consider a case where $\beta = 0$, i.e., there are no fluctuations in the size of

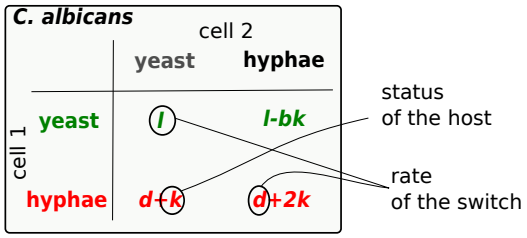

Figure 5.28.: The y2h and h2y switching rates. Cell 1 will change the phenotype at rate color-coded in the table. Parameter k is variable and expresses the status of the host's immune system. Parameters l and d are the functions of parameter n which indicates the nutrient availability.

population, phenotypic changes occur based only on pairwise interactions. From Figure 5.29 we observe that a mix of both forms will always be observed in the population.
From the analysis presented in Figure 5.29 we can draw the conclusion that a partially compromised immune system, i.e., with a reduced ability to recognize the yeast cells and

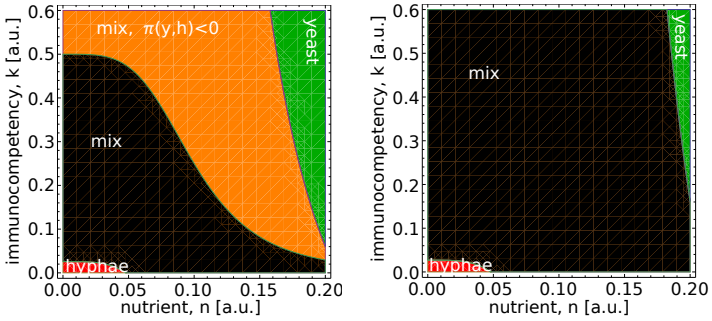

(a) $\beta = 0$, $b = 2$
Mild (green) and strong (red) infection is marked

(b) $\beta = 0$, $b = 0.05$

Figure 5.29.: Stable population profiles. Variable are the status of the host's immune system k and the nutrient resources n. Black and orange regions represent the coexistence of both yeast and hyphae. The orange region couples the parameters values for which the rate of switch $\tau(y, h)$ is negative. (a) The yeast/hyphae ratio in the population is always kept in the range $(0, 1)$. Hence, regions of mild and strong infection are marked, i.e., green region corresponds to high yeast type content ($> 95\%$) and red region to high hyphae fraction ($> 95\%$). (b) A decrease in b in $\tau(y, h) = l(n) - b \cdot k$. Region of strong infection (red) is not affected but in general the population becomes more pathogenic. The yeast fraction decreases and mild infection (green) establishes only for more active immune system and in better nutritional conditions.

ability to prevent them from switching, increases the rate of yeast to hyphae transition and, hence, a more pathogenic population will establish. This is simulated by decreasing b in the y2h switching rate $\tau(y, h) = l(n) - b \cdot k$. In game theoretical model presented in the previous section, a more pathogenic population would establish as an outcome of the enhanced competition between yeast and hyphae form. But, the competition between the cells was induced there by decreasing the fitness of yeast cells due to a higher PMNs' attraction. It is important to stress the assumptions about the nature of interactions in populations in both models. In the model of switching the status of the host's immune system controls fungal phenotypic states. In this case, the host-pathogen interactions establish how the population profile shifts. The fungi are in permanent contact with its host that determines the direction of their phenotypical switch. Here, all the cells undergo phenotypic switch, unlike in the game theoretic model, where cells are committed to their phenotype and only their proliferation rates vary.

Environmental conditions determine the population profile

Yeast to hyphae and hyphae to yeast rates of switching are controlled by the status of the host's immune system. The host's ability to distinguish between the two forms of the fungi are crucial in establishing the balance between yeast and hyphae cells content

in the population. The immunocompetent host prevents the y2h switch (Figure 5.23). In Figure 5.30 we see how the strength of the host's immune system response affects the population profile. The profile is modeled with Equation 5.17. We observe that the more

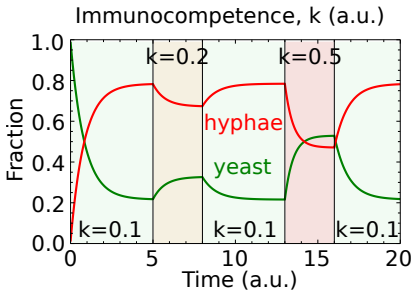

Figure 5.30.: Population profile for various levels of the host's immunocompetence. Simulations of Equation 5.17 with parameters values $v = 1$, $K = 0.1$, $\delta = 4$, $n = 0.05$ and $\beta = 0$. The higher the host's immune system ability to recognize the fungi, the more efficiently is blocked y2h transition and the faster is h2y rate and, hence, the less hyphae are present.

active is the host's immune system the less hyphae is present in the population (Figure 5.30). With an increase of the strength of the host's immune response the population response time, PRT, is also reached faster (see §5.3.4 for definition). The yeast cells will more likely switch to hyphae when sensing sparse nutritional conditions (Figure 5.27). In order to decrease the y2h switch, the rate $\tau(y, h) = l - b \cdot k$ must be reduced. It means that the host immune response must be activated to higher extent. In rich nutritional conditions this is not a good strategy as in rich nutrient $\tau(y, h)$ is more sensitive to the immune system's activity and it could become negative for hyperactive immune cells.

Modifications in the y2h and h2y switching rates

The model presented in Figure 5.23 is our 'master model'. In this section, its variants are used for the analysis of other hypothesis. As first, I consider a scenario where the hyphae-to-yeast switch is not affected by the activity of the host's immune cells (Figure 5.31a). It means that the host can reduce only the y2h transition rate. In this model variant, the h2y transition is triggered solely by the nutritional conditions. In the modified model when varying the strength of the host's immune response only $\tau(y, h)$ changes, since both $\tau(h, y) = \tau(h, h) = d$ in this model. From the analysis of Figures 5.31c and 5.31d we can conclude that in the modified model higher fractions of hyphae will establish when compared to the 'master model' (compare yellow bars). In both models fraction of hyphae drops with an increased strength of the immune system. Increased host's immunocompetency results in an increase of the PRTs in the modified model, in contrary to what is observed for the 'master model' (compare blue bars in both figures). In conclusion, it is advantageous for the host to control both y2h and h2y switching rates as it reduces the time needed to establish balance in the microbial

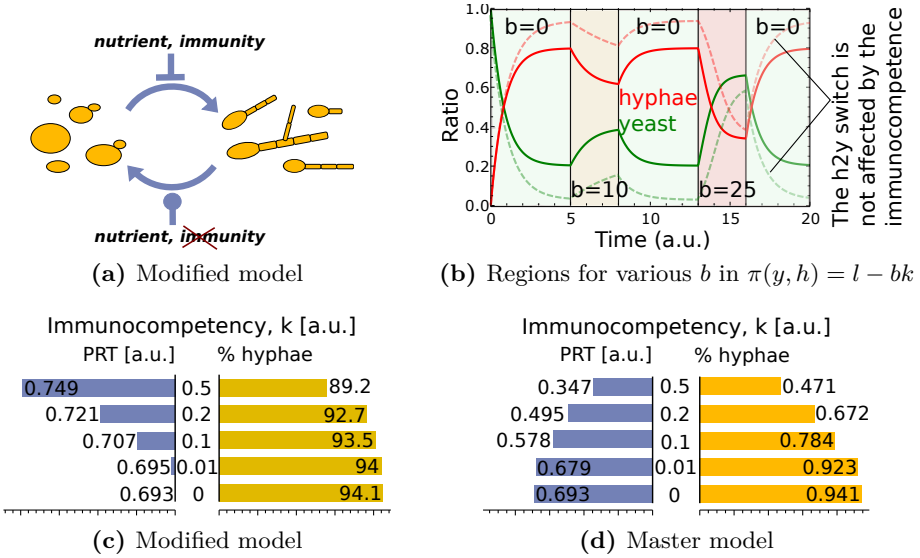

(a) Modified model **(b)** Regions for various b in $\pi(y,h) = l - bk$

(c) Modified model **(d)** Master model

Figure 5.31.: Population dynamics when h2y switching rate is not affected by the host. Simulations were performed with following parameters values $v = 1$, $K = 1$, $\delta = 4$, $n = 0.5$. (a) h2y transition is not affected by the status of the host's immune system. (b) In the modified model (dotted lines), the population reaches a higher hyphae fraction when compared to the master model (solid lines). (c, d) PRTs and hyphae fractions between the two models are compared when varying the strength of the host's immune system k.

population.

With help of the model of switching dynamics in the fungal population we can now give an answer to following questions:

- Why is the fungus switching between two distinct, but still genetically identical, morphological states?
- Switching between yeast form and hyphal form has associated costs related to the changes in gene expression pattern resulting in, e.g., a reconstruction of the cell wall, etc. What is then the advantage from the switch?

To answer the above posed questions two variants of the master model are considered. This time I look at the fungal burden and not at the yeast/hyphae ratios. I analyze the effect of deleting either h2y or both y2h and h2y switch on the fungal burden. Following models are being compared (Figure 5.32):

- (1) The master model which has implemented both y2h and h2y switch. Considered is the ODE model given in Equation 5.14 and parameters are set to $v = 1$, $K = 0.1$, $\delta = 4$, initial number of yeast cells is set to $n_1^0 = 1000$ and initial number of hyphae cells is set to $n_2^0 = 10$. α_1 and α_2 are given in Appendix D.

- (2) In model 2 the transitions y2h and h2y are not considered. Each cell type can only reproduce giving birth to exactly the same cell type. Replication is the only process that influences the temporal changes of yeast and hyphae cells numbers. See Appendix D for the equations.
- (3) In model 3 the switch from hyphae to yeast is blocked. In this context hyphae is a resistant form, i.e., once the hyphae phenotype is acquired it will not switch back to the yeast form. See Appendix D for the equations.

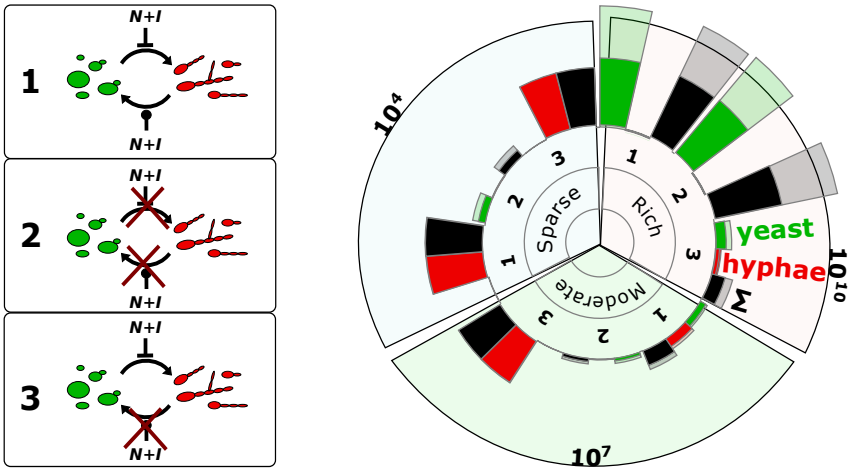

Figure 5.32.: Comparison of the master model and its two variants. Fungal burden is a scoring measure for the best model. On the right, rich, moderate and sparse nutrient conditions are considered and compared are all the three models in each of the conditions. In each situation yeast (green bars), hyphae (red bars) and total fungal burden (black bars) are plotted. In rich nutrient model 1 and model 2 are the leading ones and the process of phenotypic switch does not greatly influence the fungal burden. For moderate nutrient, a model with a resistant phenotype (model 3) is the leading one. For sparse nutritional conditions, it does not matter if hyphae is a resistant form or not, phenotypic switch increases the fitness of the fungal population. Lighter bars store the results for the immunocompromised host ($k = 0.001$), darker - for the healthy host ($k = 0.003$).

Simulations of the models reveal that in rich nutritional conditions activation of the machinery to change the phenotype is not necessary advantageous as both, the model with y2h and h2y switch (model 1) and the model with no switch in any of the directions (model 2), are performing equally well and lead to similar fungal burdens. However, already for moderate nutritional conditions the ability to switch the phenotype becomes advantageous as it increases the fungal burden. In such conditions the model with hyphae as a resistant form (model 3) performs the best. In very pure nutritional conditions, it does not matter whether hyphae is resistant or not since both models increase the fitness of the population leading to a higher fungal burden when compared to the model with no switch allowed (model 2). Decreasing the strength of the host's immune response k

leads to similar conclusions and it is depicted in Figure 5.32 with bars in lighter colors. In rich nutritional conditions and for an immuno-not-competent host the fungal burden drastically increases. In moderate and sparse nutritional conditions, decreased efficiency of the host's immune system response does not significantly influence the resulting fungal burden. Only when switch in both directions is implemented (model 1) efficiency of the host's immune system response affects the fungal burden in moderate nutrient.

5.4.5. Discussion

Different hypothesis on the nature of the host-pathogen interactions are considered and for each there are supporting experimental evidences. One possibility is that according to the environmental conditions fungal cells reprogram their gene expression pattern and change to a pathogenic and dangerous form to its host [Hube, 2011]. Other hypothesis assumes that fungal population consists of both benign and dangerous form and depending on the environmental conditions either one or another form is favorable and dominates the population [Kumamoto & Pierce, 2011]. The model of switching dynamics presented in this section considers yet another view on the nature of the host-pathogen interactions. It assumes that the pathogen and the host are constantly interacting and the fungus continuously adjusts its state according to the environmental conditions. Such view has also an experimental basis [Mochon et al., 2010, Rosenbach et al., 2010, Hube, 2011].

When developing a 'master model' (Figure 5.27) it was assumed that in the microbial population pairwise interactions take place. Each cell has a propensity to acquire certain phenotype and it varies according to the current population profile. It is assumed that all the cells undergo phenotypic switch unlike to the game theoretic model, where cells are committed to their phenotype. With an appropriate experimental data set we can study to what extent immune system affects the switching dynamics. One could analyze whether the rate of switch is in proportional relationship with nutritional conditions or whether there is a cutoff value that activates the switch. The cutoff might vary depending on y2h or h2y switch. A key experiment would be to test how the differentiable strength of yeast cells' recognition influence the population profile, since it would allow us to answer the question whether pairwise interactions establish game dynamics interactions in fungal population or control the dynamics of switch. The analysis of the model variants revealed that fungi developed the mechanisms that allow them for phenotypic changes in order to increase the population fitness when nutrients are sparse. Although there are costs associated with the phenotypical transition, it is advantageous to undergo the transition as it increases the population size, and therefore, a probability the population will survive in harsh conditions. We have seen that in rich nutritional conditions the switch is not necessary (Figure 5.32). Decreased host's immunocompetency leads to even higher fungal burden, especially in rich nutritional conditions.

In immunocompromised patients a disruption of the host microflora due to e.g., antimicrobial drug treatment, etc., is very often associated with an increased fungal burden. In this case a disruption in the microflora could also be seen as a situation where more

nutrients become available to the fungus due to elimination of the species competing for common resources. This fits the model's predictions where in a better nutrient a higher fungal burden occurs (Figure 5.32). Interestingly, the lose of functionality in the host's immune system response would not significantly influence the fungal burden when moderate or sparse nutrient environment is considered. One explanation to consider could be that in pure nutritional conditions the phenotypic switch from yeast to hyphae is promoted. Costs associated with the morphological transition might be already so large that the additional costs associated with proliferation can not be compensated from the available nutrient. Assuming that the cells interact and adjust the population profile accordingly, models presented in this section and in the previous one, could be used for studying what is the nature of the fungal interactions and if then how the host contributes to these.

5.5. Discussion

In this chapter I apply two approaches to study fungal population dynamics. In both cases the microbial interactions are understood in a pairwise context but the nature of these interactions differ in each model. I refer to the population with low hyphae content as a benign population that does not cause any harm to its host. A population with a high hyphae content is seen as a pathogenic one that damages the host. As such both in the game theoretical model and the model of switching dynamics partially compromised functionality of the immune system (PMNs in the first one; generally immune system in the second one) can aid the fungal population to become more pathogenic. However, in the game theoretical model when varying PMNs recognition of the yeast form (without changing PMNs capability to recognize hyphae cells) a decrease in yeast killing leads to a development of less pathogenic population (Figure 5.21a), whereas in the model of switching decreased ability of the immune system to interact with the yeast form could aid the population to become more pathogenic (Figure D.1). The appropriate experimental data would allow us to assess what is the nature of the interactions between the cells. Below, I analyze consequences of distinct assumptions that I made when applying each of the approaches.

- In section §5.3, I apply the game theoretical framework. I use the replicator equation to study evolutionary game dynamics interactions assumed to be played in microbial populations. I assume that the candida population consists of cells that have various predispositions to express either yeast or hyphae phenotype. Depending on the environmental conditions either one or the other phenotype is more advantageous and dominates the population. In some conditions the population can appear phenotypically homogenous but in some other conditions distinct phenotypes can be isolated what is determined by the cells predispositions. In line with the assumption, it would be possible due to the presence of cells in the population that conceal their true phenotype, and which becomes expressed only when external conditions allow for that (a hypothesis proposed in [Kumamoto & Pierce, 2011]). In some conditions, one type is under pressure, i.e. less favorable and with a reduced fitness what leads to a decrease in the cell numbers. Whereas the other cell type in new environmental conditions becomes more advantageous, acquires its phenotype, its proliferation rate increases, and hence, it becomes more pronounced in the population. But there is no switching between the phenotypes and each new born cell acquires the phenotype of the parental cell.

- In section §5.4, I assume that presence of distinct phenotypes in the population results from the switching between one form and the other one. It is assumed that all cells can undergo the yeast to hyphae and hyphae to yeast transition. In this context, the environmental conditions and communication between the cells establish the rates of switching, and not the rates of proliferation. Simulations of

the model of switching dynamics show that the fungal burden greatly increases in a weakened host and in a nutrient-rich environment. These conditions could reflect a scenario where a sick patient is given a therapy. For instance, antibacterial drug treatment destroys the balance in the microflora, microbes are eliminated and, thus, candida cells have access to more nutrients. In both immunocompetent and immuno-not-competent hosts this results in an increased fungal burden where the rate of yeast cells' proliferation increases. In the model of switching dynamics the immune system response prevents the phenotypical transitions. If we would like to consider how the phagocytic activity affects the switch then we would have to apply different expressions for $\tau(s_i, s_j)$ for s_i, $s_j \in \{y, h\}$ (see §5.4.4 and Figure 5.28) in such a way that the cells are eliminated from the system.

The models presented in this chapter can be further extended, e.g., by combining both of the presented approaches, etc. As such, the game theoretical approach can be incorporated into the model of switching dynamics as a substitute for α_1 and α_2 (Equation 5.14). It would be interesting to consider applications of this sort of approaches to study more complex microbial communities that consist of more than two cell types or strains. By establishing evolutionary games one could identify the strains that are cooperating or competing with each other what might not be trivial to assess experimentally when many strains are facing each other.

6. Discussion

Fungal infections are striking medical problems. Understanding the biology of fungal pathogens is necessary for a successful treatment, but also in prevention, since many infections have a nosocomial background. The yeast *Candida albicans* is an isolate causing the majority of human fungal infections. Detailed analyses of the cycle of candida infection will reveal crucial attributes of the fungus that allow it to invade a human. *C. albicans* is a habitant of human microflora and gastrointestinal tracts. Whilst it displays a commensal life style in the healthy individuals, the immuno-not-competent patients are particularly susceptible to *Candida* infection. This is facilitated due to the fungus' ability to switch between a variety of morphological states, i.e., yeast, hyphae, and pseudohyphae. Ability to undergo phenotypic transition to display a hyphae form is an important fungus' virulence factor. Hyphae are more prone to attach to the host tissues, a step necessary in the invasion and penetration of the host's epithelial and endothelial cells. In mouse model of systemic candidiasis, the non filamentous candida cells are not able to disseminate [Lo et al., 1997]. Consequently, the phenotypic transition could be considered as a potential therapeutic target [Jacobsen et al., 2012]. Prior to fungal invasion, a colonization of the mucosa by the fungi takes place. The colonization is associated with an increased fungal burden and accumulation of hyphal cells in the microbial population. During the course of infection, *C. albicans* cells experience changes in the environmental conditions that occur due to a fungi penetration to new host niches. The fungi can survive in its human host due to an ability to adapt to the fluctuations in external conditions. The fungal adaptation is achieved via activation of molecular mechanisms that lead to changes in genes expression patterns.

At different stages of the infection the fungi cope with different types of stresses, e.g., oxidative stress due to an activity of the host phagocytic cells, or thermal shock due to a fever. Understanding of how the fungus manages to successfully inhabit different human niches is crucial in combating this human pathogen [Tyc & Klipp, 2011]. In this thesis, I explore several aspects of the host-*Candida albicans* interactions. In each chapter I discuss different features of fungi interactions with its host, e.g., adaptation to thermal stress, or evolution of the population profile dynamics. For each problem a different computational technique is applied. The host-pathogen interactions are very complex, but using mathematical models we can investigate their mutual dependencies, and we can provide the relevant hypothesis regarding the basis of these interactions.

We can consider various granularity levels for studying how the fungi and the host influence one another. We either consider the molecular interactions within the fungal cells activated by the host's microenvironment, e.g., conditions imposed by the phago-

cytic cells, or by zooming out, we can view the host-pathogen interactions as an interplay between different host and fungal cells types. I assume that the dynamics of the fungal population profile are governed by the pairwise interactions among fungal cells, that are in addition regulated by the host's responses and environmental conditions. Different hypothesis are considered in order to assess the nature of types of interactions necessary to explain certain properties observed in the dynamics of the population profile.

The results presented in this thesis are divided into three parts. As first, I present a mathematical model that describes dynamics of molecular interactions upon the heat stress application. Next, I construct an agent-based model of fungal colonization of the epithelial cells. The model is then used to analyze the effect of various drug doses on fungal population dynamics. In the last chapter of this thesis, I investigate dynamics of the fungal population that are result of microbial pairwise interactions. Below I summarize the results of my work and discuss possible models' extensions.

Adaptation to thermal insults

An essential condition for an organism to survive in fluctuating environment is the ability to respond, quickly and effective, to the changes in outer world. During the course of infection *C. albicans* cells have to cope with a variety of stresses. One of them is a thermal upshift due to development of fever in the attacked host. This problem is addressed in Chapter 3 where the focus is on how the dynamic properties of molecular interactions allow the cells to adapt to thermal insults. A dynamic model of heat stress response in *C. albicans* is described and represented by a set of ordinary differential equations. The model is supported with experimental data obtained for two heat shocks: (1) application of 37°C heat stress to the cells cultivated at 30°C, and (2) a transfer of the cells from 30°C to 42°C. Key measurements for the model were the investigation of the dynamics of phosphorylated Hsf1 and *HSP90*mRNA in both stress conditions, and they are used to parameterize the ODE model. The ODE model captures the principal dynamics of thermal adaption in the fungus what is observed by comparing simulation results to the experimental data of phosphorylated Hsf1, as well as by examining the fold induction of Hsf1's target gene, *HSP90*mRNA. The presented model is one of the first to discuss dynamic interactions of molecules activated upon heat stress response in the human fungal pathogen *C. albicans*. The ODE model is based on the assumption that the Hsp90 protein is a key regulator in the candida heat stress response, which is governed via downregulation of Hsf1 transcriptional activity. The study of the adaptation to heat stress revealed several features of the system's dynamics.

- An instant phosphorylation of Hsf1 and its gradual dephosphorylation is viewed as an adaptation process of the system to the thermal shock. The system displays perfect adaptation what can be observed in Hsf1 complete dephosphorylation within the time frame investigated in the study. The perfect adaptation is observed in every condition tested, including sequential heat shocks treatments, during ap-

plication of stepwise heat shocks, or upon a gradual temperature increase. The perfect adaptation of the system is in agreement with the published experimental results where cells cultivated at different growth temperatures were never displaying phosphorylation of Hsf1 in steady cultures [Nicholls et al., 2009].

- The simulations of the model indicated a transient molecular memory in the system. The molecular memory is examined by looking at the deviations in the dynamics of the phosphorylation levels of Hsf1 (Hsf1P) during a second heat stress with respect to the dynamics of Hsf1P observed upon a single treatment of the system with a heat stress of the same strength. The simulations of the model show reduced levels of Hsf1P in the second heat shock, but it holds only for short time break intervals between applications of the two heat shocks. Extending the time lap between two 42°C heat shocks results in a loss of the molecular memory, and in Hsf1P dynamics closer to the Hsf1P dynamics obtained for a single heat stress treatment. A complete loss of molecular memory has been observed in the model's simulations for 120 minutes of recovery time. The model's feature was later experimentally verified and confirmed.

- The system when pretreated with a mild heat shock becomes more resistant to a severe shock. Investigated is the dynamics of phosphorylated Hsf1 levels during a 30°C-37°C-42°C stepwise heat shock. The simulations of the model point at a reduced activation of Hsf1 in a 42°C for the cells pretreated with a 37°C heat shock with respect to the cells that were instantly given a 42°C heat shock. The model's feature was later experimentally verified and confirmed.

- An activation of the transcription factor Hsf1 is essential in the *C. albicans* virulence. At the final stage, the model was used to examine dynamics of phosphorylated Hsf1 in a scenario that mimics development of fever in the host. This was achieved by imposing a slow temperature changes on the system. The simulations of the model showed a transient activation of Hsf1 in every condition tested. The transient activation always resulted in a perfect adaptation of the system, and hence, a complete loss of Hsf1 phosphorylation.

Agent-based modeling approach

In Chapter 4, I describe an agent-based modeling approach that is used for the analysis of how interactions of pre-programmed autonomous entities establish population dynamics. In the model three types of cells interact: yeast cells, hyphal cells, and host phagocytic cells - PMNs. Microbial population is then treated with a type of a drug that decreases the fungal proliferation rate. The simulations of the model indicate that a treatment of a fungi population with a high-dose of the hypothetical drug reduces the fungal burden, and reduces the inflammation. On the contrary the system is able to recover from the lower-dose drug treatment, and exhibits back an inflammation comparable to the one

occurring in the system with untreated cells. Basing on the analysis of the system it is then concluded that there is a drug's dose threshold for an efficient treatment. Also, depending whether we look at a short-term or at a long-term effect of the drug on fungal population the threshold of maximal drug's efficiency changes. In the follow up studies it would be interesting to analyze the differences in the fungal clearance when applying drugs with different functionality, e.g., a drug that blocks the germ tube formation, or a drug that upregulates the activity of the innate immune system. In the analysis of the system one should compare the differences in the course of infection in different treatment scenarios, by examining the distribution of the inflammation around the epithelium.

Pairwise interactions in fungal populations

The powerful feature of *C. albicans* is the ability to grow in distinct morphological forms, where yeast and hyphae, for a number of reasons, attract the most of attention in the scientific community. For instance, yeast form facilitates the dissemination of the fungi during the invasive candidiasis, whereas hyphae are necessary to cross the host barriers. Penetration of the host tissues by the hyphae paves a way for the yeast form to entering other host niches. The ability to develop germ tubes is believed to greatly contribute to the virulence of the pathogen [Lo et al., 1997].

- In §5.3, I develop a model that is based on the assumption that two distinct fungal cells types, yeast and hyphae, are always present in the fungal population, and in some environmental conditions the hyphal cells only display a phenotype of the yeast cells. In different conditions, different fungal forms become favorable. In this case, the favored fungal form will express its phenotype and invade the population. I assume the pairwise interactions to be a trigger that establishes the population profile, i.e., proportions of both cells types. From this study we observe that in certain conditions cooperative behavior in microbial populations is plausible. The simulations of the model show that cooperative behavior in general increases the fungal burden and establishes less pathogenic population, understood here as less hyphae present in the population. A competition among the yeast and hyphal cells decreases the size of the population, but on the other side the subpopulation of hyphae increases. In theory, an ability to change the cells' behavior appears to be crucial during invasive candidiasis. While cooperation is crucial to invade the host and disseminate to different tissues, it can be argued that during a colonization of the internal organs, e.g., kidney, a competitive type of interactions may take place. From a game theoretical perspective, during the course of infection the types of interactions shift from Snowdrift game toward Prisoners' dilemma.

- In §5.4, pairwise interactions in the microbial population establish the systems' dynamics. This time, however, it is considered that all of the cells in the population constantly change, back and forth, between yeast and hyphal states. The model of

switching dynamics between the two fungal forms is represented by a set of ordinary differential equations. The model is used to examine whether the population benefits when cells change phenotypically. The results of the model indicate that the phenotypical changes occurring in the microbial population are advantageous under certain conditions. Either in moderate or in sparse nutritional conditions, the population is more likely to survive in case the cells are able to change phenotypically. In other words, the phenotypic switch in the population takes place in order to keep the fungal burden as high as possible.

In the follow up studies one could combine both modeling approaches. For instance, in the model of switching dynamics (given in Equation 5.14) one could incorporate game theoretical based rates of proliferations in both subpopulations (α_1 and α_2). Some of the studies indicate that fungi constantly have to adapt to the host's status and environmental conditions (i.e., model of switching presented in §5.4). Other studies indicate that a change occurs in the fungi's gene expression pattern that results in deviation from a commensal to a pathogenic style of life [Hube, 2011] (a hypothesis expressed by a game theoretic based model presented in §5.3 where cells are expressing their assigned phenotype). A combined model could then account for both views, where depending on the conditions, either one or both of the models remain valid. This holds because the environmental conditions could force either a payoff matrix or a rates of switches matrix to be represented by a zero matrix.

$\sim \cdot \sim \cdot \sim$

Systems biology is a field that aims at understanding biological processes through applications of diverse computational methods. The processes that occur in a living world often reveal non linear dynamics whose outcome is not possible to be predicted without models' simulations. Therefore computational approaches are largely utilized and being developed. Depending on the type of available data, biological processes can be analyzed considering various granularity levels. We can either look at the organization of the inner content of the cell, or restrict ourselves to study processes on a cellular level by considering solely cell to cell interactions. The work presented in this thesis is a collection of various computational approaches that when taken together span several aspects of host-pathogen interactions, and allow us to look at the interactions from different angles. The structure of the computational model, however, is based on the observed evidences what brings me to the next point in the discussion.

Mutual interactions not only in biological system

The parameterization of mathematical models can be achieved only when experimental data are available. It is important to discuss the structure of the model with experimentalists throughout the process of model development as this is the only way to assure that the model represents a biological problem that we sick to understand. Discussing the structure of the model is important in order to avoid unnecessary complexity or on the other end, simplicity. Since mechanisms underlying the functionalities of living organisms are complex and display non linear dynamics, we might capture the most essential properties of these processes only when combining experimental data with computational analyses. Collaboration between experimentalists and theoreticians is essential and can be successful only when both aim at common goal.

When planning a project one always has to consider time necessary to establish experimental data, time required for repetitions of each experiment, and later, time for checking model's predictions in the experiments that is necessary for either validation of the model or its rejection. Six to twelve months should be considered for this part of the work. Construction and parameterization of a model is also a time consuming process with a similar length. This holds for many biological problems that one would want to study. Thus, to avoid any delay it is important to use the experimental data appropriately, and hence, often contact the experimental partner in order to know the experimental procedures, and construct a model with enough complexity level.

Models and biological questions

Most of biological systems are characterized by non linear dynamics. Thus, mathematical models can help us to understand the mechanisms that govern general dynamical behavior of the system. A complexity level of the mathematical model is dependent on the amount and kind of available data. Often the model's structure simplifies biological processes what can not be viewed as a wrong interpretation of the biological phenomena that we study. If such a simplified model is able to reproduce the biological data set, and provide us with novel testable predictions on the functionality of the system, then it is useful.

In summary, biological question and type of available data determine a computational technique that should be applied, and also the granularity level that has to be considered. Qualitative models, e.g., Boolean models, can be applied to study genes regulatory networks with microarray data. Such models can predict the resulting genes profiles after stimulation of the system with some other inducer. However, with Boolean models we can not investigate a temporal evolution of systems' dynamics. Investigation of dynamic properties of the system require application of other techniques, e.g., ODE models, or rule based modeling. Microbial systems can be investigated either on a molecular or cellular level, and I elaborate on these points in the next two subsection.

Modeling molecular interactions

Ordinary differential equations (ODEs) are most commonly applied to study dynamics of molecular networks. However, ODE models contain kinetic constants that need to be parameterized, what makes models largely dependent on experimental data. Every ODE model has to pass through an iterative systems biology cycle (discussed in §1.2.2). The lone ability of the model to reproduce experimental data is not sufficient to accept the structure of the model. A confidence in the model's structure increases every time the model's predictions could be confirmed in the experiments.

Mathematical analysis of a constructed model is important. For instance, sensitivity analysis (SA) can be used in order to identify crucial steps in the model that influence the most the system's dynamics. The SA technique can be helpful especially when studying systems displaying complex behavior, such as systems with multiple stable steady states, or with oscillations.

In Chapter 3, I applied time dependent response coefficients (RCs) for the analysis of the model of heat stress response in *C. albicans*. This technique is an extension of the standard SA and it allows us to study the impact of small perturbations in parameters values on the entire trajectories of model's state variables. By studying RCs we could see that in the whole model of thermal adaptation only few events actually influence dynamics of Hsf1 phosphorylation. These included the negative regulation of phosphorylated Hsf1 via binding to Hsp90, recruitment of Hsp90 to form complexes with damaged proteins, and Hsp90 production. Taken together the processes that involve Hsp90 protein govern most of the control control over the system's dynamics.

Modeling cellular interactions

Candida albicans population is influenced by e.g., components of the microflora, wealth status of its host, and many other environmental signals. In weakened patients the yeast *C. albicans* becomes pathogenic. Hence, the understanding of how different signals from the environment constitute to a pathogenic function of the fungus will reduce the effort in combating the microbe. Mathematical models can describe these processes considering various granularity levels. Again, as we have seen in Chapter 3, the modeling of molecular interactions can provide us with information how intracellular signaling leads to a specific function of the cell, e.g., adaptation to a heat stress, etc. In this case, the experimental data used for modeling usually are not a single cell data, and describe the average dynamics of the population in given conditions. Therefore, most of ODE models are average approximation of molecular networks' dynamics. Moreover, ODE models do not take into account spatial distribution of the molecules, and hence, we can not claim whether by including spatial distribution we would still capture the system's dynamics. We can however apply other computational techniques to study properties of systems considering spatio-temporal axes, for instance, agent-based modeling (ABM) approach allows for that. There are many advantages of ABM techniques. As first, behavior of

each agent can be described by set of rules that are better to handle than multivariable functions often appearing in ODE models. We can consider the fungi population with cells that are either synchronized, or not, and compare how these influence the outcome. Agents in the model can also have implemented features like adaptation to stimuli or learning processes. Such processes can not be straightforward implemented in ODE models, which have tendency to average the dynamics.

On the other end, we can focus on cellular interactions in microbial populations. Through understanding the effect of either pairwise or multiple cells interactions (which can have positive, negative or neutral impact on the interacting cells) we can assess the types of interactions in microbial communities, e.g., competition, cooperation, etc. (Figure 5.2, [Faust & Raes, 2012]). In this context, cellular interactions can sometimes be viewed as games that are being played among the cells. In other cases one can consider pairwise interactions in microbial communities that establish the rates at which certain events occur. These concepts were applied in Chapter 5. In context of fungal colonization of the epithelial cells, knowing types of interactions between microbes would help the manipulation of the fungal population dynamics via, e.g., decreasing the abundance of pathogenic strains. Computational methods that I adapted in Chapter 5 can serve as conceptual frameworks for assessing the question whether the fungi communicate in order to perform functions that would not be possible to arise from a single cell level, or not.

A single model does not make it the model

The baker's yeast *Saccharomyces cerevisiae* is a model organism for studying responses of the cell to external stimuli. For instance, adaptation to an osmotic stress is being extensively studied. There are many mathematical models that describe aspects of osmoadaptation in this yeast [Klipp et al., 2005, Schaber & Klipp, 2008, Zi et al., 2010, Kühn et al., 2010]. Each of the models considers different granularity levels and each is constructed basing on different assumptions. Nevertheless, all of them, to some extent reveal new details describing the mechanisms of the osmoadaptation process.

The in Chapter 3 presented and discussed ODE model of *C. albicans* thermal adaptation is only one of the first dynamic models that describes the heat stress response in this human fungal pathogen. Although it gives insights into our understanding of the mechanism of molecular adaptation to heat stress in the pathogen we need follow up studies where other boundaries and assumptions are considered.

Modeling without experimental data

In the time of emergent experimental data sets computational techniques are necessary in the analysis of the data in order to reveal the most of information behind the experimental results. Ironically, theoreticians often have to confront the problem of lack of

experimental data, what should not prevent theoreticians from developing mathematical models. Qualitative models, even if not parametrized, are a good basis for stimulating discussions, initiating collaborations, and encouraging experimentalists to perform relevant experiments. Even having only qualitative models in hand, simulations of these models can help to bring our point across, and bring other's attention to the question we would like to study in more detail.

Concluding remarks

In this thesis I highlight different levels of complexity that one can consider when investigating host-pathogen interactions. Depending on the problem the granularity of models may change, but also mathematical formalisms. In Chapter 3, I focused on modeling of the intracellular molecular interactions activated with stimuli relevant to those encountered *in vivo*. Zooming out, in Chapter 4, I studied how the interactions between fungal and host cells lead to overall population dynamics. The ABM presented there may serve as a platform for testing hypothesis on functionality and efficiency of different antifungal drugs. The model definitely needs follow up studies, in which one could propose the optimal scenarios for treatment of the fungal infections basing on the analysis of the results from application of combinations of different hypothetical drugs. In Chapter 5, assuming pairwise interactions in fungal population, two models were proposed. Each of the two models is based on the assumptions which are conceptually very distinct, and that define the outcome of the fungal interactions, i.e., either proliferation, or phenotypic switch takes place. Basing on experimental data one can examine whether fungal populations invading the host consist of cells that communicate in order to attack the host, or wether the cells undergo the phenotypic transition in order to survive in changing environment. In all of the studies presented in this thesis, I discussed the potential theoretical follow-up studies and possible integration with an experimental side.

Taken together, the study presented here, shows that we can learn about the host-pathogen interactions by comparing different mathematical models. By looking at the host-pathogen interactions from different angles different assumptions to the model are made, and different model boundaries are set. But yet, from each approach we can derive testable hypothesis on the nature of these interactions.

The work presented in this thesis is a part of the research project funded by the European Commission through the FINSysB Marie Curie Initial Training Network (PITN-GA-2008-214004).

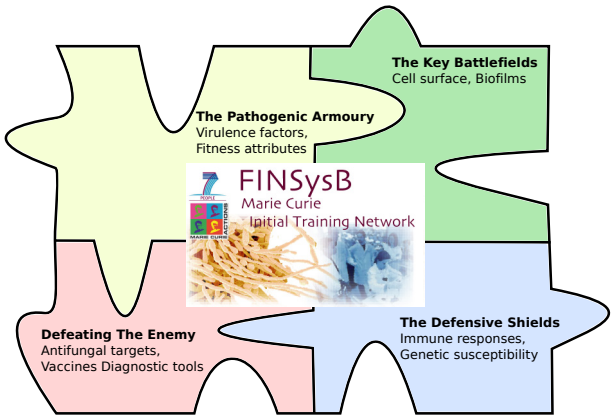

Figure 6.1.: FINSysB consortium. Different approaches only when combined together will reveal the biology of *Candida albicans* infection.

A. Heat shock response in *Candida albicans*

Dynamic model of the heat shock response

Here, I present a set of ODEs that describes the model of adaptation to the heat stress discussed in Chapter 3. In Table A.1 given are differential equations that model all the reactions and regulatory events according to the model structure presented in Figure 3.2. In Table A.2 collected are used kinetic rate laws and in Table A.3 given are parameter values that are used for simulations presented in Chapter 3.

$\frac{d[\mathrm{K}]}{dt} = +v_{1_b} - v_{1_f}$
$\frac{d[\mathrm{K}^*]}{dt} = -v_{1_b} + v_{1_f}$
$\frac{d[\mathrm{I}]}{dt} = -v_{2_b} + v_{2_f}$
$\frac{d[\mathrm{I}^*]}{dt} = +v_{2_b} - v_{2_f}$
$\frac{d[\mathrm{Hsf1}]}{dt} = -v_3 + v_{5_b} - v_{5_f}$
$\frac{d[\mathrm{Hsf1P}]}{dt} = +v_3 - v_4$
$\frac{d[\mathrm{Hsf1Hsp90}]}{dt} = +v_4 - v_{5_b} + v_{5_f}$
$\frac{d[\mathit{HSP90}\mathrm{mRNA}]}{dt} = +v_9 - v_{10}$
$\frac{d[\mathrm{Hsp90Complex}]}{dt} = -v_{6_b} + v_{6_f} - v_8$
$\frac{d[\mathrm{Hsp90}]}{dt} = -v_4 + v_{5_b} - v_{5_f} + v_{6_b} - v_{6_f} - v_7 + v_{11}$

Table A.1.: Mathematical model of heat stress adaptation in *C. albicans*. The set of ordinary differential equations describes the model presented in Figure 3.2. Each v_i describes a reaction rate. v_i that enters with positive sign on the right side of equation indicates an accumulation of given state variable; either due to a mass flow or a production. Reaction rate v_i with negative sign on the right side of equation indicates a depletion of considered state variable; either due to a mass flow or a degradation.

Kinetic rate laws that are used for describing the dynamics of heat shock model

$$
\begin{aligned}
v_{1_f} &= k_{1_f} \mathrm{T_K} \tfrac{[\mathrm{K}]}{K_{M_1}+[\mathrm{K}]} \\
v_{1_b} &= k_{1_b} [\mathrm{I}^*] \tfrac{[\mathrm{K}^*]}{K_{M_2}+[\mathrm{K}^*]} \\
v_{2_f} &= k_{2_f} \tfrac{[\mathrm{I}^*]}{K_{M_3}+[\mathrm{I}^*]} \tfrac{1}{\mathrm{T_K}} \\
v_{2_b} &= k_{2_b} [\mathrm{K}^*] \tfrac{[\mathrm{I}]}{K_{M_4}+[\mathrm{I}]} \\
v_3 &= k_3 [\mathrm{K}^*] \tfrac{[\mathrm{Hsf1}]}{[\mathrm{Hsf1}]+K_{MP}} \\
v_4 &= k_4 [\mathrm{Hsf1P}][\mathrm{Hsp90}] \\
v_{5_f} &= k_{5_f} [\mathrm{Hsf1}][\mathrm{Hsp90}] \\
v_{5_b} &= k_{5_b} [\mathrm{Hsf1Hsp90}] \\
v_{6_f} &= k_{6_f} [\mathrm{Hsp90}] \cdot \mathrm{T_H} \\
v_{6_b} &= k_{6_b} [\mathrm{Hsp90Complex}] \\
v_7 &= k_7 [\mathrm{Hsp90}] \\
v_8 &= k_8 [\mathrm{Hsp90Complex}] \\
v_9 &= k_9 \mathit{Hsf1P}_0 + k_{pr}([\mathrm{Hsf1P}] - \mathit{Hsf1P}_0) \\
v_{10} &= k_{10} [\mathit{HSP90}\mathrm{mRNA}] \\
v_{11} &= k_{11} \mathit{HSP90}\mathrm{mRNA}_0 + k_{tr}([\mathit{HSP90}\mathrm{mRNA}] - \mathit{HSP90}\mathrm{mRNA}_0)
\end{aligned}
$$

Table A.2.: Rate laws. Mass action or Michaelis-Menten kinetics were used for individual reactions. $[\cdot]$ indicates concentration of the respective state variable.

Parameters values used for the simulations of the heat shock model

Parameter value	Comment
$T_K = 1 \times 10^0$, $T_H = 1 \times 10^0$	30°C
$T_K = 1.49 \times 10^3$, $T_H = 1.14 \times 10^1$	37°C
$T_K = 2.57 \times 10^3$, $T_H = 1.68 \times 10^2$	42°C
$k_{1_f} = 7.74 \times 10^{-8}$, $K_{M_1} = 6.11 \times 10^{-3}$	Rate constant of protein kinase K activation and Michaelis-Menten constant
$K_{M_2} = 1 \times 10^{-10}$	Michaelis-Menten constant for protein kinase deactivation
$k_{2_f} = 1.2 \times 10^{-6}$, $K_{M_3} = 3.87 \times 10^{-3}$	Rate constant of inhibitor I activation and Michaelis-Menten constant
$K_{M_4} = 4.31 \times 10^{-4}$	Michaelis-Menten constant for inhibitor deactivation
$k_3 = 3.22 \times 10^1$, $K_5 = 2.52 \times 10^1$	Phosphorylation of Hsf1 rate constant and Michaelis-Menten constant
$k_{5_f} = 1.1 \times 10^7$	Rate constant of Hsf1 and Hsp90 association
$k_{6_b} = 1 \times 10^{-2}$	Dissociation rate constant of Hsp90 from Hsp90Complex
$k_7 = 2.26 \times 10^0$	Rate constant of Hsp90 degradation
$k_8 = 2.35 \times 10^0$	Rate constant of Hsp90Complex degradation
$k_9 = 3.24 \times 10^4$	Basal *HSP90*mRNA production
$k_{pr} = 5.38 \times 10^{-1}$	Rate constant of *HSP90*mRNA production
$k_{tr} = 3.88 \times 10^{-1}$	Rate constant of Hsp90 protein production
Steady state assumption	
$k_{1_b} = k_{1_f} \frac{K_0}{K_0 + K_{M_1}} \frac{K_0^* + K_{M_2}}{K_0^* \cdot I_0^*}$	Rate constant of K^* to K transition
$k_{2_b} = k_{2_f} \frac{I_0^*}{I_0^* + K_{M_3}} \frac{I_0 + K_{M_4}}{I_0 \cdot K_0^*}$	Rate constant of I to I^* transition
$k_4 = k_3 \frac{K_0^* \cdot Hsf1_0}{K_5 + Hsf1_0} \frac{1}{Hsf1P_0 \cdot Hsp90_0}$	Dephosphorylation rate constant
$k_{5_b} = \frac{k_{5_f} \cdot Hsp90_0 \cdot Hsf1_0 + k_4 \cdot Hsf1P_0 \cdot Hsp90_0}{Hsf1Hsp90_0}$	Rate constant of Hsf1 dissociation from the complex Hsf1Hsp90
$k_{6_f} = (k_{6_b} + k_8) \frac{Hsp90_{Complex_0}}{Hsp90_0}$	Rate constant of Hsp90 binding to unfolded proteins
$k_{10} = k_9 \cdot \frac{Hsf1P_0}{HSP90\text{mRNA}_0}$	*HSP90*mRNA degradation rate constant
$k_{11} = \frac{k_7 \cdot Hsp90_0 + k_8 \cdot Hsp90_{Complex_0}}{HSP90\text{mRNA}_0}$	Basal production of Hsp90 protein

Table A.3.: Parameter values. Given are numerical values used for the simulations of the main model (Figure 3.2) presented in Chapter 3. Parameters' description is given in the table.

Model 2

Given are the equations that describe 'model 2' discussed in Chapter 3 and depicted in Figure 3.15. In Table A.4 stored are all of the state variables that appear in the 'model 2' together with the initial conditions used for simulations of the model. The model was parameterized using the experimental data presented in Figure 3.6 and Figure 3.7. In Table A.5 given are the ODEs that describe 'model 2', and its kinetic rate laws are in Table A.6. Parameters values are stored in Table A.7.

Name	Short description	Initial value
K	Inactive kinase	$K_0 = 1 \times 10^{-2}$
K*	Active kinase	$K_0^* = 1 \times 10^{-6}$
I	Inactive inhibitor	$I_0 = 3.56$
I*	Active inhibitor	$I_0^* = 1 \times 10^{-10}$
Hsf1	Heat shock transcription factor	$Hsf1_0 = 2.05 \times 10^{-4}$
Hsp90	Heat shock protein	$Hsp90_0 = 3.67 \times 10^{-1}$
Hsf1K*	Hsf1 coupled with K*	$Hsf1K_0^* = 5 \times 10^{-10}$
Hsf1P	Phosphorylated Hsf1	$Hsf1P_0 = 1 \times 10^{-8}$
Hsf1Hsp90	Hsp90 coupled with Hsf1	$Hsf1Hsp90_0 = 1 \times 10^{-2}$
Hsp90Complex	Hsp90 bound to unfolded proteins	$Hsp90_{Complex_0} = 5.02 \times 10^{-1}$
*HSP90*mRNA	mRNA	$HSP90\text{mRNA}_0 = 3.53 \times 10^{-1}$

Table A.4.: Species in Model 2. Given are, both nomenclature and initial values used for simulations of Model 2.

$$
\begin{aligned}
\frac{d[\text{K}]}{dt} &= +v_{1_b} - v_{1_f} \\
\frac{d[\text{K}^*]}{dt} &= -v_{1_b} + v_{1_f} - v_{3_b} + v_{3_f} + v_4 \\
\frac{d[\text{I}]}{dt} &= -v_{2_b} + v_{2_f} \\
\frac{d[\text{I}^*]}{dt} &= +v_{2_b} - v_{2_f} \\
\frac{d[\text{Hsf1}]}{dt} &= +v_{3_b} - v_{3_f} + v_{6_b} - v_{6_f} \\
\frac{d[\text{Hsf1K}^*]}{dt} &= -v_{3_b} + v_{3_f} - v_4 \\
\frac{d[\text{Hsf1P}]}{dt} &= +v_4 - v_5 \\
\frac{d[\text{Hsf1Hsp90}]}{dt} &= +v_5 - v_{6_b} + v_{6_f} \\
\frac{d[\text{Hsp90}]}{dt} &= -v_5 + v_{6_b} - v_{6_f} + v_{7_b} - v_{7_f} - v_8 + v_{12} \\
\frac{d[\text{Hsp90Complex}]}{dt} &= -v_{7_b} + v_{7_f} - v_9 \\
\frac{d[HSP90\text{mRNA}]}{dt} &= +v_{10} - v_{11}
\end{aligned}
$$

Table A.5.: Mathematical model of heat stress adaptation in *C. albicans*. Set of ODEs describing molecular dependencies in Model 2 (Figure 3.15).

$$v_{1_f} = k_{1_f} T_K \frac{[\mathrm{K}]}{K_{M_1}+[\mathrm{K}]}$$
$$v_{1_b} = k_{1_b} [\mathrm{I}^*] \frac{[\mathrm{K}^*]}{K_{M_2}+[\mathrm{K}^*]}$$
$$v_{2_f} = k_{2_f} \frac{[\mathrm{I}^*]}{K_{M_3}+[\mathrm{I}^*]} \frac{1}{T_K}$$
$$v_{2_b} = k_{2_b} [\mathrm{K}^*] \frac{[\mathrm{I}]}{K_{M_4}+[\mathrm{I}]}$$
$$v_{3_f} = k_{3_f} [\mathrm{K}^*][\mathrm{Hsf1}]$$
$$v_{3_b} = k_{3_b} [\mathrm{Hsf1K}^*]$$
$$v_4 = k_4 [\mathrm{Hsf1K}^*]$$
$$v_5 = k_5 [\mathrm{Hsf1P}][\mathrm{Hsp90}]$$
$$v_{6_f} = k_{6_f} [\mathrm{Hsf1}][\mathrm{Hsp90}]$$
$$v_{6_b} = k_{6_b} [\mathrm{Hsf1Hsp90}]$$
$$v_{7_f} = k_{7_f} [\mathrm{Hsp90}] \cdot T_H$$
$$v_{7_b} = k_{7_b} [\mathrm{Hsp90Complex}]$$
$$v_8 = k_8 [\mathrm{Hsp90}]$$
$$v_9 = k_9 [\mathrm{Hsp90Complex}]$$
$$v_{10} = k_{10} \mathit{Hsf1P}_0 + k_{pr}([\mathrm{Hsf1P}] - \mathit{Hsf1P}_0)$$
$$v_{11} = k_{11} [\mathit{HSP90}\mathrm{mRNA}]$$
$$v_{12} = k_{12} \mathit{HSP90}\mathrm{mRNA}_0 + k_{tr}([\mathit{HSP90}\mathrm{mRNA}] - \mathit{HSP90}\mathrm{mRNA}_0)$$

Table A.6.: Rate laws for Model 2. Mass action or Michaelis-Menten kinetics were used for individual reactions. $[\cdot]$ indicates concentration of the respective state variable.

Parameter value	Comment
$\mathrm{T_K} = 1 \times 10^0$, $\mathrm{T_H} = 1 \times 10^0$	30°C
$T_K = 4.66891 \times 10^3$, $T_H = 2.114 \times 10^1$	37°C
$T_K = 9 \times 10^3$, $T_H = 2 \times 10^2$	42°C
$k_{1_f} = 2.34169 \times 10^{-8}$	Rate constant of K to K* transition
$K_{M_1} = 6.11008 \times 10^{-3}$	Michaelis Menten constant for reaction 1_f
$K_{M_2} = 2.30642 \times 10^{-6}$	Michaelis Menten constant for reaction 1_b
$k_{2_f} = 1.19693 \times 10^{-6}$	Rate constant of I* to I transition
$K_{M_3} = 3.8656 \times 10^{-3}$	Michaelis Menten constant for reaction 2_f
$K_{M_4} = 4.31539 \times 10^{-4}$	Michaelis Menten constant for reaction 2_b
$k_{3_b} = 6.84494 \times 10^{-8}$	Dissociation rate constant from the complex Hsf1K*
$k_4 = 5 \times 10^{-1}$	Phosphorylation of Hsf1P rate constant
$k_{6_f} = 1.10367 \times 10^7$	Rate constant of Hsf1 and Hsp90 association
$k_{7_b} = 1 \times 10^{-2}$	Dissociation rate constant of Hsp90 from Hsp90Complex
$k_8 = 2.25552 \times 10^0$	Rate constant of Hsp90 degradation
$k_9 = 2.35332 \times 10^0$	Rate constant of Hsp90Complex degradation
$k_{10} = 4.36811 \times 10^4$	Basal *HSP90*mRNA production
$k_{pr} = 5.38 \times 10^{-1}$	Rate constant of *HSP90*mRNA production
$k_{tr} = 3.88472 \times 10^{-1}$	Rate constant of Hsp90 protein production
Steady state assumption	
$k_{1_b} = k_{1_f} \frac{K_0}{K_0 + K_{M_1}} \frac{K_0^* + K_{M_2}}{K_0^* \cdot I_0^*}$	Rate constant of K* to K transition
$k_{2_b} = k_{2_f} \frac{I_0^*}{I_0^* + K_{M_3}} \frac{I_0 + K_{M_4}}{I_0 \cdot K_0^*}$	Rate constant of I to I* transition
$k_{3_f} = (k_{3_b} + k_4) \frac{Hsf1K_0^*}{K_0^* \cdot Hsf1_0}$	Rate constant of K* binding to Hsf1
$k_5 = k_4 \frac{Hsf1K_0^*}{Hsf1P_0 \cdot Hsp90_0}$	Dephosphorylation rate constant
$k_{6_b} = \frac{k_{6_f} \cdot Hsp90_0 \cdot Hsf1_0 + k_5 \cdot Hsf1P_0 \cdot Hsp90_0}{Hsf1Hsp90_0}$	Rate constant of Hsf1 dissociation from the complex Hsf1Hsp90
$k_{7_f} = (k_{7_b} + k_9) \frac{Hsp90_{Complex_0}}{Hsp90_0}$	Rate constant of Hsp90 binding to unfolded proteins
$k_{11} = k_{10} \cdot \frac{Hsf1P_0}{HSP90\mathrm{mRNA}_0}$	*HSP90*mRNA degradation rate constant
$k_{12} = \frac{k_8 \cdot Hsp90_0 + k_9 \cdot Hsp90_{Complex_0}}{HSP90\mathrm{mRNA}_0}$	Basal production of Hsp90 protein

Table A.7.: Parameter values. Given are numerical values used for the simulations of Model 2 presented at the end of Chapter 3. Parameters' description is given in the table.

B. Agent-based model

To study *Candida albicans* interactions with its human host an agent-based model (ABM) has been constructed using the program NetLogo [Wilensky, 1999]. When constructing an ABM defined has to be a world where agents could live. In NetLogo the world is called 'patches', which is divided into a grid of squares where each square is a single 'patch'. The agents are called 'turtles'. The turtles are entities that behave according to rules specified by the user in the 'observer'. In the observer should be implemented rules that define the properties of each agent. Also patches can display some properties and they can interact with turtles. So called 'links' can be used to connect any two agents in the model. The worlds in the model discussed in Chapter 4 are epithelial cells. Turtles are *C. albicans* cells (that can proliferate) and neutrophils (type of cells from the innate immune system) which are attracted by *C. albicans* population. The agents interact with each other and with the patches. Below presented is the code of ABM that describes a *C. albicans* population colonizing epithelial cells. The whole process is tightly regulated by a vast range of signals coming from fungal cells and also influenced by the fungi' interactions with PMNs. In this model, the molecular processes that may occur within cells are neglected and only general features are implemented, e.g., nutrient starvation triggers hyphal development, hyphae cause inflammation, and in turn, patches release cytokines that recruit PMNs to the system. Parameters of the model are collected in Table B.1.

```
;; Agents in the model
breed[yeasts yeast]
breed[hyphae hypha]
breed[PMNs PMN]

;; Agents parameters: energy - gained from nutrient available on patches
turtles-own [energy]
;; Patches parameters: cytokines (seen as a gradient of green) - released by a patch with hyphae
;; portals - entry for phagocytic cells when green gradient appears
;; nutrition - a parameter that stores the levels of nutrient in the model
patches-own [cytokine portal nutrition]

to setup
```

```
  clear-all
  setup-patches
  setup-yeasts
  setup-PMNs
  do-plots
end

to setup-patches
  ;; Initial condition: each patch has one unit of nutrient
  ask patches [ set nutrition 1]
  ;; Coordinates of the portals for PMNs entry
  let entrancex1 -16 let entrancey1 24
  let entrancex2 16  let entrancey2 24
  let entrancex3 -16 let entrancey3 -24
  let entrancex4 16  let entrancey4 -24
  ;; Assignment of 1 to portal - in order to specify where to seed PMNs
  ask patches [if pxcor = entrancex1 and pycor = entrancey1 [set portal 1 set pcolor 63]]
  ask patches [if pxcor = entrancex2 and pycor = entrancey2 [set portal 1 set pcolor 63]]
  ask patches [if pxcor = entrancex3 and pycor = entrancey3 [set portal 1 set pcolor 63]]
  ask patches [if pxcor = entrancex4 and pycor = entrancey4 [set portal 1 set pcolor 63]]
end

to setup-yeasts
  set-default-shape yeasts "circle"
  create-yeasts initial-number-yeasts
  ask yeasts
    [ setxy random-xcor random-ycor
      set size 0.6
      set color red
      set energy birth-energy ]
end

to setup-PMNs
  set-default-shape PMNs "PMNshape"
  create-PMNs initial-number-PMNs
  ask PMNs
    [ setxy random-xcor random-ycor
      set color blue ]
end

to go
  if ticks >= 1500 [stop]
  ;; Basal PMNs' recruitment rate not affected by the cytokine gradient
  seed-PMNs
  ;; Basal removal of PMNs - in order to avoid system explosion
  remove-PMNs
  diffuse-cytokine
  move-PMNs
  ask PMNs [kill-yeasts]
  ask PMNs [kill-hyphae]
  consume-nutrient
  metabolize
  reproduce-yeasts
  form-hyphae
  check-dead-fungi
  restore-nutrient
  tick
  do-plots
end
```

```
;; Specify whether to seed PMNs
;; PMNs are seeded also if no inflammation: set yeast cell's metabolism to 0
;; The higher is the value of cytokine the more PMNs are seeded into the system
to seed-PMNs
  ask patches [
    ifelse seed-PMNs? [
      if portal = 1 [
        set pcolor 63
        if (random 100 + cytokine) > seed-random [
        sprout-PMNs 1
        ask PMNs [set color blue] ]
      ]
     ]
   [ ]
  ]
end

;; PMNs' survival rate is set to 2% per tick
to remove-PMNs
  ask PMNs [ if (random 100 < PMN-die-random) [die] ]
end

to diffuse-cytokine
  ask patches [
    ;; Hyphae with energy < 0 (dead hyphae) do not cause inflammation
    if count hyphae-here with [energy > 0 ] > 0
    [set cytokine ( count ( hyphae-here with [energy > 0 ] ) * 50 ) ]
    set cytokine cytokine * 0.99
    if shownutrient? = FALSE [set pcolor scale-color green cytokine 0 100]
    ]
  diffuse cytokine 0.9
end

;; PMNs are the only agents in the model that can move
to move-PMNs
  ask PMNs [
;; PMN that has ingested a fungus can move only when the phagocytosis is completed (when PMN's energy is 0)
    if energy > 0 [set energy energy - 1]
    if energy = 0 [ ifelse random 75 > 50 [rt random 360 fd 1] [
      move-to patch-here
      let p max-one-of neighbors [cytokine]
      if [cytokine] of p > cytokine [ face p ] wiggle-PMNs ] ]
  ]
end

to wiggle-PMNs
  rt random 45
  lt random 45
  fd 1
end

;; The function is adapted from:
;; Wilensky, U. (1997). NetLogo Wolf Sheep Predation model
;; http://ccl.northwestern.edu/netlogo/models/WolfSheepPredation
to kill-yeasts
  let prey one-of yeasts-here
  if prey != nobody
    [ ask prey [die] set energy 5 ]
```

```
end

to kill-hyphae
  let prey one-of hyphae-here
  if prey != nobody
    [ ask prey [die] set energy 5 ]
end

to consume-nutrient
  ask yeasts [ if (nutrition = 1)
    [ set nutrition 0
      set energy (energy + energy-from-nutrient) ]
  ifelse show-energy?
    [set label energy]
    [set label ""]
  ]
  ;; Dead hypha can not gain energy from nutrient
  ask hyphae with [energy > 0][ if nutrition = 1 [
      set nutrition 0
      set energy (energy + h-energy-from-nutrient * energy-from-nutrient) ]
  ifelse show-energy?
    [set label energy]
    [set label ""]
  ]
end

to restore-nutrient
  ifelse restore-nutrient? [
  ask patches [
    if random 100 < 3 [ set nutrition 1 ]
    if shownutrient? = TRUE and nutrition = 1 [ set pcolor green ] ]
  ]
  [ ]
end

to metabolize
  ask yeasts [
    set energy energy - metabolism
    ifelse show-energy?[set label energy][set label ""] ]
  ask hyphae with [energy > 0][
    set energy energy - h-metabolism * metabolism
    set label "" ]
end

to reproduce-yeasts
  ifelse drug-treatment?
  [
   ;; Drug is applied at tick 400 and remains constant
    ifelse ticks > 400
    [ask yeasts [
      if energy > drug * division-threshold * birth-energy [set energy energy - drug * birth-energy
        hatch 1 [lt random 90 fd 1 set energy birth-energy]]
      ]]
    [ask yeasts [
      if energy > division-threshold * birth-energy [set energy energy - birth-energy
       hatch 1 [lt random 90 fd 1 set energy birth-energy]]
      ]]
  ]
  [ ask yeasts [
```

```
    if energy > division-threshold * birth-energy [
      set energy energy - birth-energy
      hatch 1 [lt random 90 fd 1 set energy birth-energy]
      ]
    ]
  ]
end

to form-hyphae
  ask yeasts [
    if energy < y2h-threshold * birth-energy
    and random 100 < y2h-random [set breed hyphae set shape "hyphaeform" set size 2 set color gray] ]
end

to check-dead-fungi
  ask yeasts [
    if energy <= 0 [set color yellow]
    ]
    ask hyphae [
    if energy <= 0 [set color yellow]
    ]
end

to do-plots
  set-current-plot "Totals"
  set-current-plot-pen "yeast"
  plot count yeasts
  set-current-plot-pen "hyphae"
  plot count hyphae with [energy >= 0]
  set-current-plot-pen "PMNs"
  plot count PMNs
end
```

Name	Short description	Value
initial-number-yeasts	Number of yeast cells at the beginning of the simulation	150
initial-number-PMNs	Number of PMN cells at the beginning of the simulation	0
birth-energy (B)	Yeast cell's energy assigned at birth	40
energy-from-nutrient (E)	Energy for a yeast cell obtained from nutrient consumption	20
h-energy-from-nutrient	Energy for a hyphae cell obtained from nutrient consumption	0.3 * E
metabolism (M)	Consumption of accumulated energy by a yeast cell	0.25
h-metabolism	Consumption of accumulated energy by a hyphae cell	0.55 * M
division-threshold	Division of the cell when its energy exceeds the threshold. A daughter cell receives the birth-energy B, which is subtracted from the mother cell's energy.	2.1
y2h-threshold	Morphological switch from a yeast to a hyphae when the energy of the cell drops below the specified threshold	0.9 * B
drug	Drug in the model decreases the fitness of the yeast cells, i.e. it rises the division threshold.	
Stochastic elements		
y2h-random	Switch from a yeast to a hyphae independently of the energy accumulated	75
seed-random	PMNs' recruitment to independently of the cytokine gradient	99.5
PMN-die-random	PMNs' death rate	2.1

Table B.1.: Parameters in ABM of the host-pathogen interactions. No fitting of the parameters to experimental data was performed. Qualitative behavior of the system is investigated.

C. Evolutionary games dynamic interactions in fungal populations

Model with nutrient consumption

Figure 5.21 and Figure 5.22 were simulated with the following model:

$$\begin{aligned}
l(n) &= \tfrac{v_y n^\sigma}{n^\sigma + k_y}, \\
d(n) &= \tfrac{v_h n^\sigma}{n^\sigma + k_h} + i, \\
\dot{y}(t) &= y(t)\left(\beta + \tfrac{y(t)}{y(t)+h(t)} l(n) + \tfrac{h(t)}{y(t)+h(t)}(p_1 l(n) - p_2 bk)\right) \\
\dot{h}(t) &= h(0)\left(\beta + \tfrac{y(t)}{y(t)+h(t)}(d(n) - k) + \tfrac{h(t)}{y(t)+h(t)}(d(n) - 2k)\right) \\
\dot{n}(t) &= v_{\text{prod}} - y(t) \cdot l(n) - h(t) \cdot (d(n) - i) \\
y(0) &= 0.1 \\
h(0) &= 0.01 \\
n(0) &= 0.5
\end{aligned} \tag{C.1}$$

The following parameters were taken:

$$v_y = 2,\ k_y = 2,\ v_h = 1,\ k_h = 1,\ \sigma = 3,\ i = 0.2,$$
$$\beta = -0.1,\ b = 0.25,\ k = 0.15,\ v_{\text{prod}} = 0.2.$$

If not otherwise specified in the legend of Figure 5.21, the values for p_1 and p_2 are set to 1. In order to induce oscillations in the system (Figure 5.22) the value of v_{prod} is set to 0.002.

D. Dynamics of phenotypic changes in fungal populations

Presented are equations that describe 'model 2' and 'model 3' discussed in Figure 5.32. Functions $d(n)$ and $l(n)$ are considered to be h2y and y2h rates of switching, respectively.

$$\begin{aligned} d(n) &= \frac{vn^{\sigma}}{n^{\sigma}+K^{\sigma}}, \\ l(n) &= 1-d(n), \quad \text{where} \\ v &= 1,\ K = 0.1,\ \sigma = 4. \end{aligned} \tag{D.1}$$

$\pi(y,\mathbf{x})$ and $\pi(h,\mathbf{x})$ are average y2h and h2y rates of switching. Both account for pairwise interactions in the fungal population and are thus given by:

$$\pi(y,\mathbf{x})=\frac{y(t)}{y(t)+h(t)}l(n)+\frac{h(t)}{y(t)+h(t)}(l(n)-k)$$

$$\pi(h,\mathbf{x})=\frac{y(t)}{y(t)+h(t)}(d(n)+k)+\frac{h(t)}{y(t)+h(t)}(d(n)+2k)$$

Both yeast and hyphae can reproduce at rates α_1 and α_2 not influenced by the pairwise interactions, but they dependent on nutrient availability and host immunocompetency, and are expressed with the following formulae:

$$\alpha_1=\frac{0.03n^3}{n^3+0.1^3}-k, \qquad \alpha_2=\frac{0.015n^3}{n^3+0.03^3}.$$

The parameter n in the above formulae indicates nutritional conditions with representative values proposed in Table D.2. The parameter k indicates the status of the host's immune system. For a healthy host $k = 0.003$ applies and for an immunocompromised host $k = 0.001$ is taken.
Results presented in Figure 5.32 were generated by simulating models described below. Considered is the case where nutritional conditions are steady and set according to the

Nutritional condition	Parameter value
rich	n(0)=0.39
moderate	n(0)=0.09
pure	n(0)=0.01

Table D.2.: Numerical values considered when referring to nutritional conditions.

values proposed in Table D.2. The data where then collected for time point $t = 600$.

Model 2. In model 2 there is no switching between the two phenotypes implemented. Only self replication processes take place.

$$\begin{aligned} \dot{y}(t) &= \alpha_1 y(t) \\ \dot{h}(t) &= \alpha_2 h(t) \\ \dot{n}(t) &= 0 \\ y(0) &= 1000 \\ h(0) &= 10 \\ n(0) &= \text{see Table D.2} \end{aligned} \tag{D.2}$$

Model 3. Model 3 given in Figure 5.32 describes the system where only yeast to hyphae transition takes place. Hyphae does not switch back to the yeast form.

$$\begin{aligned} \dot{y}(t) &= \alpha_1 y(t) - y(t)\pi(y, \mathbf{x}) \\ \dot{h}(t) &= \alpha_2 h(t) + y(t)\pi(y, \mathbf{x}) \\ \dot{n}(t) &= 0 \\ y(0) &= 1000 \\ h(0) &= 10 \\ n(0) &= \text{see Table D.2} \end{aligned} \tag{D.3}$$

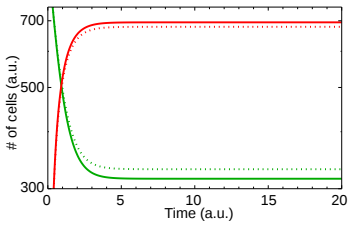

Figure D.1.: Host immune response exerted on yeast form influences fungal burden. Simulations of 'model 1' (Figure 5.32) for two different values of b in $\tau(y, h) = l - bk$. b expresses immune system strength exerted on the yeast form. Considered are: $k = 0.2$, $\alpha_1 = \alpha_2 = 0$, $n = 0.05$. Green: yeast; Red: hypha. (Dotted lines) $b = 1$, yeast and hyphae are equally influenced by immune system activity. (Solid lines) $b = 0.5$, a decrease in the immune system control of y2h switch results in a more pathogenic population; more hyphae is observed.

Bibliography

[Ackermann et al., 2008] Ackermann, M., Stecher, B., Freed, N. E., Songhet, P., Hardt, W. D., & Doebeli, M. (2008). Self-destructive cooperation mediated by phenotypic noise. *Nature*, 454(7207), 987–990.

[Alberts et al., 2002] Alberts, B., Johnson, A., Lewis, J., Raff, M., Roberts, K., & Walter, P. (2002). *Pathogens, Infection, and Innate Immunity in Molecular Biology of the Cell. 4th edition.* New York: Garland Science.

[Ali et al., 1998] Ali, A., Bharadwaj, S., O'Carroll, R., & Ovsenek, N. (1998). HSP90 interacts with and regulates the activity of heat shock factor 1 in Xenopus oocytes. *Mol. Cell. Biol.*, 18, 4949–4960.

[Alon, 2006] Alon, U. (2006). *An Introduction to Systems Biology: Design Principles of Biological Circuits (Chapman & Hall/CRC Mathematical & Computational Biology).* Chapman and Hall/CRC, 1 edition.

[Ananthan et al., 1986] Ananthan, J., Goldberg, A. L., & Voellmy, R. (1986). Abnormal proteins serve as eukaryotic stress signals and trigger the activation of heat shock genes. *Science*, 232, 522–524.

[Arguelles, 1997] Arguelles, J. C. (1997). Thermotolerance and trehalose accumulation induced by heat shock in yeast cells of Candida albicans. *FEMS Microbiol. Lett.*, 146, 65–71.

[Avery, 2006] Avery, S. V. (2006). Microbial cell individuality and the underlying sources of heterogeneity. *Nat. Rev. Microbiol.*, 4(8), 577–587.

[Baker et al., 2010] Baker, S. M., Schallau, K., & Junker, B. H. (2010). Comparison of different algorithms for simultaneous estimation of multiple parameters in kinetic metabolic models. *J Integr Bioinform*, 7(3).

[Bassler & Losick, 2006] Bassler, B. L. & Losick, R. (2006). Bacterially speaking. *Cell*, 125, 237–246.

[Bastidas et al., 2009] Bastidas, R. J., Heitman, J., & Cardenas, M. E. (2009). The protein kinase Tor1 regulates adhesin gene expression in *Candida albicans*. *PLoS Pathog.*, 5, e1000294.

[Behnsen et al., 2007] Behnsen, J., Narang, P., Hasenberg, M., Gunzer, F., Bilitewski, U., Klippel, N., Rohde, M., Brock, M., Brakhage, A. A., & Gunzer, M. (2007). Environmental dimensionality controls the interaction of phagocytes with the pathogenic fungi Aspergillus fumigatus and Candida albicans. *PLoS Pathog.*, 3, e13.

[Bellu et al., 2007] Bellu, G., Saccomani, M. P., Audoly, S., & D'Angio, L. (2007). DAISY: a new software tool to test global identifiability of biological and physiological systems. *Comput Methods Programs Biomed*, 88, 52–61.

[Bennett & Johnson, 2005] Bennett, R. J. & Johnson, A. D. (2005). Mating in *Candida albicans* and the search for a sexual cycle. *Annu. Rev. Microbiol.*, 59, 233–255.

[Berman & Sudbery, 2002] Berman, J. & Sudbery, P. E. (2002). Candida Albicans: a molecular revolution built on lessons from budding yeast. *Nat. Rev. Genet.*, 3, 918–930.

[Binder, 2006] Binder, R. J. (2006). Heat shock protein vaccines: from bench to bedside. *Int. Rev. Immunol.*, 25(5-6), 353–375.

[Biswas et al., 2007] Biswas, S., van Dijck, P., & Datta, A. (2007). Environmental sensing and signal transduction pathways regulating morphopathogenic determinants of *Candida albicans*. *Microbiol. Mol. Biol. Rev.*, 71, 348–376.

[Bonabeau, 2002] Bonabeau, E. (2002). Agent-based modeling: methods and techniques for simulating human systems. *Proc. Natl. Acad. Sci. U.S.A.*, 99 Suppl 3, 7280–7287.

[Bray, 2003] Bray, D. (2003). Molecular networks: the top-down view. *Science*, 301(5641), 1864–1865.

[Brown & Gow, 1999] Brown, A. J. & Gow, N. A. (1999). Regulatory networks controlling *Candida albicans* morphogenesis. *Trends Microbiol.*, 7, 333–338.

[Brown & Leach, 2011] Brown, A. J. & Leach, M. D. (2011). Personal communication.

[Bruggeman & Westerhoff, 2007] Bruggeman, F. J. & Westerhoff, H. V. (2007). The nature of systems biology. *Trends Microbiol.*, 15(1), 45–50.

[Cao et al., 2006] Cao, F., Lane, S., Raniga, P. P., Lu, Y., Zhou, Z., Ramon, K., Chen, J., & Liu, H. (2006). The Flo8 transcription factor is essential for hyphal development and virulence in *Candida albicans*. *Mol. Biol. Cell*, 17, 295–307.

[Cheetham et al., 2007] Cheetham, J., Smith, D. A., da Silva Dantas, A., Doris, K. S., Patterson, M. J., Bruce, C. R., & Quinn, J. (2007). A single MAPKKK regulates the Hog1 MAPK pathway in the pathogenic fungus Candida albicans. *Mol. Biol. Cell*, 18(11), 4603–4614.

[Dabrowa & Howard, 1984] Dabrowa, N. & Howard, D. H. (1984). Heat shock and heat stroke proteins observed during germination of the blastoconidia of Candida albicans. *Infect. Immun.*, 44(2), 537–539.

[Dalle et al., 2010] Dalle, F., Wachtler, B., L'Ollivier, C., Holland, G., Bannert, N., Wilson, D., Labruere, C., Bonnin, A., & Hube, B. (2010). Cellular interactions of Candida albicans with human oral epithelial cells and enterocytes. *Cell. Microbiol.*, 12, 248–271.

[De Virgilio & Loewith, 2006] De Virgilio, C. & Loewith, R. (2006). Cell growth control: little eukaryotes make big contributions. *Oncogene*, 25, 6392–6415.

[Deveau & Hogan, 2011] Deveau, A. & Hogan, D. A. (2011). Linking quorum sensing regulation and biofilm formation by Candida albicans. *Methods Mol. Biol.*, 692, 219–233.

[Dugatkin et al., 2008] Dugatkin, L. A., Dugatkin, A. D., Atlas, R. M., & Perlin, M. H. (2008). Cheating on the edge. *PLoS ONE*, 3, e2763.

[Duina et al., 1998] Duina, A. A., Kalton, H. M., & Gaber, R. F. (1998). Requirement for Hsp90 and a CyP-40-type cyclophilin in negative regulation of the heat shock response. *J. Biol. Chem.*, 273, 18974–18978.

[El-Sayed et al., 2012] El-Sayed, A. M., Scarborough, P., Seemann, L., & Galea, S. (2012). Social network analysis and agent-based modeling in social epidemiology. *Epidemiol Perspect Innov*, 9, 1.

[Elliott & Kiel, 2002] Elliott, E. & Kiel, L. D. (2002). Exploring cooperation and competition using agent-based modeling. *Proc. Natl. Acad. Sci. U.S.A.*, 99 Suppl 3, 7193–7194.

[Enjalbert et al., 2003] Enjalbert, B., Nantel, A., & Whiteway, M. (2003). Stress-induced gene expression in Candida albicans: absence of a general stress response. *Mol. Biol. Cell*, 14, 1460–1467.

[Evans, 2010] Evans, S. E. (2010). Coping with Candida infections. *Proc Am Thorac Soc*, 7, 197–203.

[Faust & Raes, 2012] Faust, K. & Raes, J. (2012). Microbial interactions: from networks to models. *Nat. Rev. Microbiol.*, 10(8), 538–550.

[Filler & Sheppard, 2006] Filler, S. G. & Sheppard, D. C. (2006). Fungal invasion of normally non-phagocytic host cells. *PLoS Pathog.*, 2, e129.

[Folcik et al., 2011] Folcik, V. A., Broderick, G., Mohan, S., Block, B., Ekbote, C., Doolittle, J., Khoury, M., Davis, L., & Marsh, C. B. (2011). Using an agent-based

model to analyze the dynamic communication network of the immune response. *Theor Biol Med Model*, 8, 1.

[Ghannoum, 1998] Ghannoum, M. A. (1998). Extracellular phospholipases as universal virulence factor in pathogenic fungi. *Nihon Ishinkin Gakkai Zasshi*, 39, 55–59.

[Goldberg, 2003] Goldberg, A. L. (2003). Protein degradation and protection against misfolded or damaged proteins. *Nature*, 426, 895–899.

[Gonzalez-Parraga et al., 2010] Gonzalez-Parraga, P., Alonso-Monge, R., Pla, J., & Arguelles, J. C. (2010). Adaptive tolerance to oxidative stress and the induction of antioxidant enzymatic activities in Candida albicans are independent of the Hog1 and Cap1-mediated pathways. *FEMS Yeast Res.*, 10, 747–756.

[Gore et al., 2009] Gore, J., Youk, H., & van Oudenaarden, A. (2009). Snowdrift game dynamics and facultative cheating in yeast. *Nature*, 459(7244), 253–256.

[Gow et al., 2012] Gow, N. A., van de Veerdonk, F. L., Brown, A. J., & Netea, M. G. (2012). Candida albicans morphogenesis and host defence: discriminating invasion from colonization. *Nat. Rev. Microbiol.*, 10(2), 112–122.

[Hall et al., 2009] Hall, R. A., Cottier, F., & Muhlschlegel, F. A. (2009). Molecular networks in the fungal pathogen Candida albicans. *Adv. Appl. Microbiol.*, 67, 191–212.

[Hawksworth, 1991] Hawksworth, D. L. (1991). The fungal dimension of biodiversity: magnitude, significance, and conservation. *Mycol Res*, 95 (6), 641–655.

[Hegde et al., 1995] Hegde, R. S., Zuo, J., Voellmy, R., & Welch, W. J. (1995). Short circuiting stress protein expression via a tyrosine kinase inhibitor, herbimycin A. *J. Cell. Physiol.*, 165, 186–200.

[Heinrich & Rapoport, 1974] Heinrich, R. & Rapoport, T. A. (1974). A linear steady-state treatment of enzymatic chains. General properties, control and effector strength. *Eur. J. Biochem.*, 42(1), 89–95.

[Higgins, 1963] Higgins, J. (1963). Analysis of sequential reactions. *Ann. N. Y. Acad. Sci.*, 108, 305–321.

[Hoops et al., 2006] Hoops, S., Sahle, S., Gauges, R., Lee, C., Pahle, J., Simus, N., Singhal, M., Xu, L., Mendes, P., & Kummer, U. (2006). COPASI–a COmplex PAthway SImulator. *Bioinformatics*, 22, 3067–3074.

[Hsieh et al., 2010] Hsieh, M. Y., Yang, S., Raymond-Stinz, M. A., Edwards, J. S., & Wilson, B. S. (2010). Spatio-temporal modeling of signaling protein recruitment to EGFR. *BMC Syst Biol*, 4, 57.

[Hube, 2011] Hube, B. (2011). Personal communication.

[Ingalls & Sauro, 2003] Ingalls, B. P. & Sauro, H. M. (2003). Sensitivity analysis of stoichiometric networks: an extension of metabolic control analysis to non-steady state trajectories. *J. Theor. Biol.*, 222, 23–36.

[Jacobsen et al., 2012] Jacobsen, I. D., Wilson, D., Wachtler, B., Brunke, S., Naglik, J. R., & Hube, B. (2012). Candida albicans dimorphism as a therapeutic target. *Expert Rev Anti Infect Ther*, 10, 85–93.

[Karlebach & Shamir, 2008] Karlebach, G. & Shamir, R. (2008). Modelling and analysis of gene regulatory networks. *Nat. Rev. Mol. Cell Biol.*, 9, 770–780.

[Kebaara et al., 2008] Kebaara, B. W., Langford, M. L., Navarathna, D. H., Dumitru, R., Nickerson, K. W., & Atkin, A. L. (2008). *Candida albicans* Tup1 is involved in farnesol-mediated inhibition of filamentous-growth induction. *Eukaryotic Cell*, 7, 980–987.

[Kitano, 2002] Kitano, H. (2002). Computational systems biology. *Nature*, 420(6912), 206–210.

[Klann et al., 2011] Klann, M. T., Lapin, A., & Reuss, M. (2011). Agent-based simulation of reactions in the crowded and structured intracellular environment: Influence of mobility and location of the reactants. *BMC Syst Biol*, 5, 71.

[Klipp et al., 2007] Klipp, E., Liebermeister, W., Helbig, A., Kowald, A., & Schaber, J. (2007). Systems biology standards–the community speaks. *Nat. Biotechnol.*, 25, 390–391.

[Klipp et al., 2009] Klipp, E., Liebermeister, W., Wierling, C., Kowald, A., Lehrach, H., & Herwig, R. (2009). *Systems Biology: A Textbook*. Number ISBN 978-3-527-31874-2. Wiley-VCH, 1 edition.

[Klipp et al., 2005] Klipp, E., Nordlander, B., Kruger, R., Gennemark, P., & Hohmann, S. (2005). Integrative model of the response of yeast to osmotic shock. *Nat. Biotechnol.*, 23, 975–982.

[Koh et al., 2008] Koh, A. Y., Köhler, J. R., Coggshall, K. T., Van Rooijen, N., & Pier, G. B. (2008). Mucosal damage and neutropenia are required for Candida albicans dissemination. *PLoS Pathog.*, 4, e35.

[Kühn, 2010] Kühn, C. (2010). *Modeling and Analysis of Yeast Osmoadaptation in Cellular Context*. PhD thesis, Humboldt Universität zu Berlin, Invalidenstrasse 42, 10115 Berlin, Germany.

[Kühn et al., 2007] Kühn, C., Kühn, A., Poustka, A. J., & Klipp, E. (2007). Modeling development: spikes of the sea urchin. *Genome Inform*, 18, 75–84.

[Kühn et al., 2010] Kühn, C., Prasad, K. V., Klipp, E., & Gennemark, P. (2010). Formal representation of the high osmolarity glycerol pathway in yeast. *Genome Inform*, 22, 69–83.

[Kumamoto & Pierce, 2011] Kumamoto, C. A. & Pierce, J. V. (2011). Immunosensing during colonization by Candida albicans: does it take a village to colonize the intestine? *Trends Microbiol.*, 19, 263–267.

[Leach et al., 2012] Leach, M. D., Tyc, K. M., Brown, A. J., & Klipp, E. (2012). Modelling the regulation of thermal adaptation in Candida albicans, a major fungal pathogen of humans. *PLoS ONE*, 7(3), e32467.

[Leidich et al., 1998] Leidich, S. D., Ibrahim, A. S., Fu, Y., Koul, A., Jessup, C., Vitullo, J., Fonzi, W., Mirbod, F., Nakashima, S., Nozawa, Y., & Ghannoum, M. A. (1998). Cloning and disruption of caPLB1, a phospholipase B gene involved in the pathogenicity of Candida albicans. *J. Biol. Chem.*, 273, 26078–26086.

[Li et al., 1982a] Li, G. C., Petersen, N. S., & Mitchell, H. K. (1982a). Induced thermal tolerance and heat shock protein synthesis in Chinese hamster ovary cells. *Int. J. Radiat. Oncol. Biol. Phys.*, 8, 63–67.

[Li et al., 1982b] Li, G. C., Petersen, N. S., & Mitchell, H. K. (1982b). Induced thermal tolerance and heat shock protein synthesis in Chinese hamster ovary cells. *Br. J. Cancer Suppl.*, 5, 132–136.

[Lionakis et al., 2011] Lionakis, M. S., Lim, J. K., Lee, C. C., & Murphy, P. M. (2011). Organ-specific innate immune responses in a mouse model of invasive candidiasis. *J Innate Immun*, 3(2), 180–199.

[Lo et al., 1997] Lo, H. J., Kohler, J. R., DiDomenico, B., Loebenberg, D., Cacciapuoti, A., & Fink, G. R. (1997). Nonfilamentous *C. albicans* mutants are avirulent. *Cell*, 90, 939–949.

[Machado et al., 2011] Machado, D., Costa, R. S., Rocha, M., Ferreira, E. C., Tidor, B., & Rocha, I. (2011). Modeling formalisms in Systems Biology. *AMB Express*, 1, 45.

[Marino et al., 2008] Marino, S., Hogue, I. B., Ray, C. J., & Kirschner, D. E. (2008). A methodology for performing global uncertainty and sensitivity analysis in systems biology. *J. Theor. Biol.*, 254, 178–196.

[Matthews et al., 2003] Matthews, R. C., Rigg, G., Hodgetts, S., Carter, T., Chapman, C., Gregory, C., Illidge, C., & Burnie, J. (2003). Preclinical assessment of the efficacy of mycograb, a human recombinant antibody against fungal HSP90. *Antimicrob. Agents Chemother.*, 47, 2208–2216.

[Mavor et al., 2005] Mavor, A. L., Thewes, S., & Hube, B. (2005). Systemic fungal infections caused by Candida species: epidemiology, infection process and virulence attributes. *Curr Drug Targets*, 6, 863–874.

[McAlister & Finkelstein, 1980] McAlister, L. & Finkelstein, D. B. (1980). Heat shock proteins and thermal resistance in yeast. *Biochem. Biophys. Res. Commun.*, 93, 819–824.

[Miller et al., 2010] Miller, J., Parker, M., Bourret, R. B., & Giddings, M. C. (2010). An agent-based model of signal transduction in bacterial chemotaxis. *PLoS ONE*, 5, e9454.

[Miller & Johnson, 2002] Miller, M. G. & Johnson, A. D. (2002). White-opaque switching in Candida albicans is controlled by mating-type locus homeodomain proteins and allows efficient mating. *Cell*, 110, 293–302.

[Miranda et al., 2009] Miranda, L. N., van der Heijden, I. M., Costa, S. F., Sousa, A. P., Sienra, R. A., Gobara, S., Santos, C. R., Lobo, R. D., Pessoa, V. P., & Levin, A. S. (2009). Candida colonisation as a source for candidaemia. *J. Hosp. Infect.*, 72, 9–16.

[Mochon et al., 2010] Mochon, A. B., Jin, Y., Ye, J., Kayala, M. A., Wingard, J. R., Clancy, C. J., Nguyen, M. H., Felgner, P., Baldi, P., & Liu, H. (2010). Serological profiling of a Candida albicans protein microarray reveals permanent host-pathogen interplay and stage-specific responses during candidemia. *PLoS Pathog.*, 6(3), e1000827.

[Moles et al., 2003] Moles, C. G., Mendes, P., & Banga, J. R. (2003). Parameter estimation in biochemical pathways: a comparison of global optimization methods. *Genome Res.*, 13(11), 2467–2474.

[Morimoto, 1993] Morimoto, R. I. (1993). Cells in stress: transcriptional activation of heat shock genes. *Science*, 259, 1409–1410.

[Morimoto, 1998] Morimoto, R. I. (1998). Regulation of the heat shock transcriptional response: cross talk between a family of heat shock factors, molecular chaperones, and negative regulators. *Genes Dev.*, 12, 3788–3796.

[Moyes et al., 2010] Moyes, D. L., Runglall, M., Murciano, C., Shen, C., Nayar, D., Thavaraj, S., Kohli, A., Islam, A., Mora-Montes, H., Challacombe, S. J., & Naglik, J. R. (2010). A biphasic innate immune MAPK response discriminates between the yeast and hyphal forms of *Candida albicans* in epithelial cells. *Cell Host Microbe*, 8, 225–235.

[Mukherjee et al., 2001] Mukherjee, P. K., Seshan, K. R., Leidich, S. D., Chandra, J., Cole, G. T., & Ghannoum, M. A. (2001). Reintroduction of the PLB1 gene into *Candida albicans* restores virulence in vivo. *Microbiology (Reading, Engl.)*, 147, 2585–2597.

[Munro et al., 2006] Munro, C., Fradin, C., Bader, O., & Hube, B. (2006). Postgenomic Approaches to Analyse *Candida albicans* Pathogenicity. In A. Brown (Ed.), *Fungal Genomics*, volume 13 of *The Mycota* (pp. 163–184). Springer Berlin Heidelberg.

[Netea et al., 2008] Netea, M. G., Brown, G. D., Kullberg, B. J., & Gow, N. A. (2008). An integrated model of the recognition of *Candida albicans* by the innate immune system. *Nat. Rev. Microbiol.*, 6, 67–78.

[Netea & Kullberg, 2010] Netea, M. G. & Kullberg, B. J. (2010). Epithelial sensing of fungal invasion. *Cell Host Microbe*, 8, 219–220.

[Neumann & Morgenstern, 1944] Neumann, J. V. & Morgenstern, O. (1944). *Theory of Games and Economic Behavior*. Princeton University Press.

[Nicholls et al., 2009] Nicholls, S., Leach, M. D., Priest, C. L., & Brown, A. J. (2009). Role of the heat shock transcription factor, Hsf1, in a major fungal pathogen that is obligately associated with warm-blooded animals. *Mol. Microbiol.*, 74, 844–861.

[Nicholls et al., 2011] Nicholls, S., MacCallum, D. M., Kaffarnik, F. A., Selway, L., Peck, S. C., & Brown, A. J. (2011). Activation of the heat shock transcription factor Hsf1 is essential for the full virulence of the fungal pathogen Candida albicans. *Fungal Genet. Biol.*, 48, 297–305.

[Noble & Johnson, 2007] Noble, S. M. & Johnson, A. D. (2007). Genetics of *Candida albicans*, a diploid human fungal pathogen. *Annu. Rev. Genet.*, 41, 193–211.

[Nowak, 2006] Nowak, M. A. (2006). Five rules for the evolution of cooperation. *Science*, 314(5805), 1560–1563.

[Odds, 1984] Odds, F. C. (1984). Ecology and epidemiology of Candida species. *Zentralbl Bakteriol Mikrobiol Hyg A*, 257, 207–212.

[Odds, 1998] Odds, F. C. (1998). *Morphogenesis in Candida, with special reference to C. albicans*. Ballière Tindall, London, UK, 2nd ed. edition.

[O'Malley & Dupre, 2005] O'Malley, M. A. & Dupre, J. (2005). Fundamental issues in systems biology. *Bioessays*, 27(12), 1270–1276.

[Pappalardo et al., 2011] Pappalardo, F., Martinez Forero, I., Pennisi, M., Palazon, A., Melero, I., & Motta, S. (2011). SimB16: modeling induced immune system response against B16-melanoma. *PLoS ONE*, 6, e26523.

[Parsek & Greenberg, 2005] Parsek, M. R. & Greenberg, E. P. (2005). Sociomicrobiology: the connections between quorum sensing and biofilms. *Trends Microbiol.*, 13(1), 27–33.

[Petersen & Mitchell, 1981] Petersen, N. S. & Mitchell, H. K. (1981). Recovery of protein synthesis after heat shock: prior heat treatment affects the ability of cells to translate mRNA. *Proc. Natl. Acad. Sci. U.S.A.*, 78, 1708–1711.

[Pfaller, 1996] Pfaller, M. A. (1996). Nosocomial candidiasis: emerging species, reservoirs, and modes of transmission. *Clin. Infect. Dis.*, 22 Suppl 2, 89–94.

[Phan et al., 2000] Phan, Q. T., Belanger, P. H., & Filler, S. G. (2000). Role of hyphal formation in interactions of Candida albicans with endothelial cells. *Infect. Immun.*, 68(6), 3485–3490.

[Pittet et al., 1994] Pittet, D., Monod, M., Suter, P. M., Frenk, E., & Auckenthaler, R. (1994). Candida colonization and subsequent infections in critically ill surgical patients. *Ann. Surg.*, 220, 751–758.

[Pogson et al., 2008] Pogson, M., Holcombe, M., Smallwood, R., & Qwarnstrom, E. (2008). Introducing spatial information into predictive NF-kappaB modelling–an agent-based approach. *PLoS ONE*, 3, e2367.

[Pogson et al., 2006] Pogson, M., Smallwood, R., Qwarnstrom, E., & Holcombe, M. (2006). Formal agent-based modelling of intracellular chemical interactions. *BioSystems*, 85, 37–45.

[Ramirez-Zavala et al., 2008] Ramirez-Zavala, B., Reuss, O., Park, Y. N., Ohlsen, K., & Morschhauser, J. (2008). Environmental induction of white-opaque switching in *Candida albicans*. *PLoS Pathog.*, 4, e1000089.

[Rieger et al., 2005] Rieger, T. R., Morimoto, R. I., & Hatzimanikatis, V. (2005). Mathematical modeling of the eukaryotic heat-shock response: dynamics of the hsp70 promoter. *Biophys. J.*, 88, 1646–1658.

[Roman et al., 2007] Roman, E., Arana, D. M., Nombela, C., Alonso-Monge, R., & Pla, J. (2007). MAP kinase pathways as regulators of fungal virulence. *Trends Microbiol.*, 15, 181–190.

[Rosenbach et al., 2010] Rosenbach, A., Dignard, D., Pierce, J. V., Whiteway, M., & Kumamoto, C. A. (2010). Adaptations of Candida albicans for growth in the mammalian intestinal tract. *Eukaryotic Cell*, 9(7), 1075–1086.

[Schaber & Klipp, 2008] Schaber, J. & Klipp, E. (2008). Short-term volume and turgor regulation in yeast. *Essays Biochem.*, 45, 147–159.

[Segovia-Juarez et al., 2004] Segovia-Juarez, J. L., Ganguli, S., & Kirschner, D. (2004). Identifying control mechanisms of granuloma formation during M. tuberculosis infection using an agent-based model. *J. Theor. Biol.*, 231, 357–376.

[Shapiro & Cowen, 2010] Shapiro, R. S. & Cowen, L. (2010). Coupling temperature sensing and development: Hsp90 regulates morphogenetic signalling in Candida albicans. *Virulence*, 1(1), 45–48.

[Shapiro et al., 2009] Shapiro, R. S., Uppuluri, P., Zaas, A. K., Collins, C., Senn, H., Perfect, J. R., Heitman, J., & Cowen, L. E. (2009). Hsp90 orchestrates temperature-dependent Candida albicans morphogenesis via Ras1-PKA signaling. *Curr. Biol.*, 19(8), 621–629.

[Sharp et al., 1999] Sharp, F. R., Massa, S. M., & Swanson, R. A. (1999). Heat-shock protein protection. *Trends Neurosci.*, 22, 97–99.

[Sudbery, 2011] Sudbery, P. E. (2011). Growth of Candida albicans hyphae. *Nat. Rev. Microbiol.*, 9(10), 737–748.

[Thorne et al., 2007] Thorne, B. C., Bailey, A. M., DeSimone, D. W., & Peirce, S. M. (2007). Agent-based modeling of multicell morphogenic processes during development. *Birth Defects Res. C Embryo Today*, 81, 344–353.

[Tyc & Klipp, 2011] Tyc, K. M. & Klipp, E. (2011). Modeling dissemination of pathogenic fungi within a host: A cartoon for the interactions of two complex systems. *J Comput Sci Syst Biol*, doi:10.4172/jcsb.S1-001.

[Urban et al., 2006] Urban, C. F., Reichard, U., Brinkmann, V., & Zychlinsky, A. (2006). Neutrophil extracellular traps capture and kill Candida albicans yeast and hyphal forms. *Cell. Microbiol.*, 8(4), 668–676.

[Wachtler et al., 2012] Wachtler, B., Citiulo, F., Jablonowski, N., Forster, S., Dalle, F., Schaller, M., Wilson, D., & Hube, B. (2012). Candida albicans-epithelial interactions: dissecting the roles of active penetration, induced endocytosis and host factors on the infection process. *PLoS ONE*, 7(5), e36952.

[Wächtler et al., 2011] Wächtler, B., Wilson, D., Haedicke, K., Dalle, F., & Hube, B. (2011). From attachment to damage: defined genes of Candida albicans mediate adhesion, invasion and damage during interaction with oral epithelial cells. *PLoS ONE*, 6(2), e17046.

[Warrender et al., 2006] Warrender, C., Forrest, S., & Koster, F. (2006). Modeling intercellular interactions in early Mycobacterium infection. *Bull. Math. Biol.*, 68, 2233–2261.

[Webb, 2007] Webb, J. N. (2007). *Game Theory: Decisions, Interaction and Evolution.* Springer.

[Weindl et al., 2007] Weindl, G., Naglik, J. R., Kaesler, S., Biedermann, T., Hube, B., Korting, H. C., & Schaller, M. (2007). Human epithelial cells establish direct antifungal defense through TLR4-mediated signaling. *J. Clin. Invest.*, 117, 3664–3672.

[Werner-Washburne et al., 1987] Werner-Washburne, M., Stone, D. E., & Craig, E. A. (1987). Complex interactions among members of an essential subfamily of hsp70 genes in Saccharomyces cerevisiae. *Mol. Cell. Biol.*, 7, 2568–2577.

[Westerhoff, 2008] Westerhoff, H. V. (2008). Signalling control strength. *J. Theor. Biol.*, 252(3), 555–567.

[Whiteway, 2000] Whiteway, M. (2000). Transcriptional control of cell type and morphogenesis in *Candida albicans*. *Curr. Opin. Microbiol.*, 3, 582–588.

[Whiteway & Bachewich, 2007] Whiteway, M. & Bachewich, C. (2007). Morphogenesis in Candida albicans. *Annu. Rev. Microbiol.*, 61, 529–553.

[Wilensky, 1999] Wilensky, U. (1999). NetLogo at http://ccl.northwestern.edu/netlogo/.

[Wilson & Hube, 2010] Wilson, D. & Hube, B. (2010). Hgc1 mediates dynamic *Candida albicans*-endothelium adhesion events during circulation. *Eukaryotic Cell*, 9, 278–287.

[Wozniok et al., 2008] Wozniok, I., Hornbach, A., Schmitt, C., Frosch, M., Einsele, H., Hube, B., Loffler, J., & Kurzai, O. (2008). Induction of ERK-kinase signalling triggers morphotype-specific killing of Candida albicans filaments by human neutrophils. *Cell. Microbiol.*, 10(3), 807–820.

[Young et al., 2004] Young, J. C., Agashe, V. R., Siegers, K., & Hartl, F. U. (2004). Pathways of chaperone-mediated protein folding in the cytosol. *Nat. Rev. Mol. Cell Biol.*, 5, 781–791.

[Zeuthen & Howard, 1989] Zeuthen, M. L. & Howard, D. H. (1989). Thermotolerance and the heat-shock response in Candida albicans. *J. Gen. Microbiol.*, 135(9), 2509–2518.

[Zi et al., 2010] Zi, Z., Liebermeister, W., & Klipp, E. (2010). A quantitative study of the Hog1 MAPK response to fluctuating osmotic stress in Saccharomyces cerevisiae. *PLoS ONE*, 5(3), e9522.

[Zipfel et al., 2008] Zipfel, P. F., Gropp, K., Reuter, M., Schindler, S., & Skerka, C. (2008). The Host Innate Immune Response to Pathogenic *Candida albicans* and Other Fungal Pathogens. In A. A. Brakhage & P. F. Zipfel (Eds.), *Human and Animal Relationships*, volume 6 of *The Mycota* (pp. 233–242). Springer Berlin Heidelberg.

[Zou et al., 1998] Zou, J., Guo, Y., Guettouche, T., Smith, D. F., & Voellmy, R. (1998). Repression of heat shock transcription factor HSF1 activation by HSP90 (HSP90 complex) that forms a stress-sensitive complex with HSF1. *Cell*, 94, 471–480.

[Zupanić-Krmek & Nemet, 2004] Zupanić-Krmek, D. & Nemet, D. (2004). Systemic fungal infections in immunocompromised patients. *Acta Med Croatica*, 58, 251–261.

List of Figures

List of Tables

Selbständigkeitserklärung

Ich erkläre, dass ich die vorliegende Arbeit selbständig und nur unter Verwendung der angegebenen Literatur und Hilfsmittel angefertigt habe.

Berlin, den 24.07.2012 Katarzyna M. Tyc